AN ANALOGUE MODEL STUDY OF ELECTROMAGNETIC INDUCTION IN THE QUEEN CHARLOTTE ISLANDS REGION

by

EDWARD SU WAH CHAN

B.Sc., University of Victoria, 1977

A THESIS SUBMITTED IN PARTIAL FULFILLMEMT

OF THE REQUIREMENTS FOR THE DEGREE OF

MASTER OF SCIENCE

in the Department

of

Physics

We accept this thesis as conforming

to the required standard

[redacted]

(H.W. Dosso) (R.E. Horita)

[redacted]

(L.K. Law) (H.M. Srivastava)

[redacted]

(T.W. Dingle) (J.T. Weaver)

Supervisors: Dr. H.W. Dosso and Dr. L.K. Law

ABSTRACT

In this thesis, electromagnetic variations in the Queen Charlotte Islands region are studied using scaled analogue model measurements and field station measurements. Contour diagrams and three-dimensional diagrams of the in-phase and quadrature parts of the model magnetic and electric field components are used to show in detail the field response to the complex coastlines and ocean channels.

The results indicate that conductive channelling of induced currents is important in Hecate Strait, the shallow ocean between the Queen Charlotte Islands and the British Columbia mainland, for both source field polarizations studied. Current deflection is observed at Rose Point for E-Polarization and at the northern and southern tips of the Queen Charlotte Islands for H-Polarization.

Model results for the simulated 4, 40, and 120 min. period variations indicate that the behaviour of the fields over the Queen Charlotte Islands are highly frequency dependent. At the eastern island coastline, for E-Polarization, H_z shows fairly large anomalies for the 4 min. period, but H_z is almost zero at this region for

40 min. period. With increasing period, current channelled into Hecate Strait decreases sharply, and proportionately the field responses for the various components shift from the in-phase to the quadrature part. H_z, H_x, E_x, and E_y show response to capes and bays. These components also respond to channelled currents in the ocean inlets. Large E_y enhancements at the end of ocean inlets indicate diffusion of current into land.

The model results show that in decreasing the depth of the conducting layer in the mantle from 200 km to 100 km, the H_z, H_x, E_x, and E_y anomalies are attenuated by 20%, and the H_y anomalies by roughly 8% over the deep ocean and by 12% over Hecate Strait for 4 min. period variations. Beyond 200 km, the change in the depth of the conducting layer has very little effect on the various field components.

The behaviour of the model and field station Parkinson arrows are found to be in reasonably good agreement, showing that the magnetic variations in this area are mainly due to the coast effects. The difference between the analogue model results and the field station results will provide information on the tectonic structure of the region.

The results of the present work will help in the determination of reference station locations for the reduction of cross-over error in marine magnetic surveys.

The results will also suggest possible locations for field stations in this area for tectonic studies.

[redacted]

(H.W. Dosso) (R.E. Horita)

[redacted]

(L.K. Law) (H.M. Srivastava)

[redacted]

(T.W. Dingle) (J.T. Weaver)

TABLE OF CONTENTS

LIST OF FIGURES

Figure Page

Figure Page

Figure Page

Figure Page

Figure Page

ACKNOWLEDGEMENTS

I would like to thank my supervisors, Dr. H.W. Dosso and Dr. L.K. Law, for suggesting the research problem and their valuable guidance throughout the research.

I would like to take this opportunity to express my appreciation to Dr. W. Nienaber, Mr. G.J. Heard and Mr. D. Hebert for many useful discussions and comments. I would like to acknowledge Mr. D. Auld for his helpful suggestions and providing the field measurement data.

Financial support for this work was in part provided through Energy, Mines and Resources, Canada Research Agreements Nos. 65-3-79 and 22-3-80. The financial support from N.S.E.R.C. Scholarships is gratefully acknowledged.

Chapter 1

INTRODUCTION

1.1 Electromagnetic Induction in the Earth

The electromagnetic variations at the surface of the earth are related to the currents induced in the conducting interior by external time-varying magnetic fields. The transient geomagnetic variations are mainly caused by current systems in the ionosphere or magnetosphere originating from the interaction of the solar wind with the earth's magnetosphere. The magnetic field variations due to these current systems cover a period range from a fraction of a second to several days. The inducing magnetic fields generate electric currents in the earth's interior which in turn produce secondary electric and magnetic fields that contribute to the total geomagnetic fields observed at the surface of the earth. The induced electromagnetic field is also affected by structures such as conducting oceans, complex coastlines, ocean channels, and islands situated near a continent. The depth of penetration in the earth of the varying fields is determined by the frequency of the variations and the conductivity of the earth. Hence, the analysis of the

variation fields at the earth's surface can yield information on the conductivity distribution within the earth.

1.2 Global Induction Studies

Electromagnetic induction studies may be divided into problems of a global nature and those of a local nature. The global induction studies regard the properties of the earth as a whole and are concerned with the average values of the conductivity distribution over regions having dimensions comparable with those of the earth. The conductivity is treated as some smooth function of latitude, longitude and distance from the centre of the earth. In solving these problems, the inducing field is expressed in terms of spherical harmonics. The effect of each harmonic is studied separately and the result of all the harmonics then superimposed.

The problem of current induced in a sphere with constant conductivity was first studied by Lamb (1883). Schuster (1889) applied the method of spherical harmonic analysis to separate the fields of external and internal origin. Price (1930, 1931) extended Lamb's solution to include aperiodic fields. Lahiri and Price (1939) considered the conductivity of the earth as a function of its radius. They applied their results to investigate the conductivity distribution of the earth to considerable

depths. Their results showed that the conductivity of the earth was uniform down to a depth of 700 km where the conductivity increased sharply to a large value. Banks (1972) also found a steep rise in the earth's conductivity at the depth of approximately 700 km.

Price (1949) developed the basic theory of induction in non-uniform thin sheets and shells. Analysis and applications were made by Ashour (1950) and Rikitake (1960). Rikitake (1961) studied the current induced in the ocean by the daily magnetic variation and discussed the problem of mutual induction between the thin crustal conducting shell and conducting material in the mantle. Bullard and Parker (1970) studied a particular model consisting of a conducting mantle, a non-conducting crust-mantle layer and a layer of conducting sediments of variable thickness.

1.3 Local Induction Studies

Local induction studies deal with regions of limited size, of the order of several hundred kilometers. In these studies, the sphericity of the earth is ignored and the earth is treated as a semi-infinite half-space with variable conductivity distribution. However, the inducing field remains of global dimension and is effectively uniform over the region being studied.

Price (1950) studied electromagnetic induction in a flat earth using a semi-infinite uniform conducting half-space, and calculated the induced fields for an arbitrary source field. A uniformly layered earth model was considered by Tikhonov (1950), Lipskaya (1953). Cagniard (1953), in his derivation of the magnetotelluric method, assumed a horizontal uniform earth with a uniform field and outlined the solutions for two-layer and multi-layer models. Wait (1954) and Price (1962) showed that Cagniard's results are valid only if the electromagnetic field is uniform over a horizontal distance of at least one skin-depth of the conducting medium. Weaver (1973) has reviewed the principal features of electromagnetic induction for a multi-layered earth by various source fields.

At many locations on the earth, the geomagnetic fields at relatively nearby stations show considerable difference. This difference remains consistant in character for fluctuations of given frequency, and forms a definite pattern for the area studied. Anomalous vertical magnetic fields over a subsurface conductivity anomaly in Northern Germany have been investigated by Schmucker (1959), Kertz (1964), and Vozoff and Swift (1968). Similar anomalous fields were observed on the North American continent by Swift (1967), Caner et al. (1969) and Schmucker (1970).

Lateral variations in conductivity have been studied by various techniques. Analytic approaches to the problem of vertical discontinuity in conductivity have been considered by several authors. D'Erceville and Kunetz (1962) considered a model for two media of different resistivities in contact along a vertical plane overlying a horizontal basement to study the effect of a fault on the earth's natural electromagnetic field. Weaver and Thomson (1972) used a similar model with induction by an external line current. Weidelt (1971) considered induction in two adjacent half-sheets with different conductivities to study the coast effect.

Analytic techniques are generally suitable for handling idealized structures with very simple geometry. More complex structures have been studied using several numerical techniques. Jones and Pascoe (1972), Lines and Jones (1973) and Brewitt-Taylor and Weaver (1976) employed the finite difference method, calculating the field values over a mesh of grid points. The finite element method, based on the principle that electromagnetic fields behave in a way as to minimize the energy of the system, was described by Zienkiewicz (1971) and used by Coggan (1971) and Reddy and Rankin (1972).

When the conductivity structure cannot be represented by simple geometric shapes, as is normally the case for actual geophysical problems, the laboratory analogue

modelling technique becomes very useful. The theory of electromagnetic scale modelling has been treated by Sinclair (1948), Strangway (1966), Ward (1967), Frischknecht (1971) and others. Modelling systems employing metal sheets to represent the conducting oceans have been used by several authors (Roden, 1964; Hermance, 1968; Launay, 1970; and Kulik et al., 1973). Since the conductivity contrast between metal and air is practically infinite, these models simulate an infinite conductivity contrast at the sea-land interface.

Dosso (1966a) developed an analogue model system using saturated salt solution to simulate earth, and graphite to simulate the ocean or other highly conducting structures. Various types of model source fields have been used, including a uniform field (Dosso, 1966a), an oscillating line current (Dosso and Jacobs, 1968; Ramaswamy and Dosso, 1977), overhead vertical and horizontal magnetic dipoles (Dosso, 1969; Thomson et al., 1972; Ogunade et al., 1974), and buried dipole sources (Ramaswamy, 1973; Ramaswamy and Dosso, 1978).

This modelling facility has been used to study a variety of model structures, such as, vertical faults and dykes (Dosso, 1966b), an anisotropic conductor (Dosso, 1969), a sphere embedded in a conducting earth (Ogunade et al., 1974; Ogunade and Dosso 1977), conducting cyclinders in a conducting earth (Ramaswamy and Dosso, 1977). Dosso

et al. (1974) have compared analogue model measurements and finite-difference numerical calculations for induction in the ocean (both constant depth and sloping floor) for a uniform inducing field. Ogunade et al. (1974) also carried out a similar comparison for a buried conducting sphere for an overhead vertical magnetic dipole source. Ramaswamy et al. (1975) compared numerical and analogue model results for electromagnetic induction for an island near a coastline. Ramaswamy et al. (1980) carried out a comparison of numerical, analogue model and field station vertical magnetic fields for the Vancouver Island region. All comparisons have shown good agreement.

1.4 Electromagnetic Induction Studies of the Coast Effect

The electromagnetic induction effects at an ocean coastline have recently been reviewed by Parkinson and Jones (1979) and Fischer (1979). The geomagnetic coast effect is characterized by the large vertical magnetic fields for the case of the inducing electric field polarized parallel to the coast. This effect was observed by Parkinson (1959) and Wiese (1962). Parkinson (1959) observed that the vertical variations were almost entirely correlated with those horizontal variations which were perpendicular to the coastline. Similar observations were made by Schmucker (1964) along the California coast, Lambart and Caner (1965) in western Canada, and Everett and

Hyndman (1967) in Australia.

Weaver (1963) considered an ocean coast model consisting of two adjacent quarter-spaces and examined the coast effect theoretically. Other analytical studies have been carried out by Parker (1968) and Brewitt-Taylor (1975). Jones and Price (1970) developed a numerical method for studying the perturbation of electric current by a sharp discontinuity of conductivity in a conductor and applied to a continental-oceanic interface. Lines and Jones (1973) extended the method and considered the three-dimensional case. The coast effect has been studied using analogue model techniques by Roden (1964), Dosso (1966c), Dosso and Jacobs (1968), Dosso (1973), Hermance (1968), Thomson et al. (1972) and Chan et al. (1981a, b).

An interesting feature in the induction studies along a coastal region is the effect of the irregular coastal contour. Jones (1974) and Jones and Lokken (1975) used the finite difference technique to investigate the channelling of current around an island near an irregular coastline and showed the effect of a shallow bay on channelling currents. Launay (1970) and Kulik et al. (1973) used metallic models to study the effect of bays and capes. Chan et al. (1981a) carried out an analogue model study of electromagnetic induction for cape and bay coastlines and found that the effects are limited to a distance approximately equal to the dimension of the bay or cape.

Geomagnetic field variations on islands near a continent have been studied by several authors, for example, the British Isles by Edwards et al. (1971), the Japanese Islands by Rikitake (1966) and Honkura (1971), and Vancouver Island, Canada by Nienaber et al. (1979b).

Three-dimensional numerical model calculations for various simplified island-shapes near a coastline have been carried out by Lines and Jones (1973), Jones and Lokken (1975) and Ramaswamy et al. (1975, 1980).

Using the analogue modelling technique, Nienaber et al. (1976) studied the electromagnetic effects of square and circular islands near a continent, and concluded that the perturbations, due to the island, of the coast effect over the continental shoreline become negligible when the channel width is larger than half the dimension of the island. Scaled analogue models of large geographical regions have also been studied, for example, Vancouver Island region (Nienaber et al., 1979a), the British Isles region (Dosso et al., 1980a), the east coast of North America (Dosso et al., 1980b).

The present work is concerned with electromagnetic induction in the Queen Charlotte Islands region, on the west coast of British Columbia, Canada. Unfortunately, only a limited amount of field station data is available for the area surveyed by the analogue model. Geomagnetic depth sounding has been carried out by Dragert (1973) and

Miller (1973) in this region. In the area south of this region, magnetotelluric survey and geomagnetic depth sounding studies have been carried out by Caner and Cannon (1965), Caner et al. (1969, 1971), Cochrane and Hyndman (1970) and Lambert and Caner (1965). These authors used field station locations extending eastward from the continental coast across geological trends to study the combined effect of the coast and conductivity structure.

1.5 Summary of the Work Carried out in this Thesis

In this thesis, electromagnetic variations in the Queen Charlotte Islands region are studied using scaled analogue model measurements and field station measurements. There is considerable interest in the exploration for hydrocarbons in the Queen Charlotte Sound - Hecate Strait region. Geomagnetic resource charting is being carried out in this area. The present work is to assist in determinating suitable reference station locations for the reduction of cross-over error in marine magnetic surveys as carried out by Auld et al. (1979). This study also suggests suitable field station locations for tectonic studies.

The behaviour of the electromagnetic variations is studied for two orthogonal orientations of a uniform horizontal inducing source field, with the electric field of the inducing field i) roughly parallel to the west coast of the Queen Charlotte Islands, the E-Polarization case,

and ii) perpendicular to the coast of the island, the H-Polarization case. The model frequencies used simulate periods of 4, 40 and 120 min. in the geophysical system.

The laboratory analogue model study includes the effect of (a) the bathymetry of the ocean surrounding the island, (b) the Queen Charlotte Island and the mainland coastline contours, (c) ocean inlets, and (d) the conducting layer at various depths within the mantle. Analogue model digital data are used to produce contour diagrams and three-dimensional diagrams of the in-phase and quadrature model field components to show in detail the responses to the complex coastlines and ocean channels.

The analogue model results are used to investigate electromagnetic induction and conductive channelling, of induced electric current, in the shallow ocean between the Queen Charlotte Islands and the mainland. Current deflection at various sections of the coastlines and current diffusion into land masses are also studied.

Geomagnetic data for the Prince Rupert and Sandspit field stations are compared with analogue model results. Parkinson arrows for the Prince Rupert, Sandspit, Tasu, Smithers and Terrace field stations are compared with those obtained from analogue model measurements.

CHAPTER 2

THE LABORATORY ANALOGUE MODEL

2.1 The Analogue Modelling Conditions and Scaling Factors

The theory of electromagnetic scale models has been discussed in detail by Sinclair (1948), Strangway (1966), Ward (1967), Frischknecht (1971), and applied by Dosso (1966a), and others, to determine the modelling conditions and scaling factors required for an electromagnetic analogue modelling system. For completeness, the modelling conditions will be developed here.

For linear isotropic media in a source-free region, Maxwell's equations in the geophysical system (in SI units) are

$$(1) \qquad \bar{\nabla}' \times \bar{E}' = -\mu' \frac{\delta \bar{H}'}{\delta t'} ,$$

$$(2) \qquad \bar{\nabla}' \times \bar{H}' = \sigma' \bar{E}' + \epsilon' \frac{\delta \bar{E}'}{\delta t'} ,$$

and in the model system are

$$(3) \qquad \bar{\nabla} \times \bar{E} = -\mu \frac{\delta \bar{H}}{\delta t} ,$$

$$(4) \qquad \bar{\nabla} \times \bar{H} = \sigma \bar{E} + \epsilon \frac{\delta \bar{E}}{\delta t} ,$$

where E and H are the electric and magnetic fields respectively, ϵ and μ are the electric permittivity and magnetic permeability, and σ, the electric conductivity. The field variables in the two systems can be related by linear transformations

$$(5) \qquad E = E' K_E , \qquad H = H' K_H ,$$

$$(6) \qquad \epsilon = \epsilon' K_e , \qquad \mu = \mu' K_m ,$$

$$(7) \qquad L = L' K_L , \qquad \sigma = \sigma' K_s , \qquad t = t' K_t ,$$

$$(8) \qquad \bar{\nabla} = \frac{1}{K_L} \bar{\nabla}' , \qquad \frac{\delta}{\delta t} = \frac{1}{K_t} \frac{\delta}{\delta t'} , \quad f = f' K_f ,$$

where K_E, K_H, K_e, K_m, K_L, K_s, K_t, K_f are the respective scale factors for the electric field, magnetic field, premittivity, permeability, length, conductivity, time and frequency.

Using (5) to (8) in (1) and (2), and rearranging terms yields

$$(9) \qquad \bar{\nabla} \times \bar{E} = - \frac{K_E}{K_H} \frac{K_t}{K_L} \frac{\mu}{K_m} \frac{\delta \bar{H}}{\delta t} = - \alpha \mu \frac{\delta \bar{H}}{\delta t} ,$$

$$(10) \qquad \bar{\nabla} \times \bar{H} = \frac{K_H}{K_E} \frac{1}{K_L} \frac{\sigma}{K_s} \bar{E} + \frac{K_H}{K_E} \frac{K_t}{K_L} \frac{\epsilon}{K_e} \frac{\delta \bar{E}}{\delta t} = \beta \sigma \bar{E} + \gamma \epsilon \frac{\delta \bar{E}}{\delta t} ,$$

These two equations must be identical to equations (3) and (4) for proper simulation. Hence, the dimensionless constants α, β and γ must be unity, and

$$(11) \qquad \frac{K_E}{K_H}\,\frac{K_t}{K_L}\,\frac{1}{K_m} = 1 \ ,$$

$$(12) \qquad \frac{K_H}{K_E}\,\frac{1}{K_L}\,\frac{1}{K_s} = 1 \ ,$$

$$(13) \qquad \frac{K_H}{K_E}\,\frac{K_t}{K_L}\,\frac{1}{K_e} = 1 \ .$$

When the displacement currents are unimportant, that is

$$\sigma|E| \gg \epsilon \frac{\delta|\bar{E}|}{\delta t} \ ,$$

the last term in each of equations (2), (4), and (10), and condition (13) can all be ignored. Furthermore, if ferromagnetic media are excluded from the system, K_m can be chosen to be 1 or ($\mu=\mu'$). Equations (11) and (12) become

$$(14) \qquad K\,\frac{K_t}{K_L} = 1 \ ,$$

$$(15) \qquad K\,K_s\,K_L = 1 \ ,$$

where $K = \frac{K_E}{K_H}$ is the ratio of model impedance to the geophysical impedance. Using the transformations (7) and (8) in (14) and (15) leads to

$$(16) \qquad K\,(f'/f)\,(L'/L) = 1 \ ,$$

$$(17) \qquad K^{-1}\,(\sigma'/\sigma)\,(L'/L) = 1 \ ,$$

the necessary and sufficient conditions for proper model

simulation of the geophysical problem.

The scaling factors are chosen to satisfy the above scaling conditions. The conductivity scaling σ'/σ is chosen to be 3×10^{-5}, so that land of conductivity 6.3×10^{-4} Sm^{-1} is respresented by saturated salt solution of conductivity 21 Sm^{-1}, and sea water with conductivity 3.6 Sm^{-1} is respresented by graphite with conductivity 1.2×10^{5} Sm^{-1}. The linear dimension scaling is chosen to be $L'/L = 5 \times 10^{5}$, in order that 1 cm in the model represents 5 km in the geophysical system. These scale factors lead to an impedance scaling of $K = 1/15$ and the frequency scaling $f'/f = 1/(75 \times 10^{5})$. Thus model frequencies of 30, 3 and 1 kHz simulate variations with periods of 4, 40 and 120 min. respectively in the geophysical scale.

2.2 Laboratory Analogue Model Description

The analogue model used in the present work is basically the same as that described by Dosso (1966a, 1973). The experimental arrangement is shown in Fig. 1. It employs a plywood tank 2.44 m x 1.68 m, filled with concentrated salt solution to a height of .63 m. The bottom of the tank is lined with a 5 cm thick layer of graphite to minimize the effects of the concrete floor below.

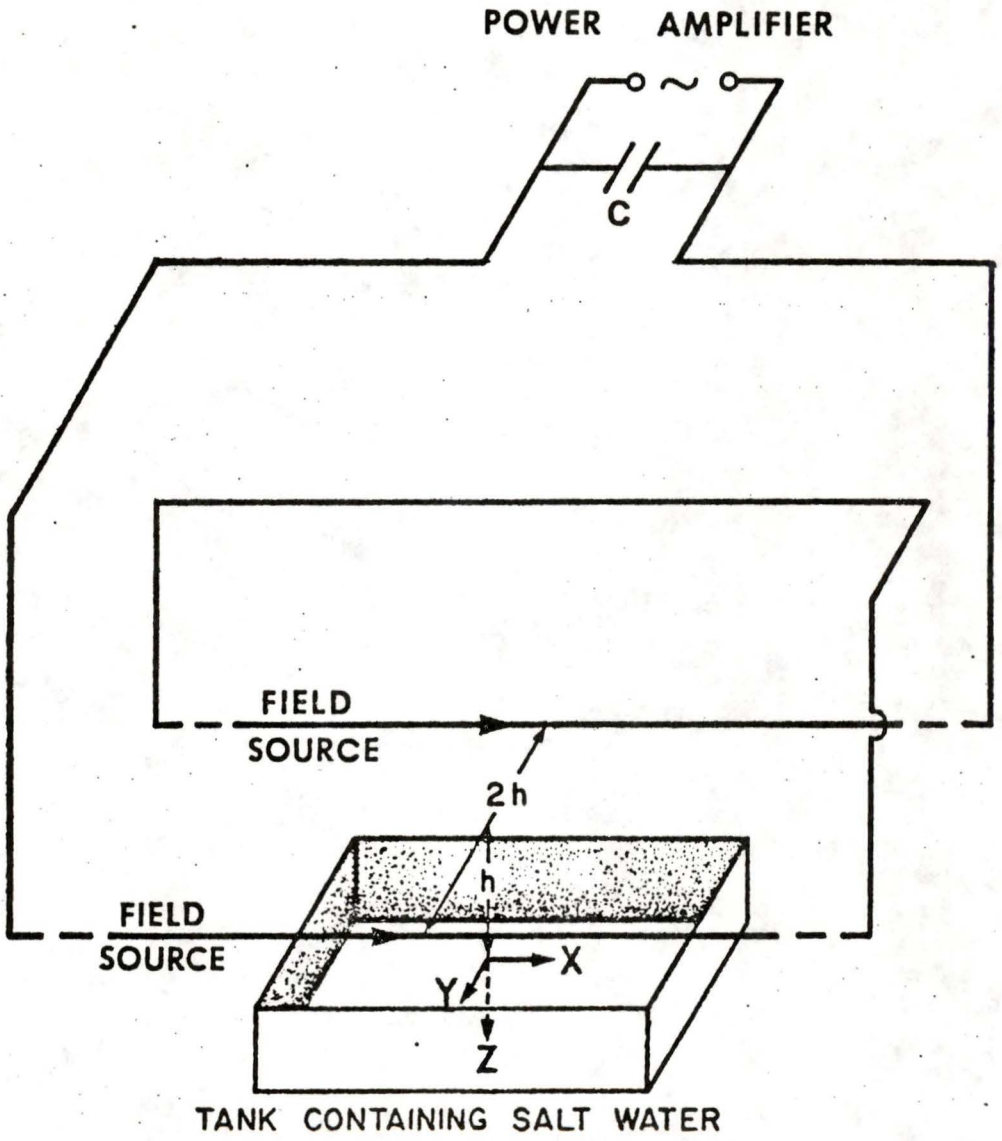

Fig. 1. The electromagnetic analogue model.

A reasonably uniform inducing field is provided by parallel line currents along two parallel wires separated by a distance of 2.4 m and suspended 1.2 m above the surface of the salt solution. A 1000-Watt Savage power amplifier (for 1 kHz and 3 kHz) and a 150-Watt McIntosh power amplifier (for 30 kHz) are used to generate the current. A variable capacitor, connected in parallel with the power amplifier, is used to tune the source circuit for resonance. The source current is continually monitored to ensure a steady source field throughout the experiment.

The two walls of the tank perpendicular to the electric field of the source are lined with stainless steel sheets. The two plates are electrically connected by a heavy copper wire outside the tank to permit induced current in the salt solution to flow parallel to the electric field of the source right to the edge of the tank. This arrangement minimizes the end effects due to the limited size of the model tank.

The two detectors used to measure the vertical magnetic field and the horizontal magnetic field are similar in design. Each detector consists of a .1 cm long coil of 250 turns of #42 wire, with inside diameter .235 cm and outside diameter .635 cm. Each coil is mounted in a lucite tube with the axis of the coil parallel to the direction of the mangetic field component being measured. The coil for the horizontal magnetic field detector is

mounted with its center .38 cm from the end of the lucite tube while the coil for the vertical magnetic field detector is mounted with its center .1 cm from the end of the tube. The horizontal electric field detector consists of three equally spaced pins in a straight line with the outer pins 1.48 cm apart. The electrodes protrude through the sealed end of a lucite tube to make contact with the salt solution. The detector is designed to measure the average horizontal electric field between the two outer electrodes and provide a suitable input to a differential amplifier.

When measuring a particular field component, the appropriate detector mounted rigidly on a motor driven carriage, moves horizontally across the surface of the tank. The recording instrumentation, as shown in Fig. 2, is designed to record the amplitude and phase as well as the in-phase and quadrature parts of the field components simultaneously.

2.3 The Queen Charlotte Islands Analogue Model

The Queen Charlotte Islands region modelled is shown in Fig. 3. With 1 cm representing 5 km, the entire model is approximately 1 m square. In the simplified map of Fig. 3, The Queen Charlotte Islands are shown as one island approximately 300 km long and ranging from approximately 25 km to 100 km wide. Thus a hole, with appropriate shape,

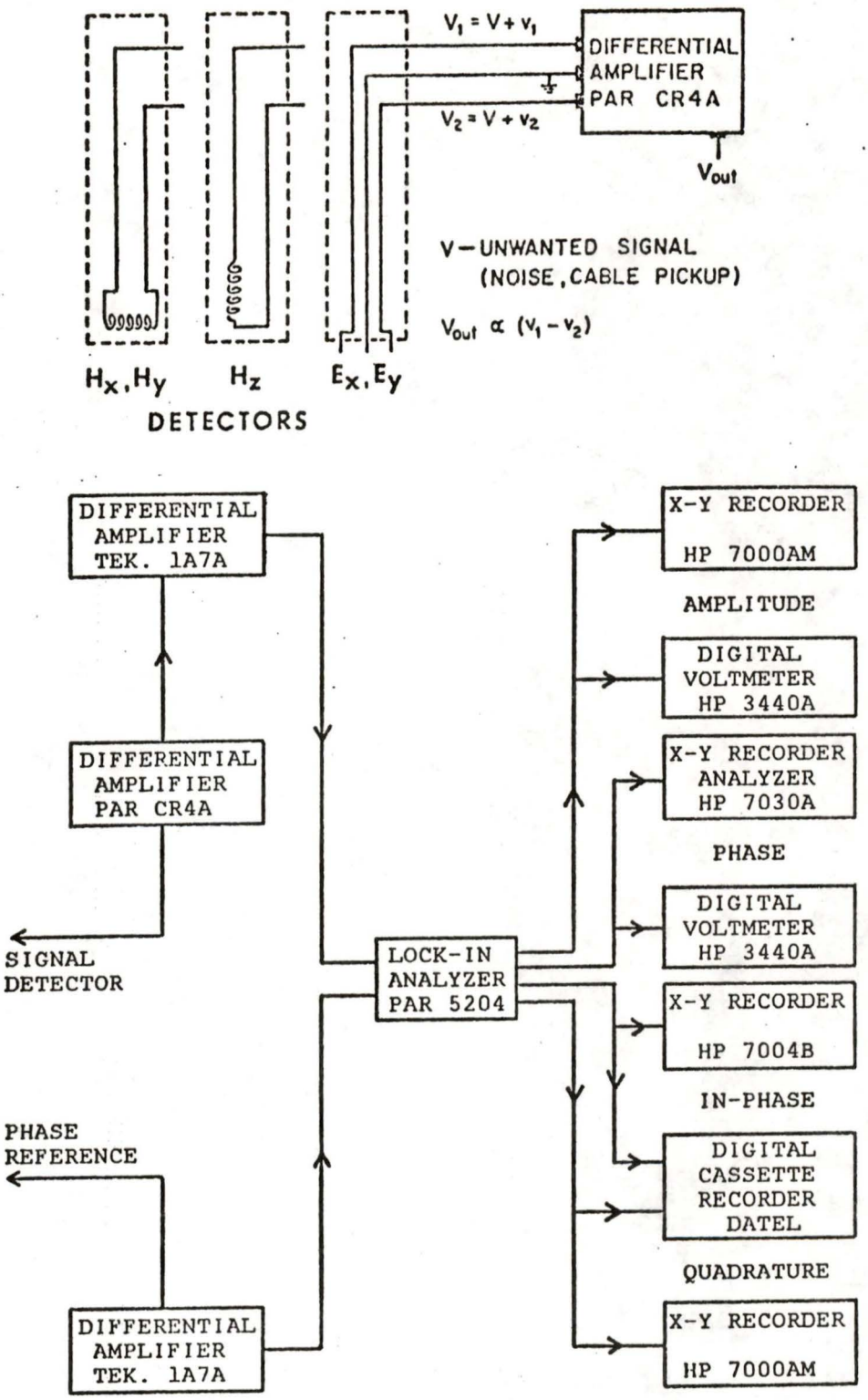

Fig. 2. The field detectors and measurement instrumentation.

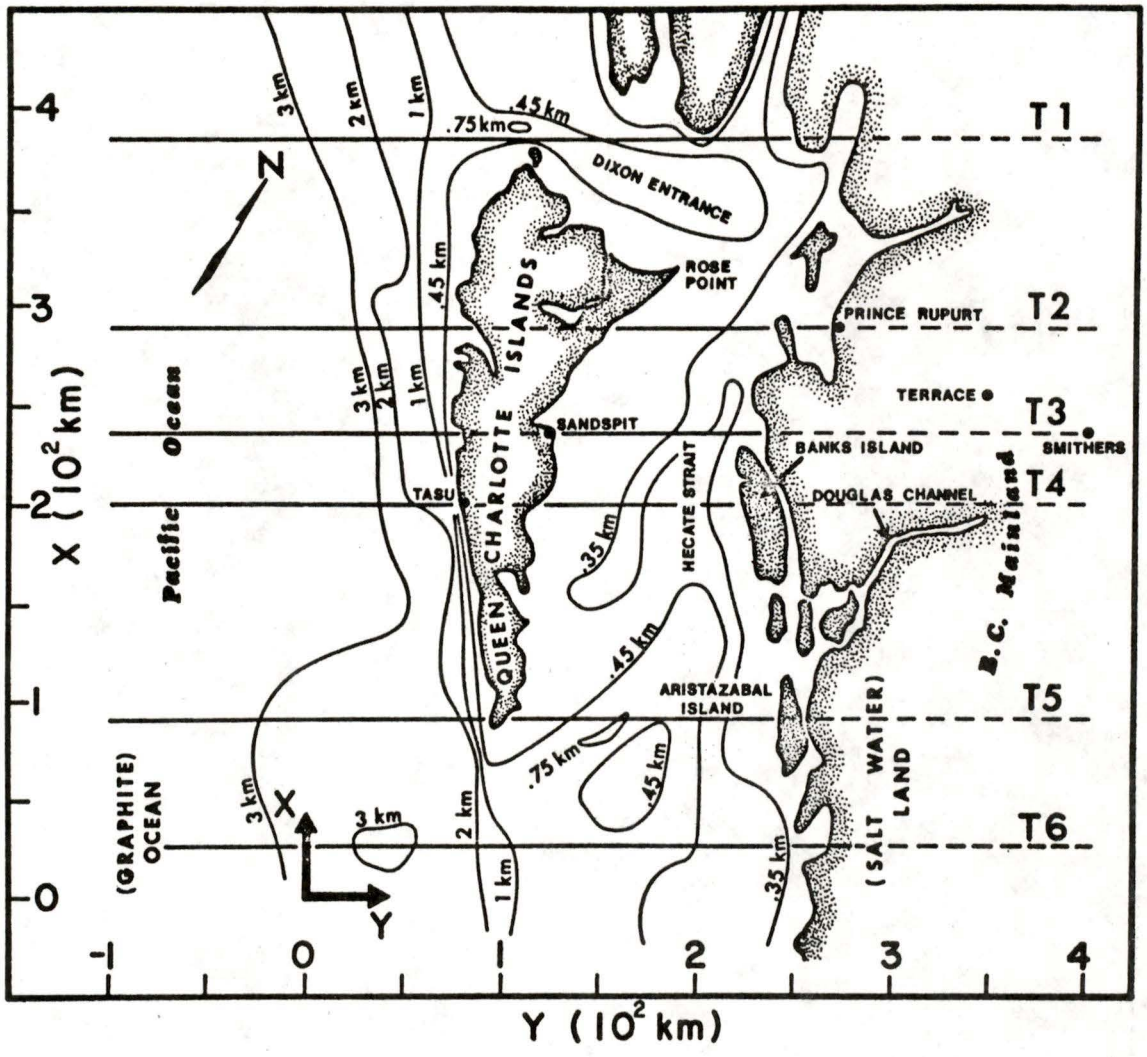

Fig. 3. Simplified map of the Queen Charlotte Islands region with bathymetric contours and locations of the model traverses.

cut in the graphite plate represents the Queen Charlotte Islands. One edge of the plate is shaped to represent the continental coastline. The shallow sea region, Hecate Strait, is underlain by the Queen Charlotte Basin consisting of Mesozoic sediments with comparatively high electrical conductivity. The model includes the effect of this uniform layer of sediments 1 km thick, with conductivity approximately 1/5 that of sea water, by increasing the model ocean depth appropriately in this area. The deep ocean is simulated by a graphite plate .7 cm thick. For the shallow regions, the graphite plate was machined to simulate the ocean depths shown in Fig. 3. A graphite plate 1 m square and 1.5 cm thick was mounted at varying depths of 20, 40 and 60 cm below the surface of the Queen Charlotte Islands graphite model to simulate depths of 100, 200 and 300 km to the high conductive layer of the earth's mantle. For E-Polarization measurements, the north and south ends of the Queen Charlotte Islands model were electrically connected to the stainless steel wall to minimizes the effects due to the limited size of the graphite model.

Chapter 3

LABORATORY ANALOGUE MODEL RESULTS

The electromagnetic response of the scaled laboratory model of the Queen Charlotte Islands region is studied for two polarizations of the source field. For the E-Polarization, the electric field of the inducing source is in the model x-direction, while for the H-Polarization, the electric field of the source is in the y-direction. Thus for the E-Polarization, the electric field of the source is roughly parallel to the continental margin and the west coast of the Queen Charlotte Islands.

In the discussion of results, the magnetic field components are denoted by H_x, H_y, H_z and the associated phase angles by Φ_x, Φ_y, Φ_z, while the horizontal electric field components are denoted by E_x and E_y and the corresponding phase angles by Ψ_x and Ψ_y. The phase angles are angles of phase lead relative to the phase angle of the "reference" H_y field at the surface of the salt solution in the absence of the model structure. The source field was held constant for all measurements by monitoring the H_y reference at a point some distance from the model in the tank. Thus, all components were measured and normalized relative to an H_y reference value at a single geographical

location.

Measurements of amplitude and phase as well as in-phase and quadrature components of the electric and magnetic fields were carried out for 84 traverses over the model. The location of the six traverses selected for discussing the amplitudes and phases of the field components are shown in Fig. 3. Dashed lines are used to show measurements over land and solid lines are used for measurements over sea.

3.1 Analogue Model Reference Fields

To examine the uniformity of the inducing field, measurements of the amplitudes and phases of the electric and magnetic field components were carried out over the concentrated salt solution in the absence of the graphite model. These measurements will be referred as the reference fields. The amplitudes and phase angles of the reference electric and magnetic fields for a traverse along $x = 0$ for the 4 min. period variations are shown in Fig. 4. The results in Fig. 4 show that the reference fields are mainly horizontal, with the electric field parallel to, and the magnetic field perpendicular to, the electric field of the inducing source. Both the amplitude and phase for each field component change little along the traverse.

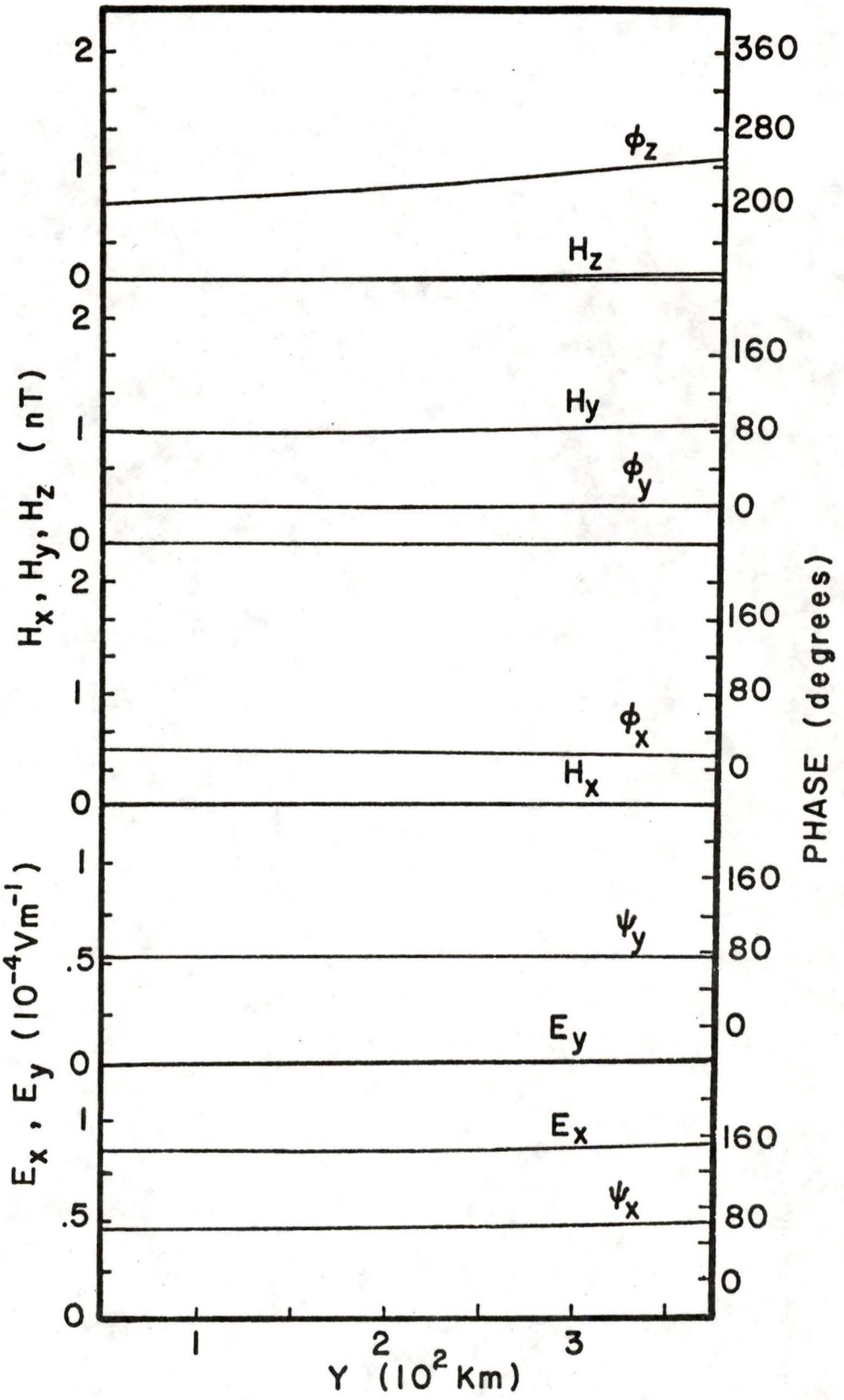

Fig. 4. Amplitudes and phases of the model reference electric and magnetic field components for a traverse along x = 0.

3.2 Model Field Amplitudes and Phases for E-Polarization of the Source Field

Analogue model measurements of the magnetic and electric field components, for a conductor within the mantle at a depth of 100 km, with a simulated 4 min. period variations for E-Polarization are shown in Fig. 5. As expected, the vertical magnetic field H_z is sharply enhanced at all sea-land interfaces as well as having maxima directly over the 2 km bathymetry contour where the ocean depth is changing rapidly off the west coast of the Queen Charlotte Islands. H_z is more enhanced, in general, over the continental coastline than over the island's eastern coastline. The weaker enhancement at the island coastline could be largely accounted for by the effect of channelled current in Hecate Strait partly cancelled by the long range effect of induced currents in the deep ocean. H_z has very sharp gradients over the Queen Charlotte Islands as shown by traverses T2 to T4. However H_z still responds to the coast even at the central region of the island. Along traverse T3, near the central region of the Queen Charlotte Islands (about 25 km from the coast), H_z continues to show values approximately 25% of those observed at the western coastline. Traverse T6 provides an example of reduced coast effect for H_z. The maximum in the coastal H_z enhancement is shifted seaward from the

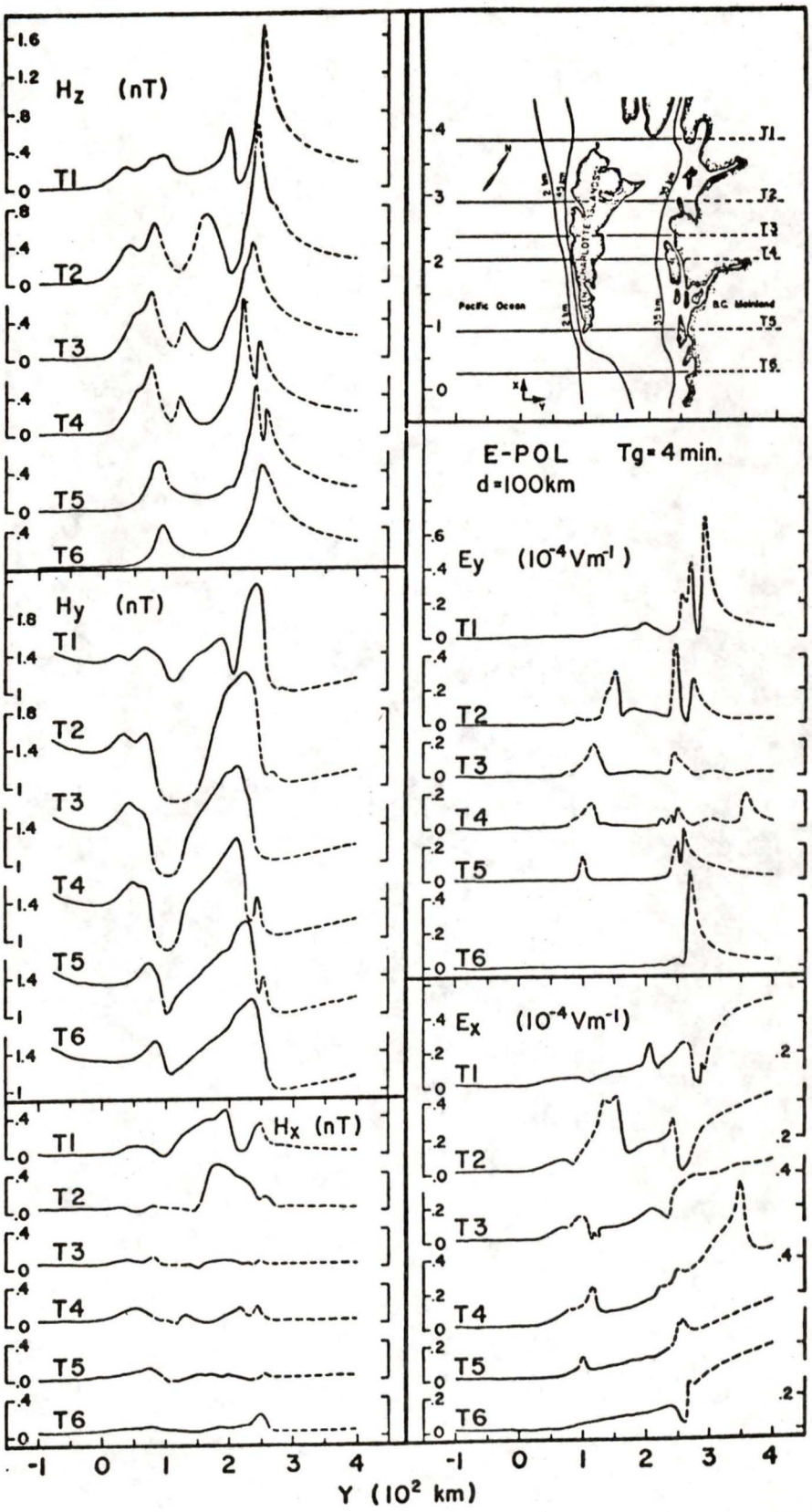

Fig. 5. Amplitudes of the field components for traverses over the Queen Charlotte Islands model for a 4 min. period for E-Polarization.

coastline, as is expected for a traverse through the central region of a bay (Chan et al. 1981a).

H_y is enhanced over the highly conducting ocean and shows large anomalies due to conductive channelling through Hecate Strait, the shallow sea between the Queen Charlotte Islands and the mainland. Local induction is expected to be less important than channelling here since the shallow sea is only of the order of 0.1 skin depth. H_y shows greater enhancement over the Rose Point area along T2, than over the channel along T5, indicating that the density of channelled current is greater at Rose Point due to deflection of current by the coastline. For traverses T2 to T4, H_y has broad minima over the island with sharp gradients towards the coastal regions. H_x, which responds to current deflected at some angle to the inducing field, shows no enhancement over the island. H_x for T6 shows an appreciable enhancement at the continental coastline due to the bay-shaped coastline. The same effects can be observed along the east coast of the Queen Charlotte Islands for both T3 and T4 as both of the traverses pass through a bay.

Channelling of current is observed in the Banks Island region (T4 in Fig. 5). Traverse T4, intersecting Banks Island, shows a sharp H_z maximum and minimum at either side of the island and a maximum at the mainland coast. Traverse T5, intersecting Aristazabal Island, shows similar features at the coasts of the island and mainland. In each

case the H_z minimum is situated at the islands' east coast where the H_z field due to current in Hecate Strait opposes that due to current in the channel between the island and the mainland. Since T5 crosses the narrow restriction in the channel, there is some diffusion of current to the left and right of the channel as indicated by the two E_y enhancements. H_x, which is associated with E_y, also shows a small enhancement here. In the traverse T4 region, the channel is approximately 30° relative to the electric field of the source, and currents are deflected to produce the E_y anomaly. A corresponding H_x enhancement is observed for this traverse. This demonstrates that the geometry of the electrical conductor in this region affects the direction of current flow.

The horizontal electric field E_x, in Fig. 5, is sharply enhanced at locations where the coastline is approximately perpendicular to E_x, for example, on the east coast of the Queen Charlotte Islands for T2. Traverse T4, shows a large E_x enhancement just north of Douglas Channel. The E_y component is enhanced near the ocean inlets. This indicates that telluric current in the ocean is channelled into the inlets and spreads out into the more resistive land. E_y has a maximum at each coastline crossing. These enhancements are due to diffusion of current into the land at the coastline. Both E_x and E_y show significant gradients everywhere over the island with values increasing

from west to east.

H_x, in the shallow sea region of Dixon Entrance for T1, and in Hecate Strait for T2, illustrates current deflection and channelling. H_x should be zero for this polarization unless current is deflected at some angle to the electric field of the source. The deflection and channelling of current indicated by the response of H_x in the shallow sea at Dixon Entrance and Hecate Strait is described further by the behaviour of Φ_x shown in Fig. 6. The phase Φ_x undergoes a 180° change between these two regions. This is due to current deflection around Rose Point.

The phase Φ_z shows a large change in crossing Hecate Strait, resembling the change in phase in crossing a line current. For traverses T2 to T4, Φ_z undergoes a change of approximately 180° in crossing the Queen Charlotte Islands. This is expected for parallel currents on either side of the Queen Charlotte Islands. The phase Ψ_y shows a 180° change across the narrow channel between Banks Island and the mainland and across the channel between Aristazabal Island and the mainland. This indicates E_y is in opposite directions for these locations in the channel. Current diffuses both to the left (into the islands) and to the right (into the mainland). This will affect the magnetotelluric responses in this area. The diffusion of current will lead to an unexpected enhancement in apparent

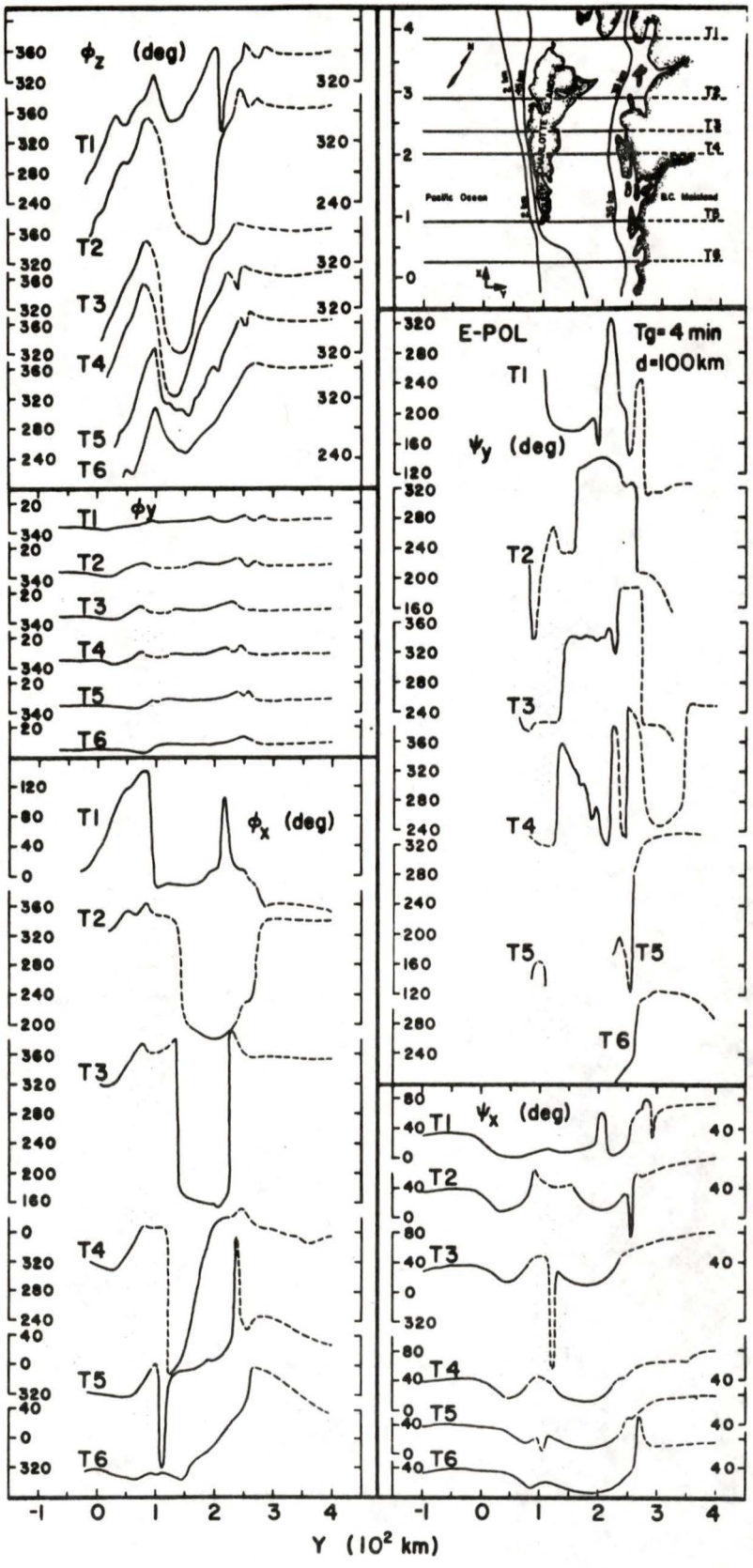

Fig. 6. Phase of field components for traverses over the Queen Charlotte Islands model for a 4 min. period for E-Polarization.

resistivity near the continental and island coastlines with the value decreasing with distance from the coasts.

Electric and magnetic field components for a simulated period of 40 min. are shown in Fig. 7. The electric and magnetic fields show smaller enhancements than for the 4 min. period results in Fig. 5. The H_z enhancements for T4 and T5 over the narrow channel between Banks Island and the mainland, and between Aristazabal Island and the mainland, observed for the 4 min. period are present for the 40 min. period results as well. There is no H_z enhancement over the east coast of the Queen Charlotte Islands, suggesting that current density in the Hecate Strait is greatly reduced. However, H_z increases rapidly in traversing westward and shows a large broad enhancement at the west coast, with amplitudes larger than those for 4 min. period. The H_y field remains enhanced with increasing period off the west coast of the Queen Charlotte Islands, but the enhancements over the shallow Hecate Strait fall off rapidly with increasing period as was the case for H_z.

The general behaviour of the electric fields for 40 min. period variations is very similar to that observed for the 4 min. period but with a much smaller gradient over the island. The E_x enhancements over the Queen Charlotte Islands and the mainland are attenuated with increasing period. This effect is more pronounced over the mainland

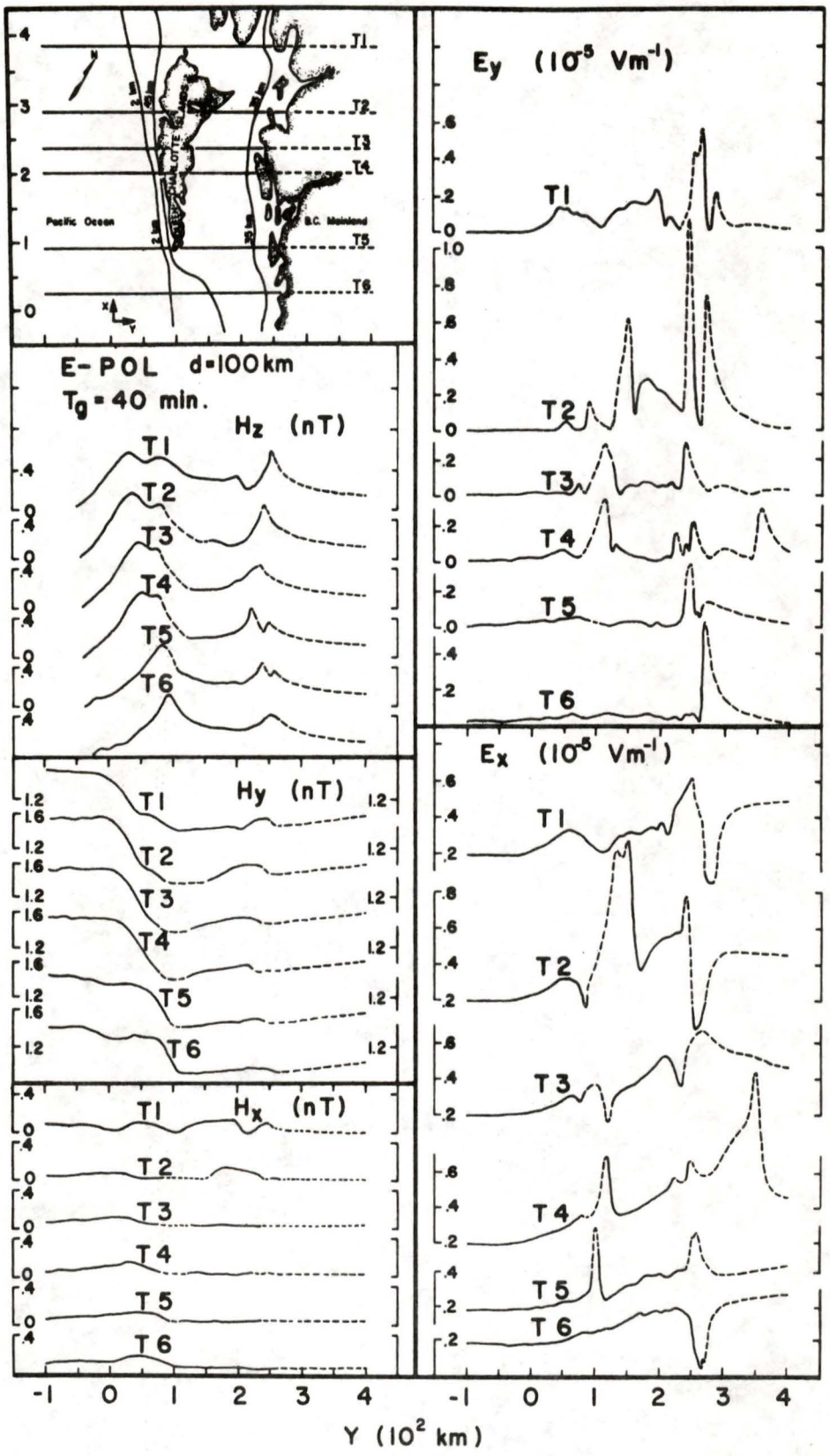

Fig. 7. Amplitudes of the field components for traverses over the Queen Charlotte model for a 40 min. period for E-Polarization.

coastal region than over the Queen Charlotte Islands, indicating less current flow in Hecate Strait for this longer period. H_x still shows enhancements over Dixon Entrance (T1) and Hecate Strait (T2), suggesting some current deflection around Rose Point. From the phase results (shown in the Appendix), Φ_x again shows a phase difference of 180° for these two locations as in the case of the 4 min. period results (Fig. 6). The phase Φ_z undergoes a change of from 60°-100° in crossing Hecate Strait.

Figure 8 shows the field components for a simulated period of 120 min. With increasing period, the magnetic field enhancements are further decreased. Conductive channelling over the narrow channel between Banks Island and the mainland is much diminished as seen in H_z for T4. The H_z enhancement over the continental margin off the west coast of the Queen Charlotte Islands is larger than the enhancements over the island and mainland coastlines. The H_y anomalies over the shallow sea (Hecate Strait) are very small, and H_x shows no enhancement in this region. The E_x response is further decreased for this longer period. With increasing period, the field over the continent decreases rapidly, indicating that the amount of current diffusing into the continent decreases with increasing period.

As the period increases, the magnetic fields fall off rapidly over the shallow Hecate Strait region as expected.

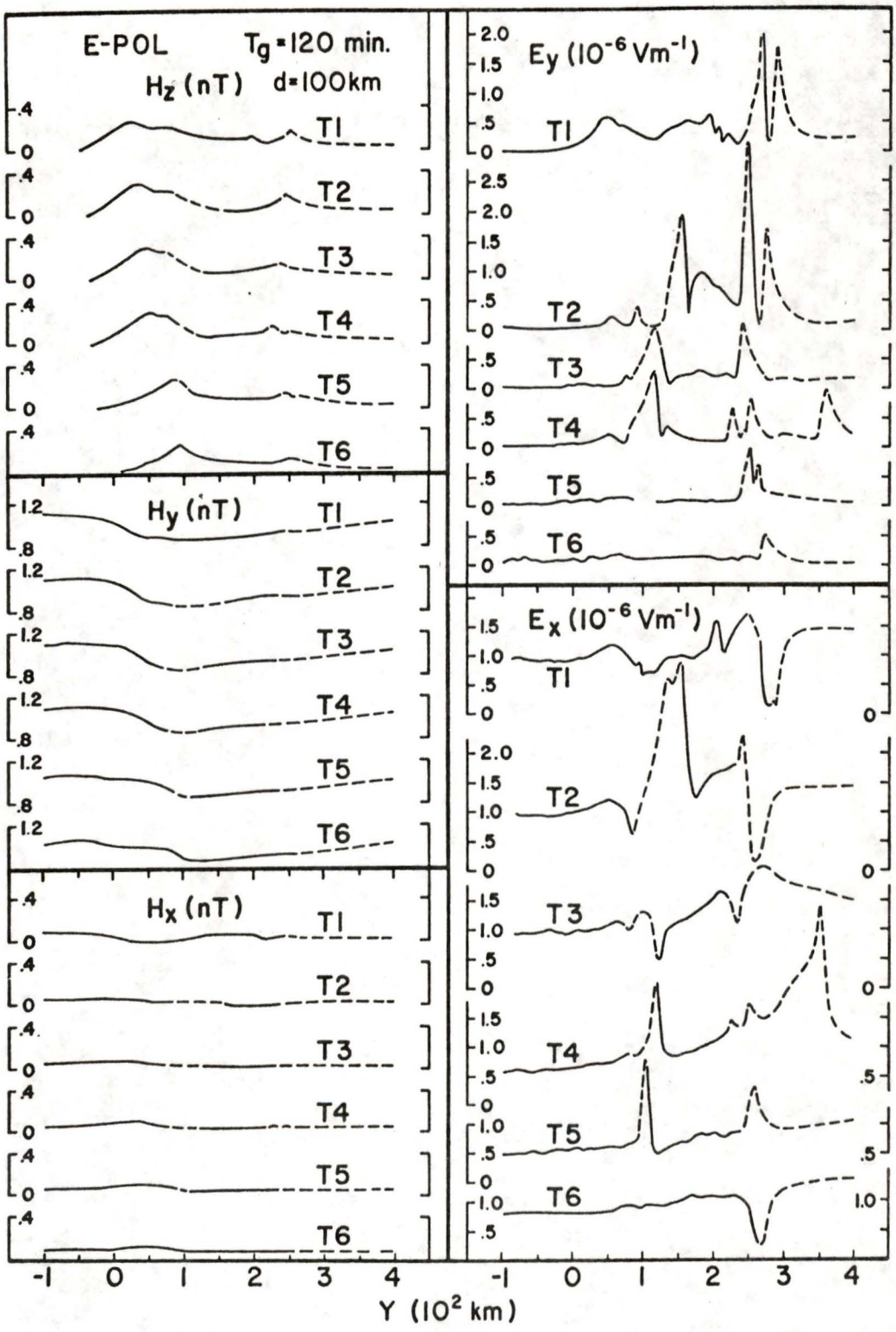

Fig. 8. Amplitudes of the field components for traverses over the Queen Charlotte Islands model for a 120 min. period for E-Polarization.

At the west island coastline, where the bathymetry changes rapidly, both H_z and H_y fields show larger enhancements at 40 min. period than at 4 min. period due to the skin depth effect. Similar behaviour of the magnetic field components, with varying period of the source field, were observed by Dosso et al. (1980) in the study of electromagnetic induction in the British Isles region.

3.3 Model Field Amplitudes and Phases for H-Polarization of the Source Field

The model results for the H-Polarization case (electric field of the inducing source roughly perpendicular to the west coast of Queen Charlotte Islands), for 4 min. period variations are shown in Fig. 9. For this polarization, the traverses are parallel to the electric field of the source, and deflected currents are now associated with E_x and H_y. The magnetic field components show a much smaller response for H-Polarization than for the previous E-Polarization. The large enhancement in H_z near the southern end (T5) of the Queen Charlotte Islands and the low broad maximum in H_z near the northern end (T1) indicate current concentrations in these regions, with current deflected around the northern and southern ends into Hecate Strait. The two maxima in H_y for T1 and T5 at these locations further indicate that current is deflected around the ends of the island and into the

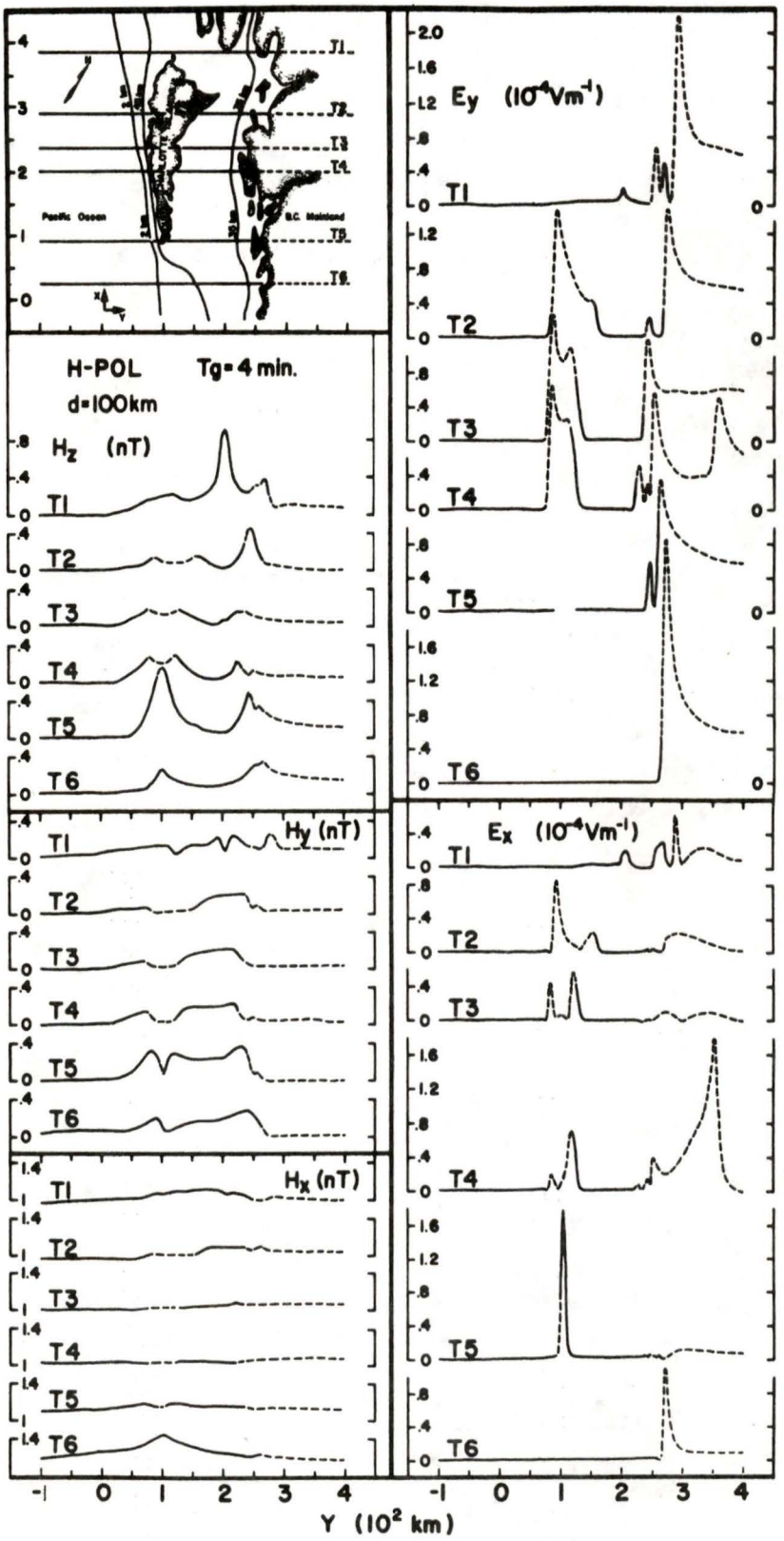

Fig. 9. Amplitudes of the field components for traverses over the Queen Charlotte Islands model for a 4 min. period for H-Polarization.

shallow sea. As a result of deflected current, H_y is enhanced in the Hecate Strait region, from where the channelled current diffuses into the mainland. H_y and H_z show very small gradients over the Queen Charlotte Islands, but show some response to the coastline. For both components, the field gradient increases as the width of the island decreases. H_y has approximately the same value over the Queen Charlotte Islands as over the continent.

E_x, for H-Polarization, is related to current channelling or deflection by the coastline. This is demonstrated by the anomalies along traverse T1 in Fig. 9, where an enhancement is seen in the vicinity of each channel or inlet near the continental coastline. The E_x enhancements on the west coast of the Queen Charlotte Islands decrease in going from T2 to T4. Traverse T2 passes through the mouth of a bay and has a large enhancement there, as the result of increased current density due to the effects of the bay for this polarization. Traverses T3 also passes through a bay, but of smaller dimension, thus leading to a smaller E_x anomaly than for T2. Traverse T4 crosses the west coast of the island in a region where the coastline is straight but has a small angle relative to the inducing field, leading to a small enhancement in E_x. The E_x enhancements on the east coast of the Queen Charlotte Islands increase in going from T2 to T4. This can be attributed to the effects of the

wedge shaped east coast. Current in this region of Hecate Strait is mainly provided by current flow around the southern tip of the Queen Charlotte Islands, and the current density in the Strait decreases with distance from the southern tip. This is also supported by the behaviour of the E_y enhancements in this region, increasing in going from T2 to T4. E_y has very sharp enhancements at all coastlines as expected for this polarization, responding to the large current concentration in the shallow ocean. E_y increases in traversing from the east to the west coast over the island. E_x and E_y both show very large gradients over the Queen Charlotte Islands (larger than the gradient for the E-Polarization case, since the induced current is roughly perpendicular to the west coast of the island for H-Polarization). For traverse T4, E_x and E_y both show substantial enhancements near the long narrow inlet (Douglas Channel), indicating high current density there. Traverses T4 and T5 show E_x and E_y enhancements near Banks Island and Aristazabal Island. H_z and H_y also have enhancements at these locations. This indicates that current channelling in the very narrow ocean channels is important for the H-Polarization as well. Traverse T6, shows an extremely large E_y enhancement over the bay shaped continental coastline, in agreement with the augmented enhancement at a bay observed by Chan et al. (1981a).

The phase results for the 4 min. period variations for the H-Polarization case are shown in Fig. 10. As in the case of E-Polarization, Φ_z changes by approximately 180° in crossing Hecate Strait. The phase Φ_z has approximately the same value on the east and west coasts of the Queen Charlotte Islands, indicating that the x-components of the currents on the two sides are in opposite directions as required for current deflected around the northern and southern ends and into Hecate Strait. The phase Ψ_x along T2 undergoes a change of approximately 180° across the Queen Charlotte Islands. Current diffuses into the land northward at the west coast and simultaneously southward at the east coast, accounting for the phase change in traversing the island. For traverse T4, Ψ_x shows a similar response. For Traverse T3, Ψ_x has the same value at both coastlines since the two coastlines are approximately parallel (see Fig. 3 for coastline shape).

Model results for a simulated 40 min. period variation for H-Polarization are shown in Fig. 11. As for the case of E-Polarization, the enhancements decrease rapidly with increasing period. In fact, except for the H_z enhancement near the northern tip of Queen Charlotte Islands, no noticable magnetic field enhancement is observed. The general behaviour of E_x and E_y is very similar to that observed for the 4 min. period, but the enhancements are diminished.

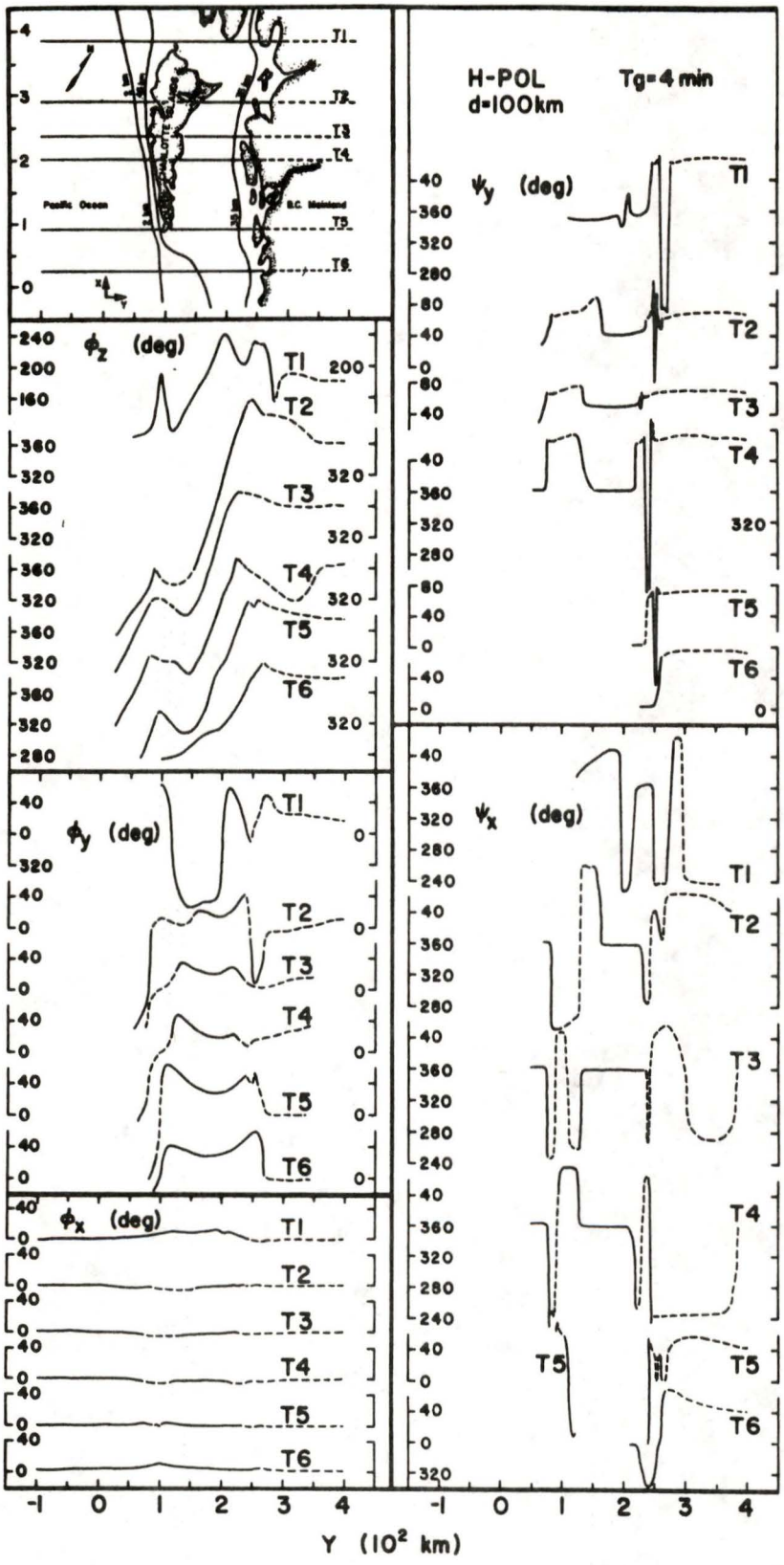

Fig. 10. Phase of field components for traverses over the Queen Charlotte Islands model for a 4 min. period for H-Polarization.

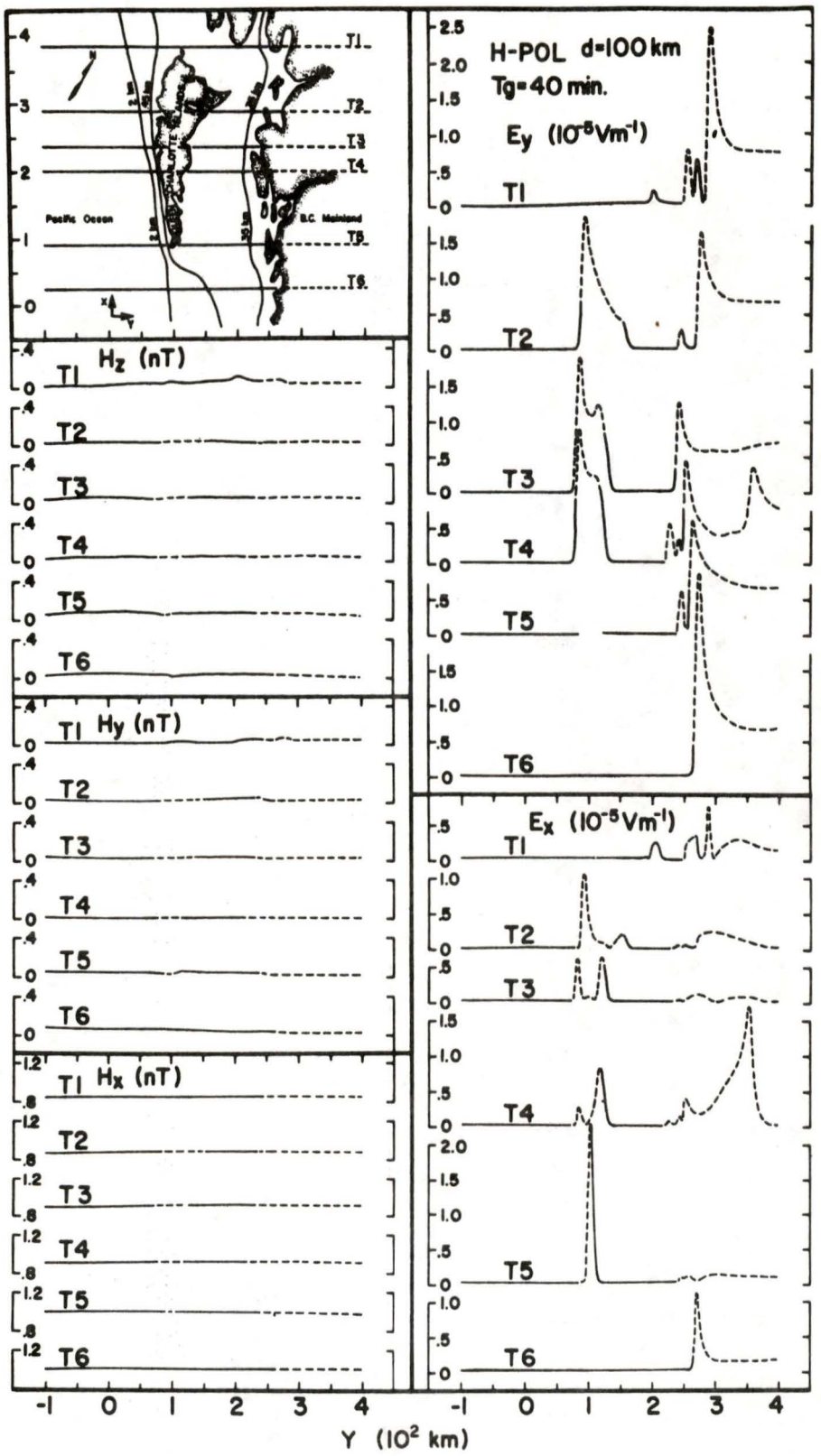

Fig. 11. Amplitudes of the field components for traverses over the Queen Charlotte Islands model for a 40 min. period for H-Polarization.

3.4 Model In-phase and Quadrature Results for E-Polarization

For the 4 min. period variations, contour diagrams and three-dimensional diagrams of the analogue model field components were produced using digital data for 81 equally spaced (1 cm spacing in the model) traverses in the y-direction. The 81 traverses covered the simulated 400 km coastal region (x = 0 to 400 km) shown in Fig. 12. For the 40 min. variations, only 21 traverses (4 cm spacing on the model) were used since the field gradients are smaller than for the shorter periods. In the digital recording, two hundred or more points with .5 cm, or less, separation were sampled along each traverse. The computer plotting routine used to produce contour diagrams of the analogue model fields was the one used earlier by Nienaber et al. (1981) for the British Isles model. The present work deals only with the results for E-Polarization, for which the electric field of the inducing source field is roughly parallel to the continental shelf and the west coast of the Queen Charlotte Islands.

Each figure showing field contours contains four diagrams. The upper diagrams show the contours for a large contour interval (for example, 0.1 nT for H_z), while the lower diagrams show the same results but with a much smaller contour interval (either 1/4 or 1/8 that of the

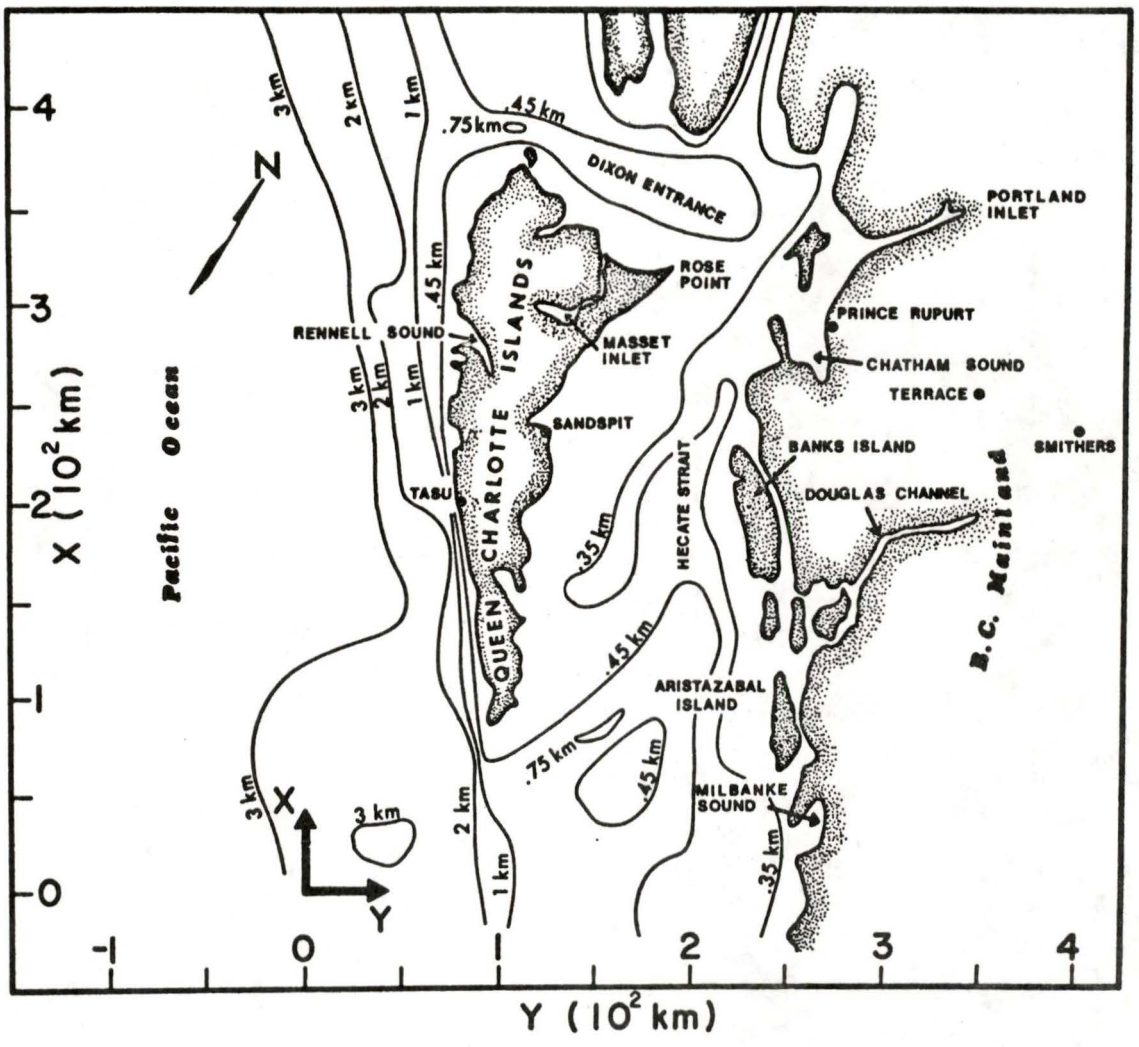

Fig. 12. Simplified map of the Queen Charlotte Islands region.

upper diagrams). The increased contour density in the lower diagrams tends to provide a rather striking detailed view of the field response to the various coastline features. Thick lines are used to delineate the coastlines only in the upper diagrams of each figure. The field contours in the upper diagrams are labelled in units of nT for magnetic fields and in units of Vm^{-1} for electric fields. The corresponding three-dimensional field diagram that follows each figure giving the field contours is particularly helpful in showing whether the field is increasing or decreasing at a given location. (Note that the z-axis scale for the three-dimensional diagrams varies from one diagram to another). All field components were normalized with respect to H_y. This was achieved by setting H_y quadrature to zero and H_y in-phase to 1 nT as reference values at a point over land far from the coast. The succeeding measurements for all components were carried out with these instrument settings.

Figure 13 shows the H_z contours for simulated 4 min. period variations. H_z in-phase increases gradually from a small value over the mainland to a maximum at the continental coastline. The field values then decrease in crossing Hecate Strait to reach some negative value at the eastern coastline of the Queen Charlotte Islands. A very large negative value is observed at Rose Point as shown by the dense concentric contours. The field values increase

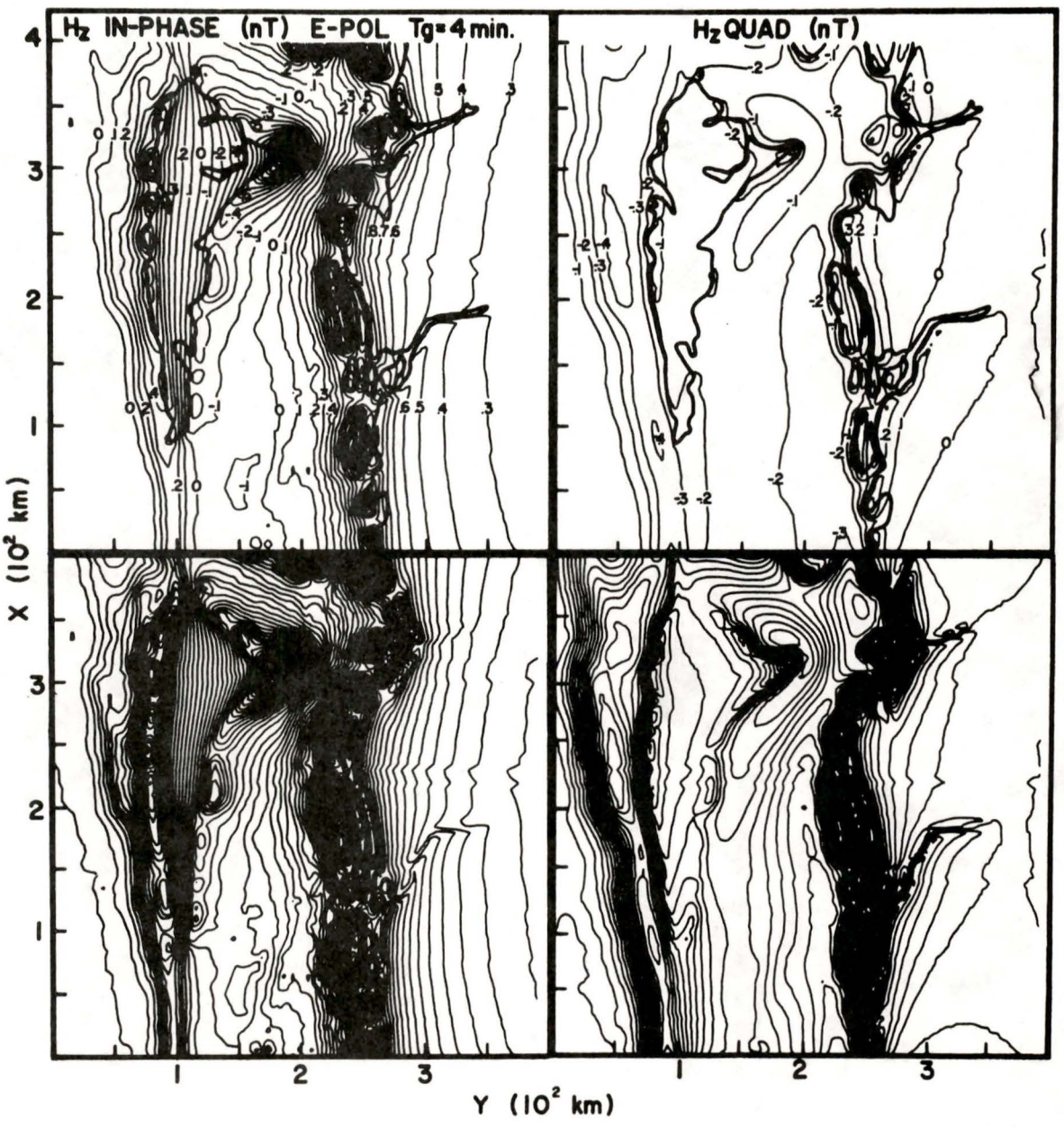

Fig. 13. Contours of the model in-phase and quadrature H_z for 4 min. period.

from east to west over the island, reaching maxima over the western island coastline. The field values then decrease over the continental margin and approach zero over the deep ocean. The sign change of the in-phase H_z, in crossing Hecate Strait, is expected due to the channelled current in the Strait resembling a line current. The large in-phase H_z observed at Rose Point indicates a large current density in this region due to current deflection at the cape-shaped coastline. The H_z quadrature shows anomalies off the western island coastline and the continental coastline. A fairly large anomaly is observed at Rose Point.

The dense in-phase H_z contours in the lower diagrams tend to delineate the shape of the island and the irregular continental coastline. This results from the large enhancements right at the coastline with the field falling off rapidly towards the central regions of the island and also seaward from the coastlines. Along the western island coastline, a series of circular contours, similar but of smaller gradient than that at Rose Point, are observed over the capes, resulting from enhanced current densities in these areas. From the dense contour plots, it is seen that both the in-phase and quadrature H_z fields show a sensitive response to the long narrow Douglas Channel, as induced current channelled into Hecate Strait is also funnelled into Douglas Channel.

The 4 min. period in-phase and quadrature H_z three-dimensional diagrams are shown in Fig. 14. All anomalies at the eastern island coastlines are negative, consistent with a phase reversal in crossing Hecate Strait. The effect of Douglas Channel is observed for both H_z in-phase and H_z quadrature.

Figure 15 provides the H_y contours for a simulated 4 min. period. H_y in-phase has values of roughly 1 nT, and H_y quadrature is approximately zero, as established by the normalization procedure, for points over land far from the mainland coastline. H_y in-phase shows anomalies seaward of all coastlines with a large maximum near Rose Point. H_y quadrature has small values in the shallow Hecate Strait and decreases to large negative values in the deep ocean. The contour lines for H_y in-phase follow the coastlines very closely and thus delineate the shape of the island. The contours are very closely spaced over the ocean, and show large gradients near all coastlines. The widely spaced contours over the mainland and the island indicate that H_y in-phase is fairly constant over land. The dense contour H_y quadrature diagram shows a large gradient along the western island coastline and the continental coastline. A substantial anomaly is observed near Rose Point in response to the deflected and channelled current. The effect of the ocean inlets is observed in both H_y in-phase and H_y quadrature with the H_y quadrature showing a

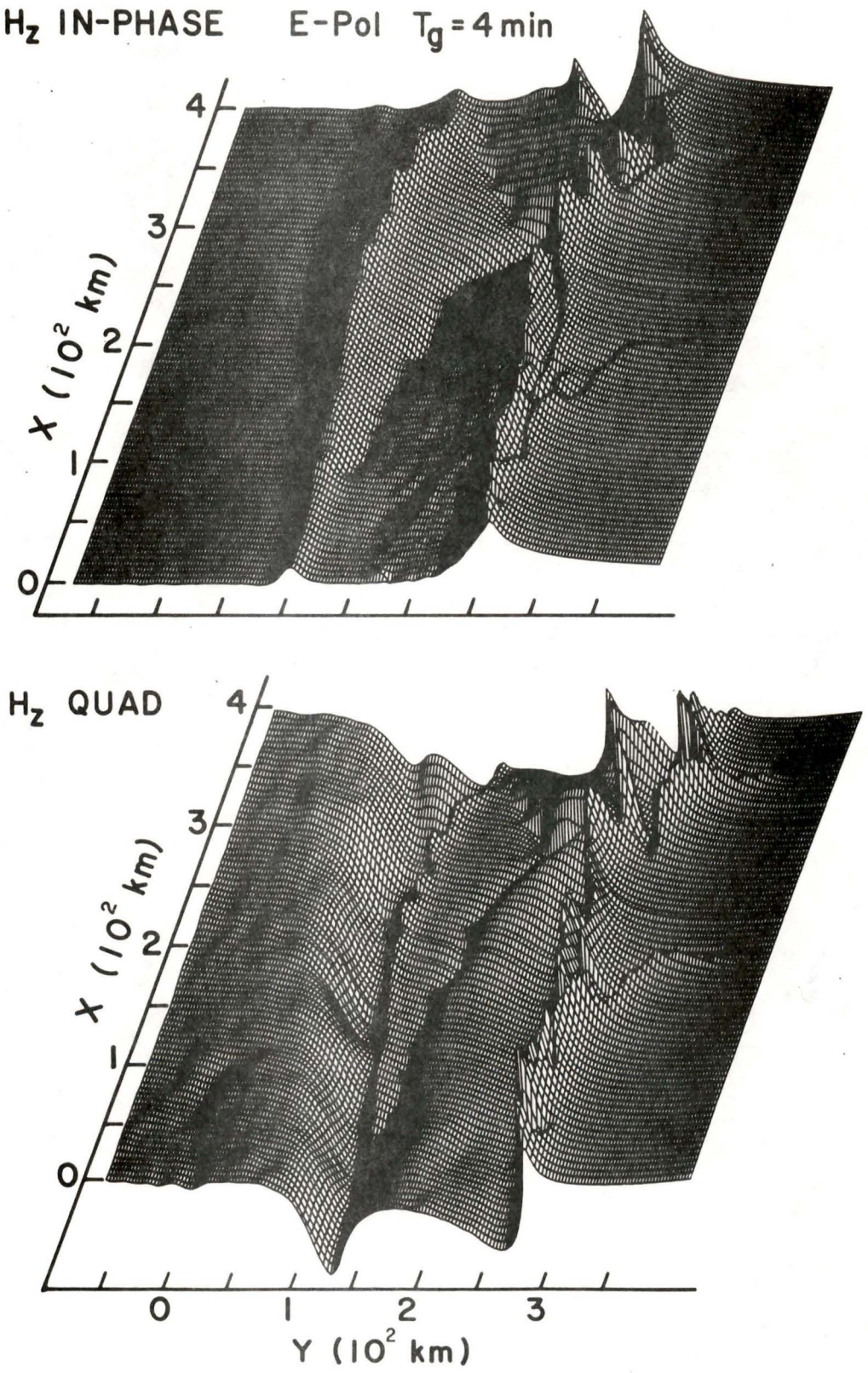

Fig. 14. Three-dimensional diagram of the model in-phase and quadrature H_z for 4 min. period.

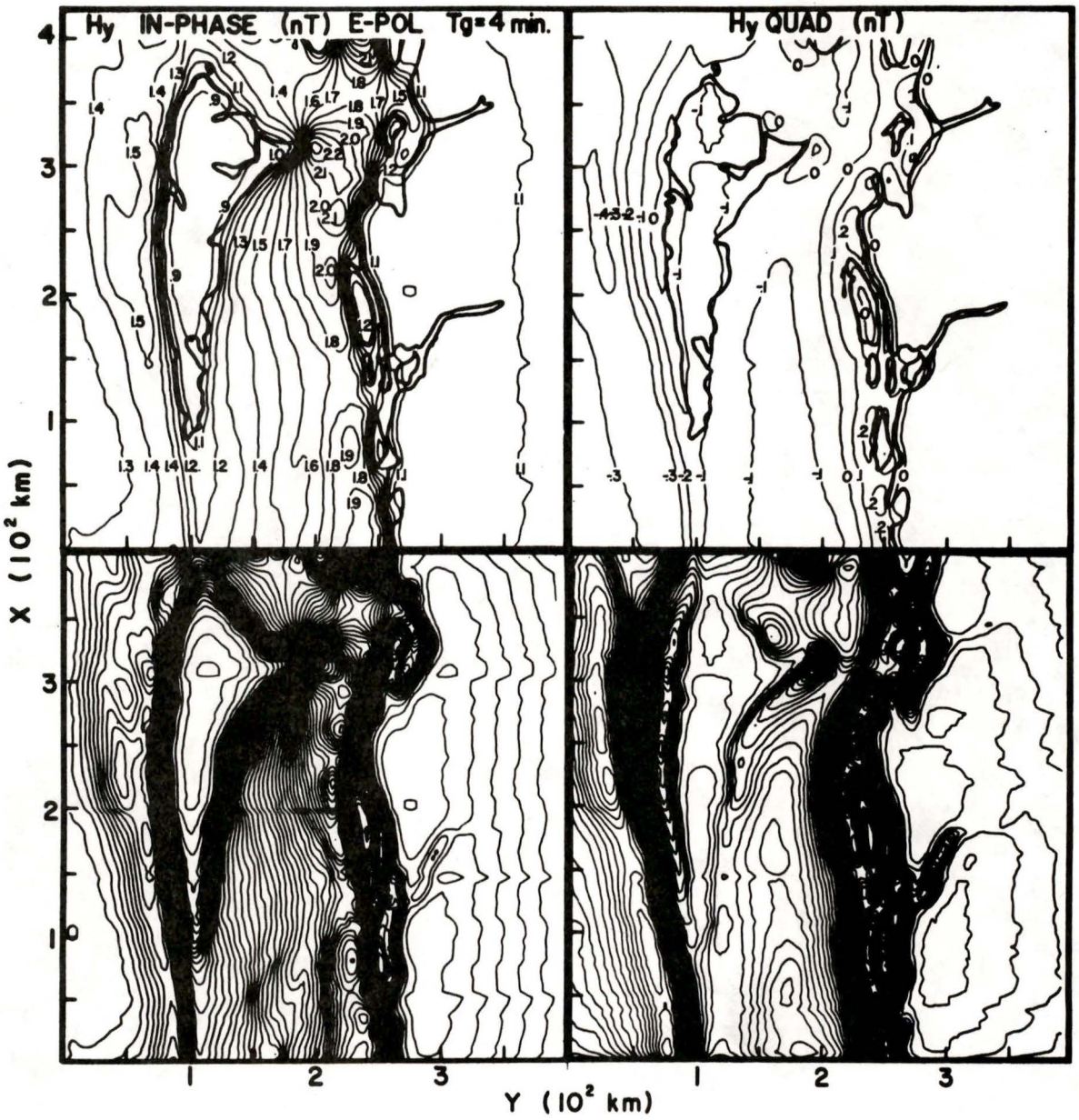

Fig. 15. Contours of the model in-phase and quadrature H_y for 4 min. period.

particularly strong response. Anomalies are observed for both the in-phase and quadrature over the continental shelf region where the ocean depth changes very rapidly.

Figure 16 provides the H_y three-dimensional diagrams for the 4 min. period. Both H_y in-phase and H_y quadrature show minima over the Queen Charlotte Islands and positive enhancements over the island and continental coastlines. H_y quadrature has a fairly large enhancement at Rose Point. Small enhancements are observed along the western island coastline near capes. Enhancements for both H_y in-phase and H_y quadrature over Douglas Channel are clearly observed.

Figure 17 shows the H_x contours for a simulated 4 min. period. Both the H_x in-phase and H_x quadrature over land and sea some distance from the coastlines are approximately zero. This is expected since, for E Polarization, H_x is zero except in the neighbourhood of deflected or channelled currents. H_x in-phase has two sets of circular contours near Rose Point, one in Dixon Entrance (positive), and the other in Hecate Strait (negative). The sign change indicates a phase reversal from north to south across Rose Point in agreement with current deflected and channelled around the wedge shaped point as described earlier. The dense contours in the lower diagrams of Fig. 17 show a series of circular contours indicating response to capes and bays along the island coastlines. Both H_x in-phase and

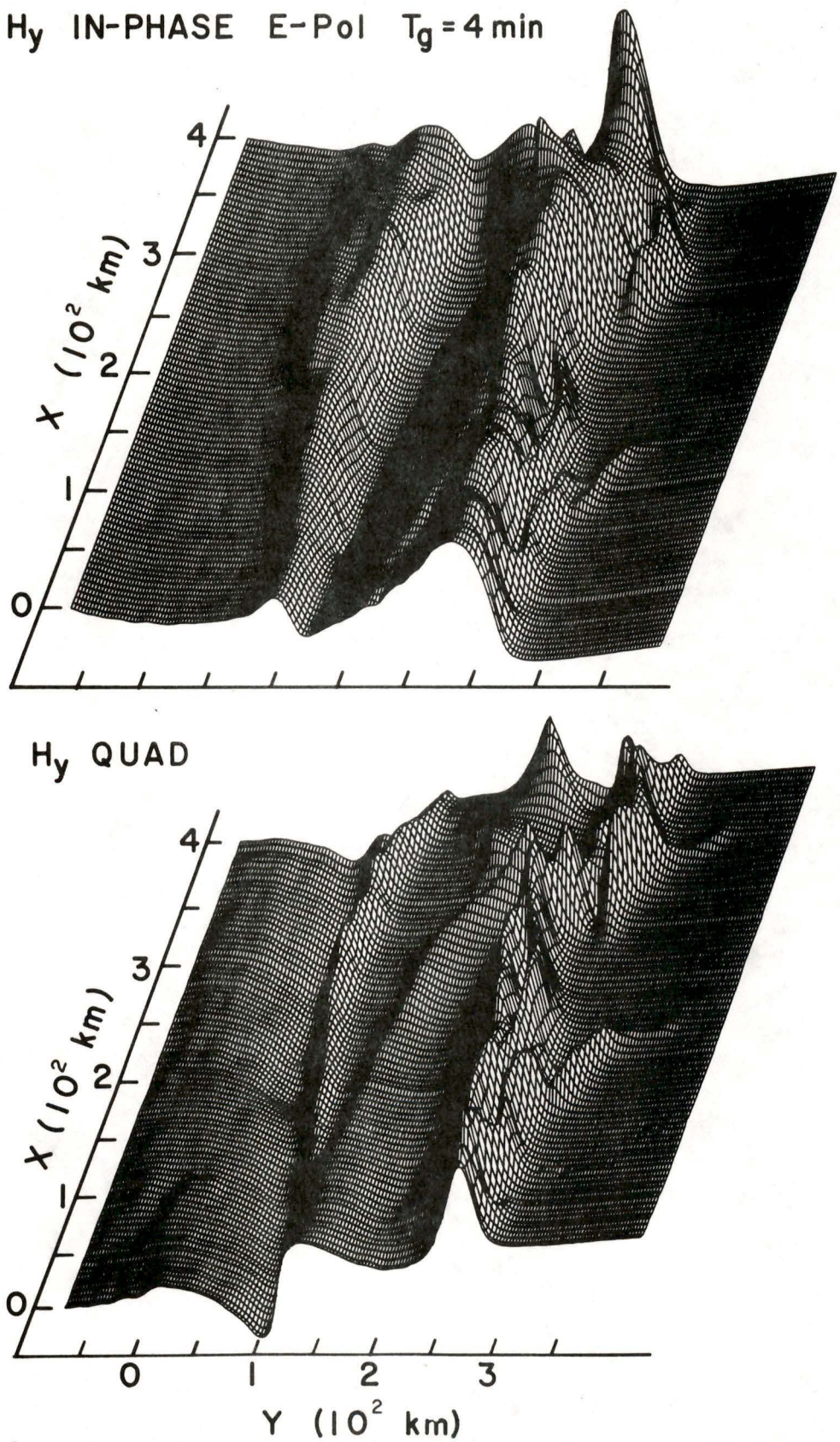

Fig. 16. Three-dimensional diagram of the model in-phase and quadrature H_y for 4 min. period.

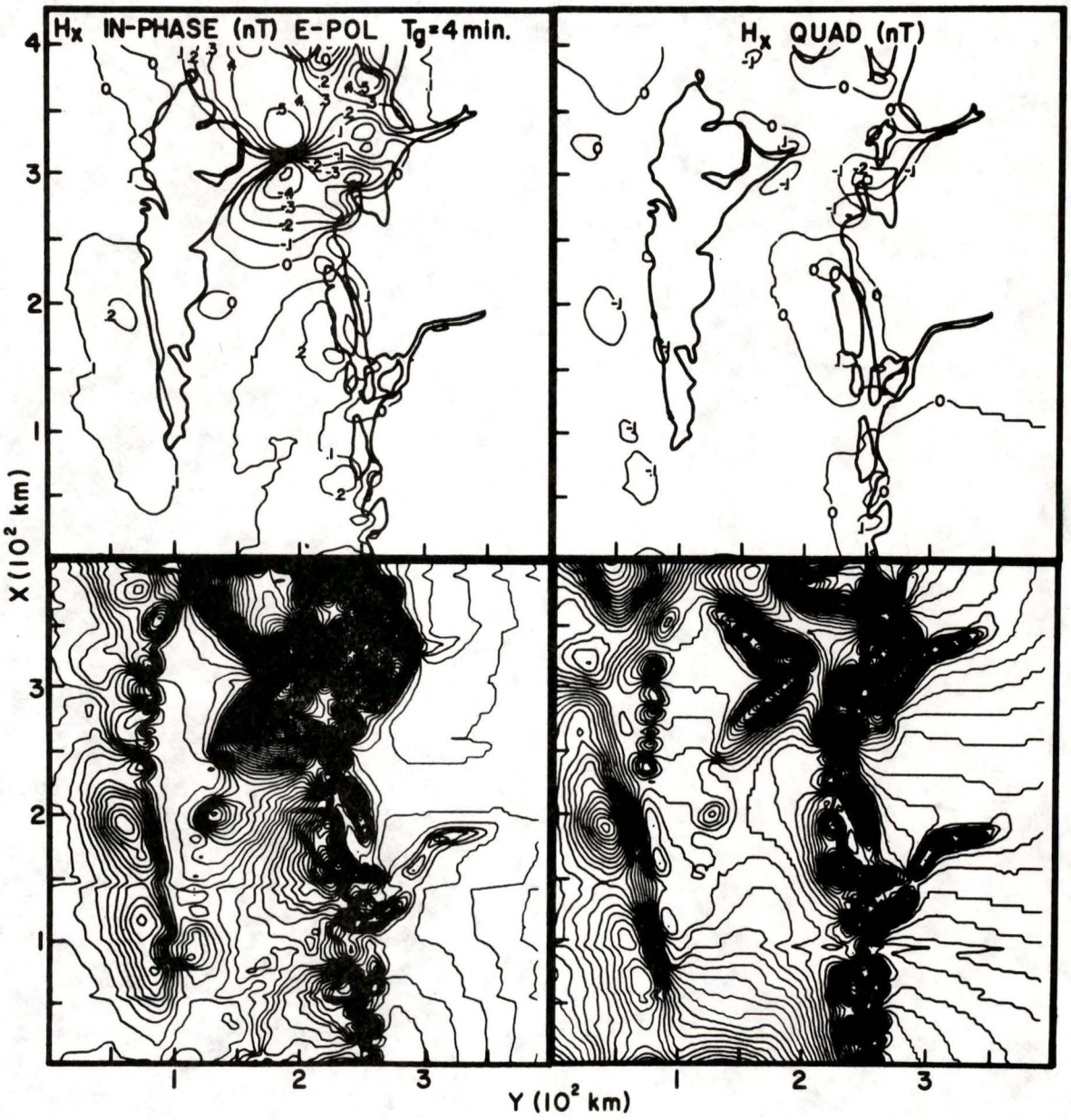

Fig. 17. Contours of the model in-phase and quadrature H_x for 4 min. period.

H_x quadrature respond to current funnelled into Douglas Channel and Portland Inlet, with a particularly sensitive quadrature response.

The H_x three-dimensional diagram for a simulated 4 min. period is shown in Fig. 18. Large enhancements in both H_x in-phase and H_x quadrature are observed between Banks Island and the mainland in response to channelling of currents. Anomalies with negative values are observed over Douglas Channel and Portland Inlet for both H_x in-phase and H_x quadrature. The channelled currents that are funnelled into the ocean inlets flow in the positive y-direction, producing the negative H_x values. Enhancements are observed in the Milbanke Sound region due to the cape-shaped coastline. H_x quadrature shows a rapidly changing field off the southwest coast of the Queen Charlotte Islands, as a result of the rapidly changing bathymetry in that region, leading to a changing density of induced and deflected current.

The E_x contour diagrams for a simulated 4 min. period are shown in Fig. 19. E_x in-phase has small values except near the wedge-shaped Rose Point, where current is deflected, and in the vicinity of Douglas Channel and Portland Inlet where current is funnelled in a direction roughly perpendicular to the electric field of the inducing source field. E_x quadrature shows a similar response as E_x in-phase except over the continent where its value

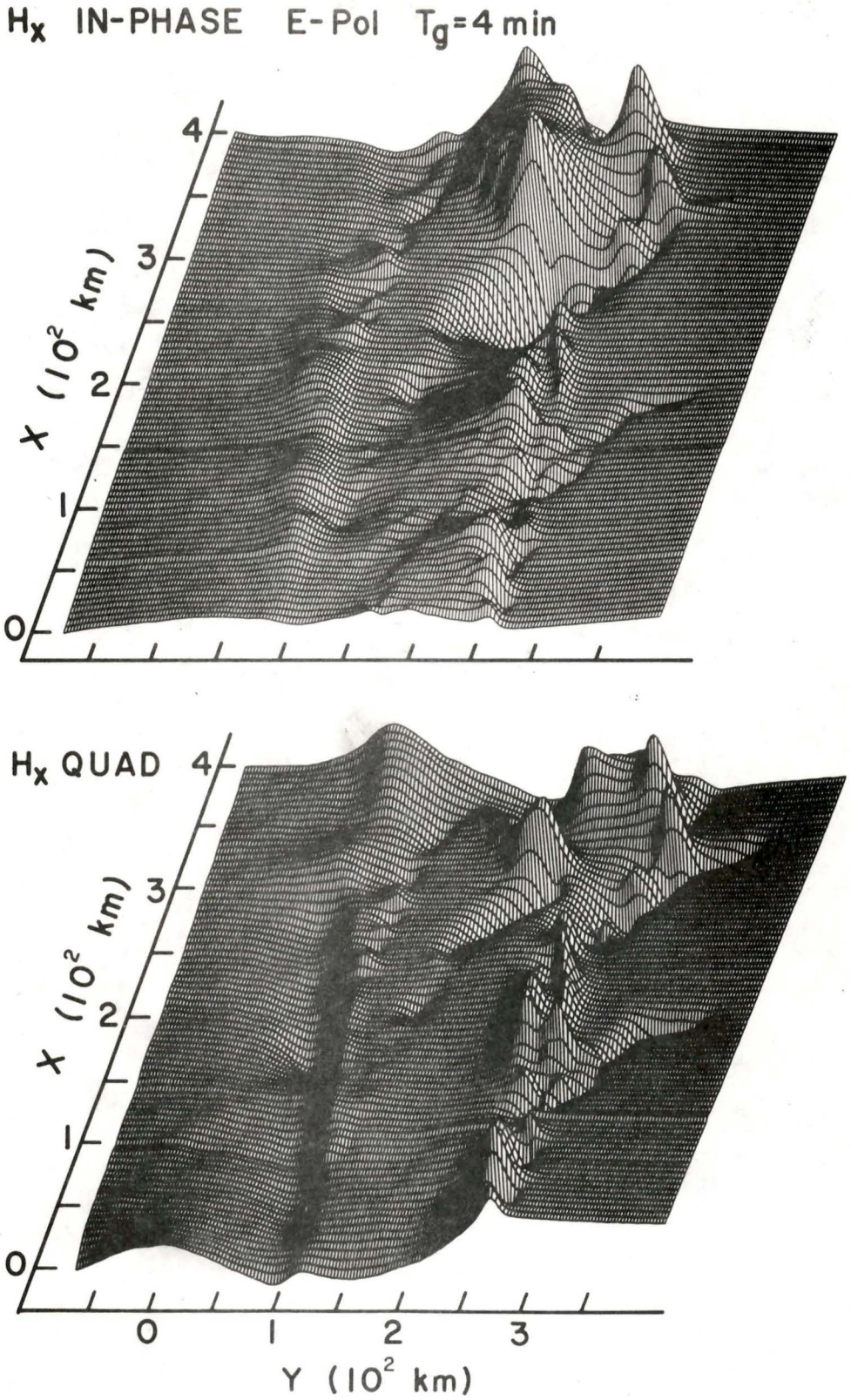

Fig. 18. Three-dimensional diagram of the model in-phase and quadrature H_x for 4 min. period.

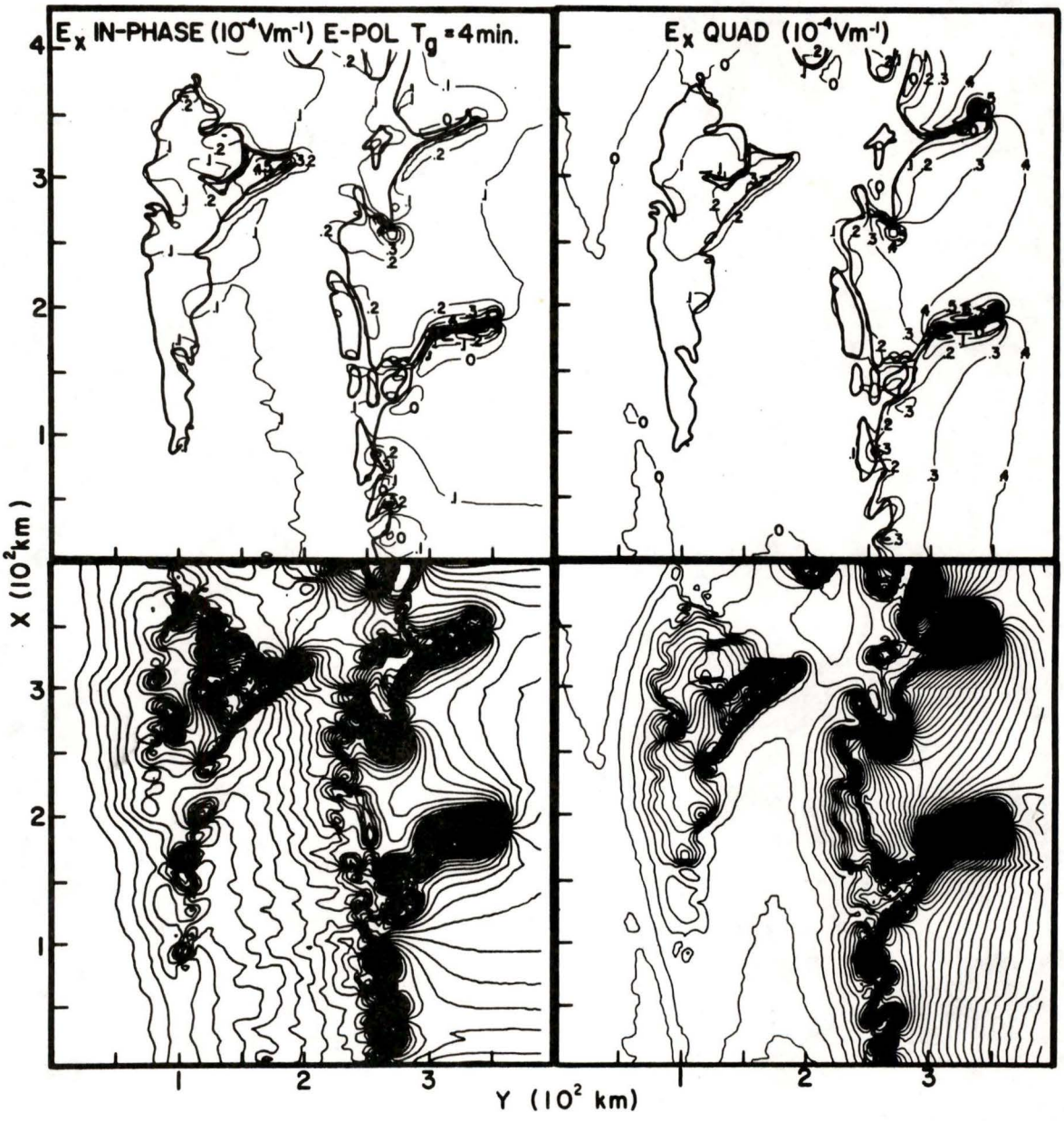

Fig. 19. Contours of the model in-phase and quadrature E_x for 4 min. period.

increases landward. The dense contours for E_x in-phase in the lower diagram show that the effects of capes and bays are important for E_x. This is illustrated by the circular contours along both island coastlines. E_x in-phase shows dense gradients along the coastlines approaching Rose Point, as well as over Douglas Channel and Masset Inlet on the Queen Charlotte Islands. At these locations, the field is at some angle to the coastlines. The dense contours for E_x quadrature also show rapidly changing gradients at the ocean inlets. Enhancements are observed for both E_x in-phase and E_x quadrature at the narrow part of the channel between Aristazabal Island and the mainland due to funnelling of channelled current.

The E_x three-dimensional diagrams are shown in Fig. 20. Enhancements are observed along the eastern island coastline south of Rose Point for both E_x in-phase and E_x quadrature. A sign reversal is observed across the ocean inlets for both E_x in-phase and E_x quadrature. The negative values at these locations suggest that channelled currents that are funnelled into the inlets are diffusing into surrounding land along the length of the inlets. Enhancements are observed landward of Chatham Sound for both E_x in-phase and E_x quadrature, indicating diffusion of telluric currents into this region.

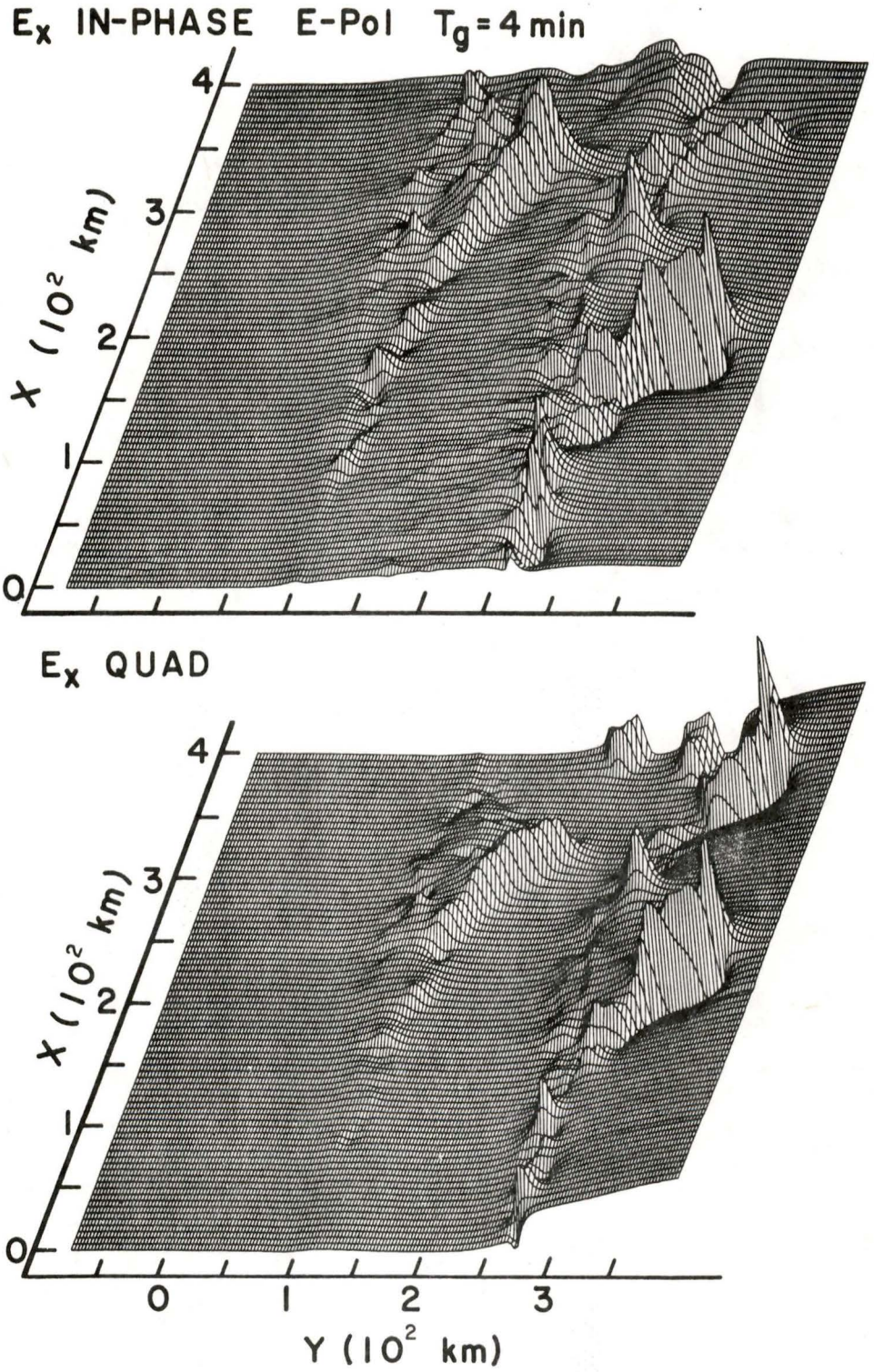

Fig. 20. Three-dimensional diagram of the model in-phase and quadrature E_x for 4 min. period.

Figure 21 shows the E_y contour diagrams for a simulated 4 min. period. Both E_y in-phase and E_y quadrature have zero values over most of the region since this component is usually zero for this polarization unless the induced current is constrained to flow at some angle relative to the electric field of the source. Both E_y in-phase and E_y quadrature contours show very large gradients at the ends of Douglas Channel and Portland Inlet, as well as on the landward side of the bay shaped Chatham Sound and Milbanke Sound. This indicates that induced currents are funnelled into these regions. The dense E_y in-phase contours in the lower diagram of Fig. 21 show small anomalies for bays of small dimension, such as Rennell Sound on the west coast of the Queen Charlotte Islands. E_y in-phase also has dense concentric contours north and south of Rose Point in response to current deflected at some angle with the electric field of the inducing source. This agrees with the response observed for the H_x component.

The E_y three-dimensional diagram is shown in Fig. 22. The anomalies at the eastern island coastlines change from positive to negative in traversing from north to south across Rose Point. This indicates that the deflected currents change direction in flowing around Rose Point. Large enhancements are observed at the ends of Douglas Channel and Portland Inlet as a result of diffusion of

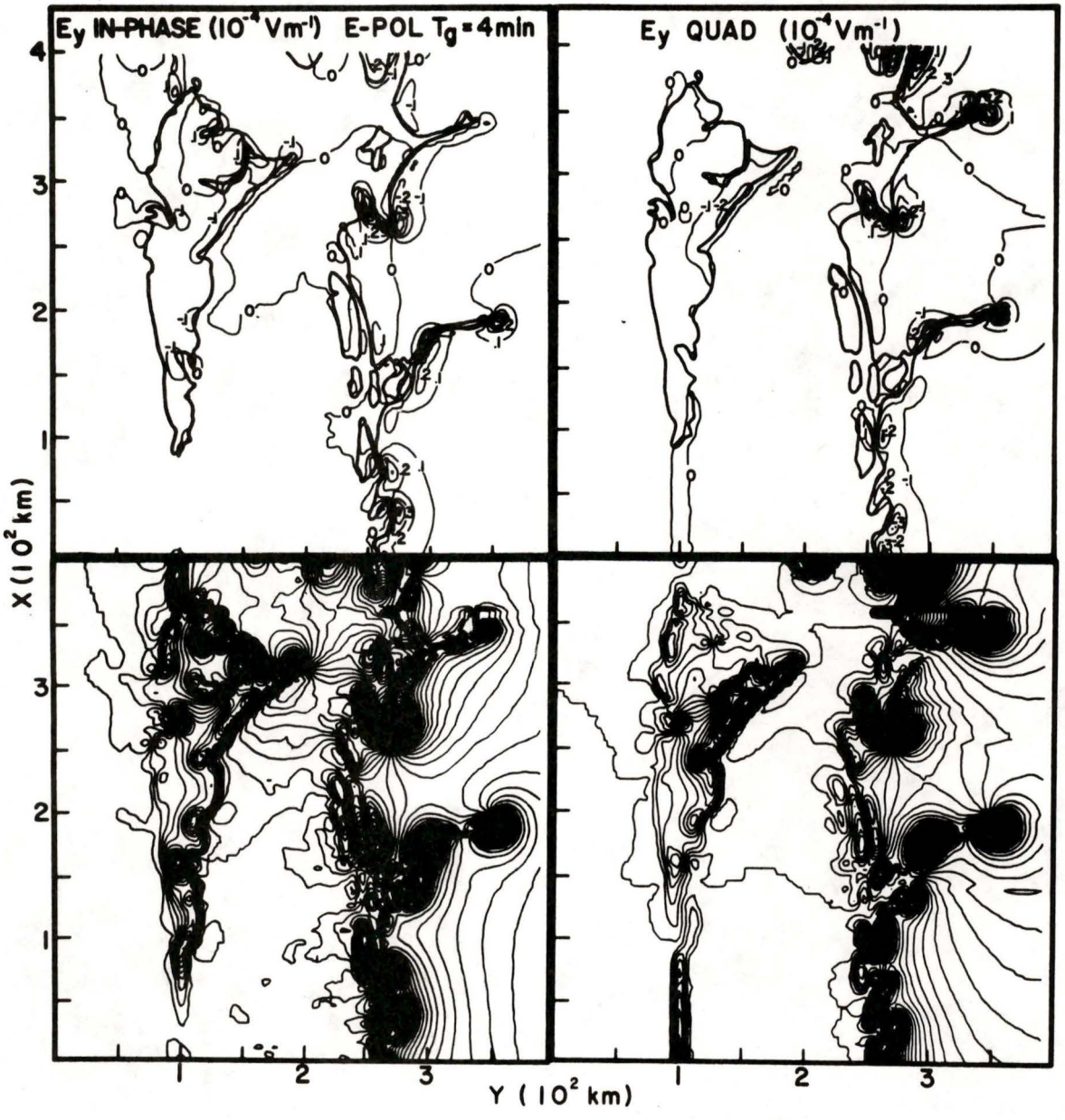

Fig. 21. Contours of the model in-phase and quadrature E_y for 4 min. period.

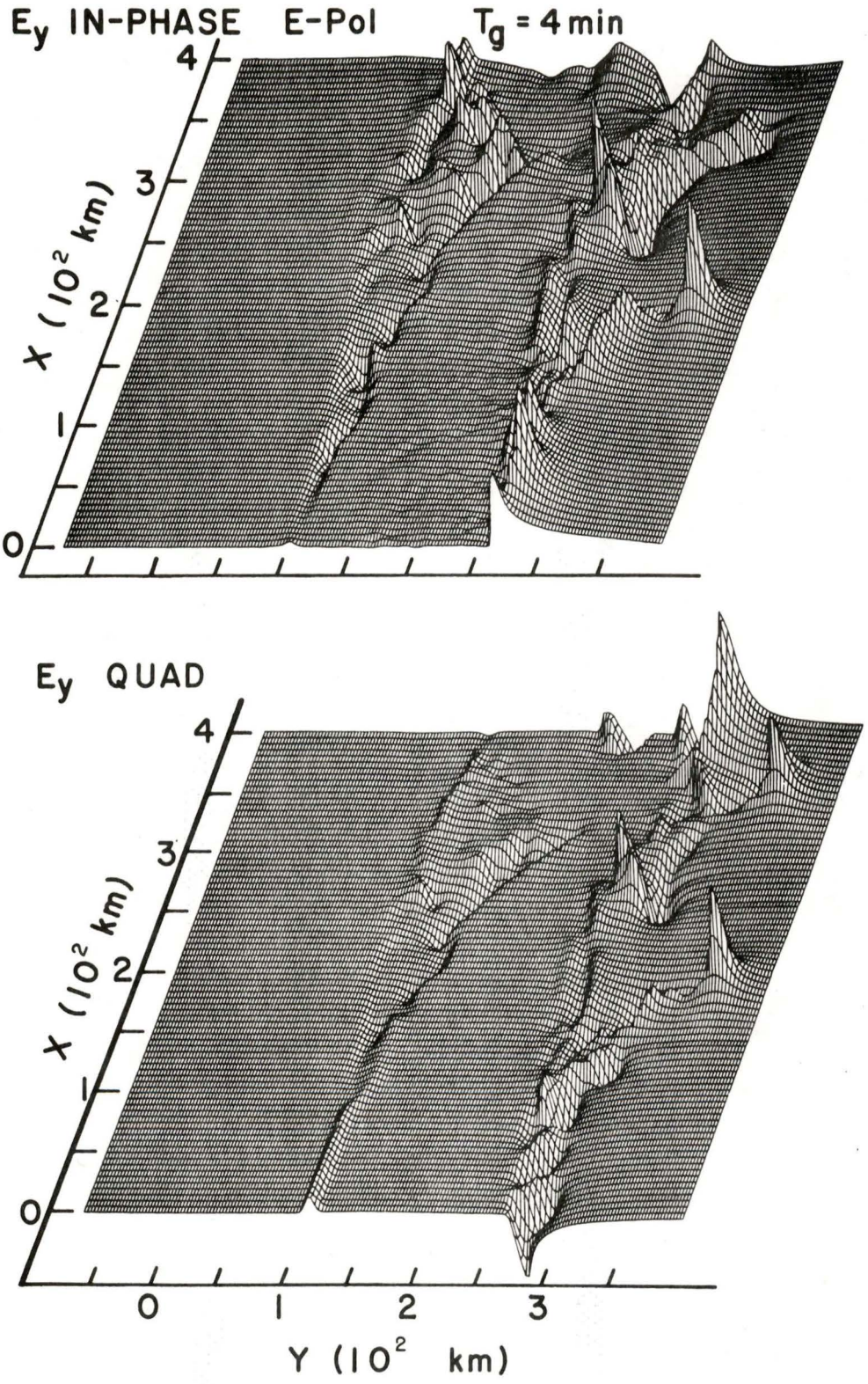

Fig. 22. Three-dimensional diagram of the model in-phase and quadrature E_y for 4 min. period.

telluric current into land. E_y in-phase has positive anomalies at the continental coastline except east of Chatham Sound, the negative value suggests diffusion of channelled current into the surrounding land. Both E_y in-phase and E_y quadrature show anomalies over the narrow channel between Banks Island and the continent indicating channelled current in this region.

The H_z, H_y and E_x components for E-Polarization for a simulated 40 min. period are shown in Figs. 23, 24, and 25 respectively. For this simulated period, the diagrams are produced using digital data for 21 traverses in the y-direction, as compared with 81 traverses for the 4 min. period measurements. This larger traverse spacing will somewhat limit the resolution of the contour lines for the 40 min. period results.

From Figure 23, H_z in-phase increases gradually traversing from the mainland towards the deep ocean. H_z quadrature for this simulated period shows greater spatial variation than H_z in-phase, that is, the field responses have been shifted from H_z in-phase to H_z quadrature. H_z quadrature increases from east to west over the mainland, reaching a maximum at the continental coastline. In crossing Hecate Strait, H_z quadrature decreases to a minimun at the eastern island coastline. A large negative value is observed at Rose Point. H_z quadrature then increases landward across the island and reaches a second

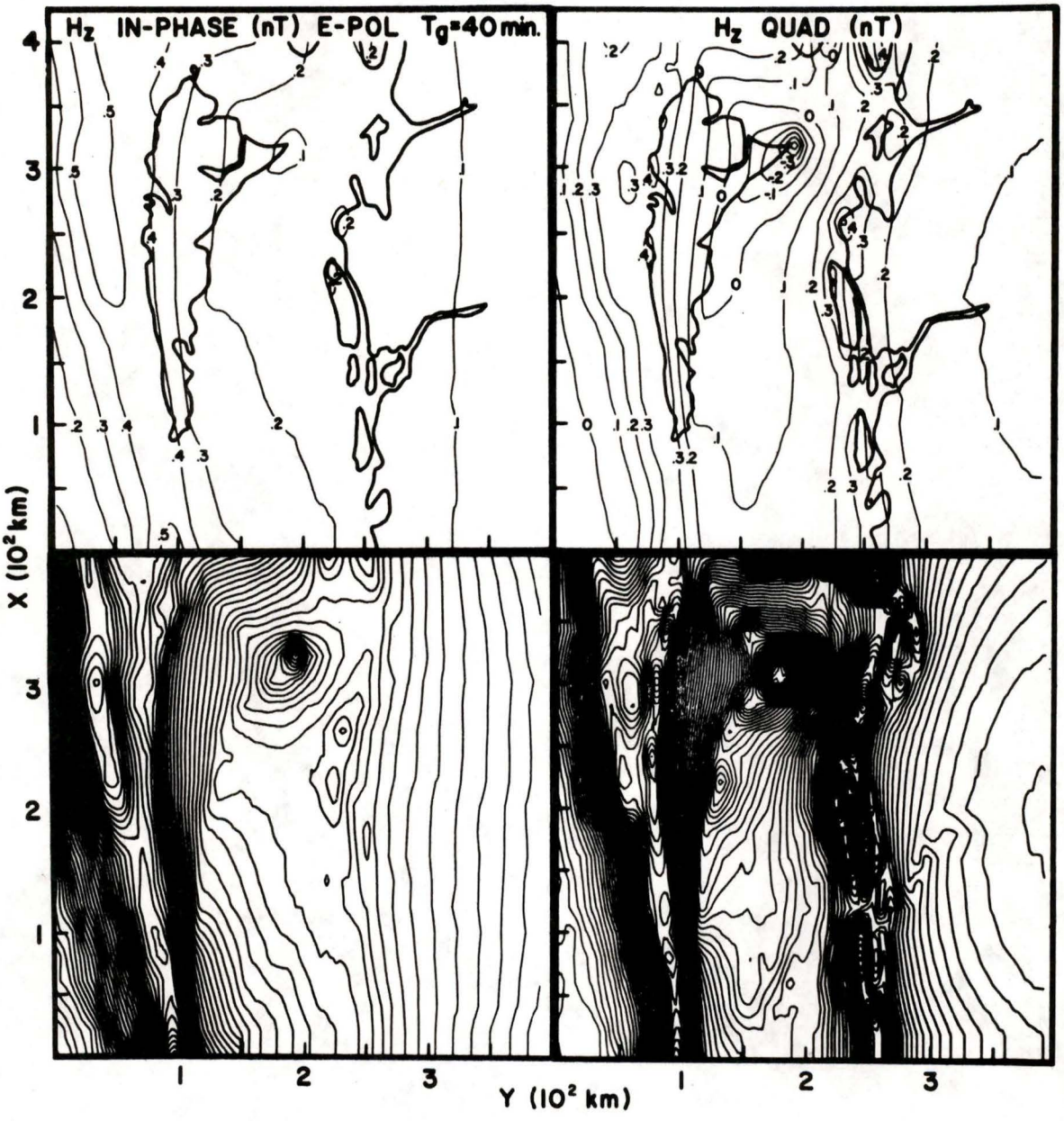

Fig. 23. Contours of the model in-phase and quadrature H_z for 40 min. period.

maximum at the western island coastline before decreasing gradually in traversing towards the deep ocean. The dense H_z in-phase contours in the lower diagram show a set of circular contours at Rose Point as was observed for the 4 min. period results. The dense H_z quadrature contours show that the effects of capes are less pronounced though still important for this longer period. The effect of the sloping continental margin to the west of the island is significant for both the in-phase and quadrature parts. Relatively large H_z gradients are observed seaward from the west coast. The effects of ocean inlets are much diminished for this longer period variation and only a small change for H_z quadrature is observed at Douglas Channel.

Figure 24 presents the H_y contour diagrams for a simulated 40 min. period. H_y in-phase shows values of approximately 1 nT everywhere except over the continental margin. H_y quadrature shows values near zero over the mainland and over the island. The field values increase in traversing from east to west reaching a maximum value on the seaward side of the continental coastline. A large maximum is observed near Rose Point. The H_y quadrature values decrease in crossing Hecate Strait and reach a minimum landward of the eastern island coastline. H_y quadrature remains fairly constant over most of the island, increasing over the western island coastline to a large

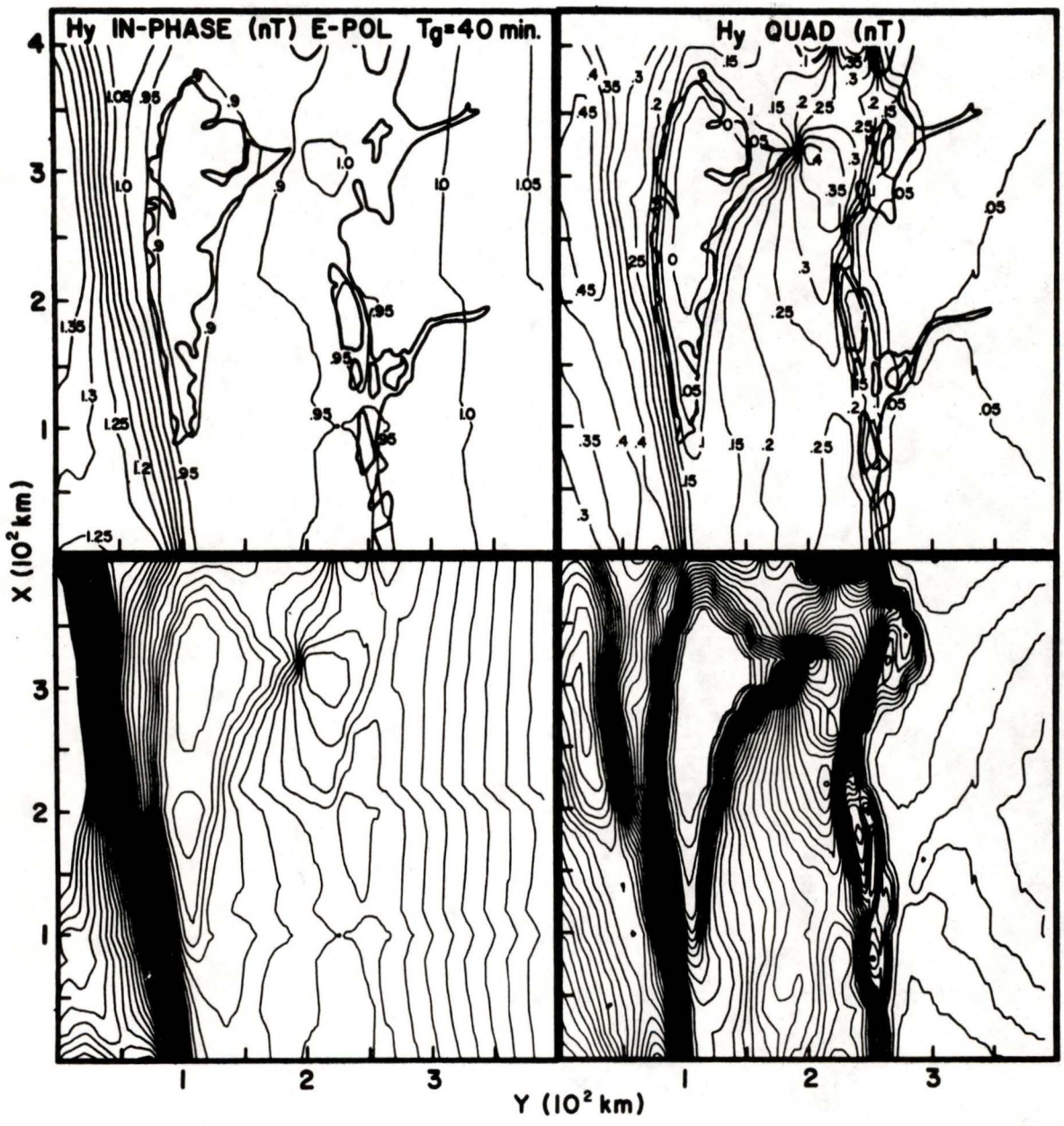

Fig. 24. Contours of the model in-phase and quadrature H_y for 40 min. period.

value over the deep ocean. The dense contours in the lower diagrams of Fig. 24 show that the contours, for both in-phase and quadrature, follow the coastline very closely as was the case for the 4 min. period results.

Figure 25 provides the E_x contour diagrams for a simulated 40 min. period. As in the case of 4 min. period, E_x in-phase shows enhancements when the coastlines are roughly perpendicular to the field. Enhancements are observed over the wedge-shaped coastline near Rose Point and at the ocean inlets, Douglas Channel, Portland Inlet and Masset Inlet. E_x quadrature shows more spatial variations than E_x in-phase for this period. Enhancements are observed at Rose Point, over Douglas Channel and landward of Chatham Sound as for the 4 min. period results. Effects of bays are observed along the eastern island coastline for both E_x in-phase and E_x quadrature. Enhancement at the narrow part of the channel between Aristazabal Island and the mainland due to funnelling of current is only observed for E_x quadrature at this longer period.

In general the results for the 4 min. and 40 min. period variations show that with increasing period, the field responses of E_x in the coastal regions shift from the in-phase to the quadrature part. Since many of these coastal anomalies, even at long periods, depend upon the behaviour of telluric currents in the deep ocean through

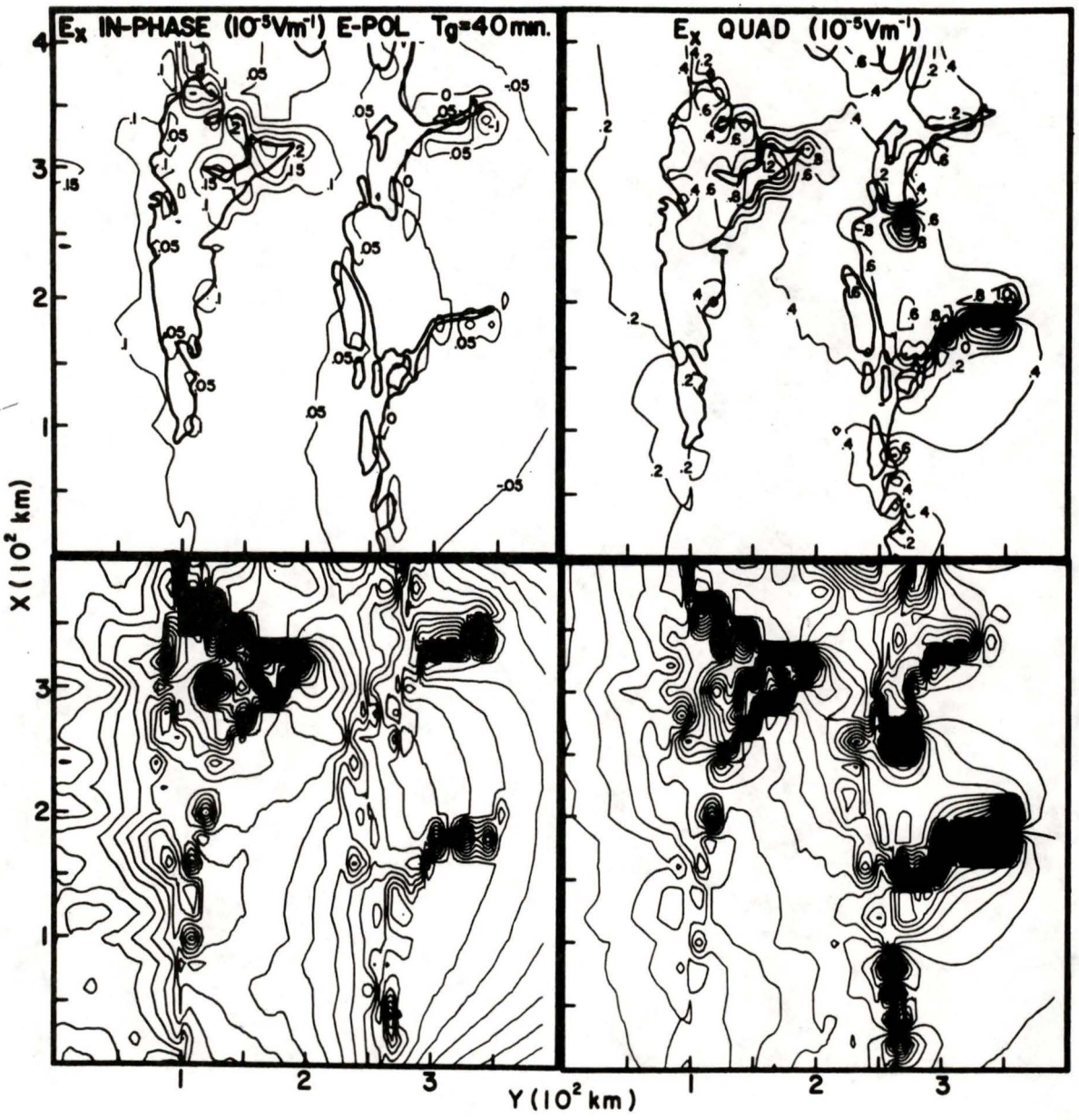

Fig. 25. Contours of the model in-phase and quadrature E_x for 40 min. period.

the channelling process, this shift to the quadrature part may be related to the increasing phase lag (with increasing period) between E_x and the electric field of the inducing source field. For 4 min. period, the deep ocean is of the order of a skin depth. Numerical calculations for a two layer model show that the observed electric field lags the inducing field by about 5° for 4 min. period, and increases to approximately 30° for 40 min. period.

The contour diagrams and the three-dimensional diagrams delineate the behaviour of the magnetic and electric field components in the Queen Charlotte Islands region in detail. They indicate locations where the field components are highly affected by the coast effect, the channelling of telluric currents, and current deflection due to the geometry of the complex coastline. As well, the results suggest suitable reference station locations for marine magnetic surreys. From the model vertical magnetic field contour diagrams, it is apparent that the vertical magnetic field is highly perturbed everywhere along the continental coastline. Thus an inland location such as Terrace or Smithers, rather than a coastal location, should be selected for reference station measurements, that could be used in the reduction of cross-over error (for example, Auld et al. 1979) in marine magnetic surveys to be carried out in the Hecate Strait region.

3.5 Model Field Amplitude Ratios

Figure 26 presents the amplitude ratios H_z/H_y and E_x/H_y for a simulated period of 4 min. The H_z/H_y ratio, often used to describe the coast effect, shows sharp enhancements at all coastlines. At the western island coastline, the ratio is fairly large but is less than 1 everywhere as expected for a straight coastline near the deep ocean for a horizontal inducing field. Enhancements are observed to be smaller along the eastern island coastline than along the western coastline, except at Rose Point where a ratio greater than 1 is recorded. This is the result of greatly increased local current density due to current channelling and deflection at the wedge-shaped coastline. Along the continental coastline, H_z/H_y is near unity everywhere and is larger than 1 at all the cape coastlines. This large ratio is accounted for by the strong channelling of current in Hecate Strait for the E-Polarization of the source field at this short period. The dense contours in the lower diagram show large gradients over the entire island except a narrow strip at the central region. This means that the fields over the entire island are influenced by the coast effect. The ratio is observed to be nearly constant near the central region of the wider portion of Hecate Strait.

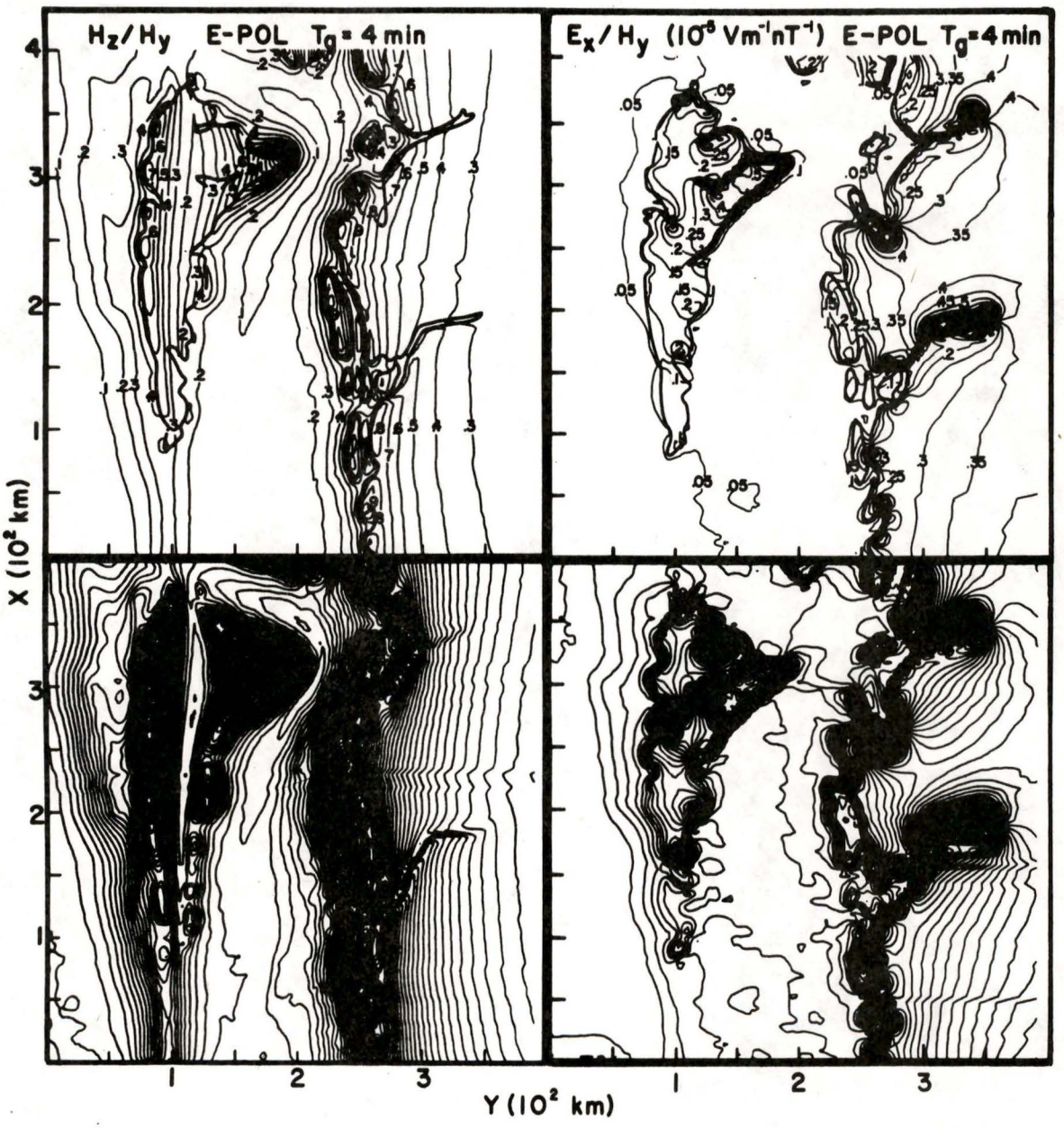

Fig. 26. Contours of the model H_z/H_y and E_x/H_y ratios for 4 min. period.

Figure 26 also presents the contour diagrams of E_x/H_y for a simulated 4 min. period. This ratio is proportional to the magnetotelluric impedance. E_x/H_y at the continental coastline is a factor of 3 smaller than the value inland. E_x/H_y at Douglas Channel is enhanced by a factor of 2 from the values at a point 20 km from the channel. This illustrates the fact that the impedance quantities are perturbed significantly by the estuarties. Circular contours are observed landward of Chatham Sound, Milbanke Sound and Rennell Sound. The enhancements at these locations are due to the bay shaped coastline. A large enhancement is observed over the channel between Aristazabal Island and the mainland. This indicates an enhanced current density in the narrow channel. The dense contours in the lower diagram show large gradients at both the eastern island coastline and the continental coastline. E_x/H_y is relatively constant over Hecate Strait.

The laboratory model simulates only a conducting ocean and a homogeneous earth underlain by a conducting layer at a depth of 100 km. Thus, the large perturbation of the model E_x/H_y for the periods studied are due to the effect of the complex coastline. Hence, magnetotelluric fields for stations in the coastal region or near a fiord, will show large response to the coastlines and thus provides limited useful information on the subsurface tectonic structure. It would be interesting to carry out magneto-

telluric sounding measurements in the Aristazabal Island region and in the vicinity of Douglas Channel to confirm the large enhancements in the E_x/H_y ratio observed in the analogue model results.

Figure 27 shows H_z/H_y and E_x/H_y for a simulated 40 min. period. H_z/H_y, though in general decreased from that for the 4 min. period results, shows enhancements at all coastlines. Along the western island coastline, H_z/H_y values are comparable to those for the 4 min. period results, but the values at Rose Point and along the continental coastline have been reduced substantially. The lower diagram shows that the coast effect attenuates more rapidly with increasing period at both the eastern island coastline and the continental coastline than at the western island coastline. This is explained by the rapid decrease in current channelling in Hecate Strait with increasing period variations, leading to a rapidly decreasing coast effect on either side of Hecate Strait. Current induced in the deep ocean, as well as current deflected westward of the Queen Charlotte Islands, rather than through Hecate Strait, continues to lead to a large coast effect at the western island coastline.

In comparing the results in Fig. 27 with those of Fig. 26, it is seen that E_x/H_y is smaller in general for the 40 min. period than for the 4 min. period variation. As observed for the 4 min. results, the E_x/H_y values at the

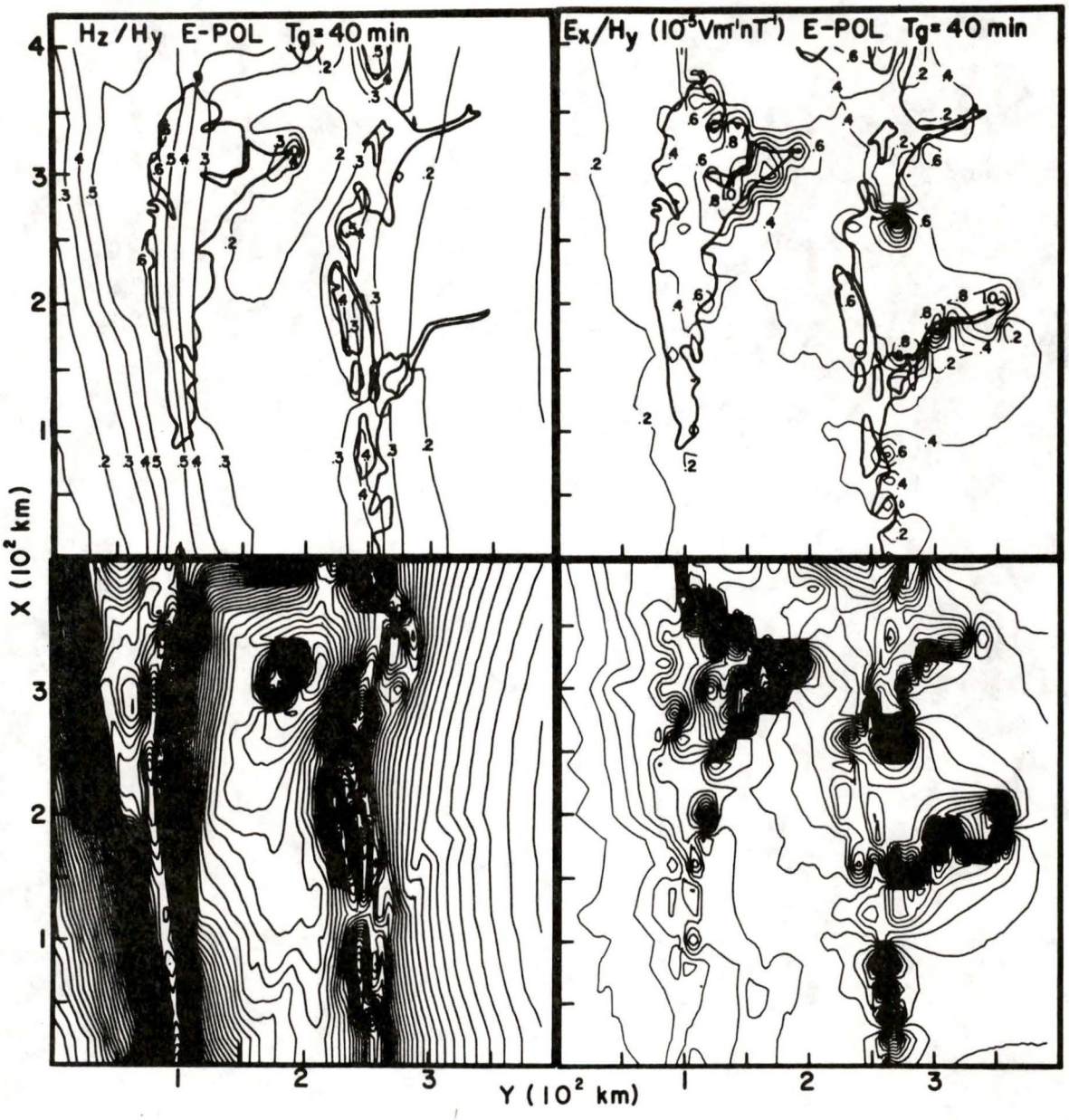

Fig. 27. Contours of the model H_z/H_y and E_x/H_y ratios for 40 min. period.

continental coastline are a factor of 3 smaller than the values observed inland. Near Douglas Channel, E_x/H_y is again enhanced by a factor of 2 over the values observed in the surrounding region. Large enhancement is observed at the bay-shaped Chatham Sound. The dense contours in the lower diagram show large gradients along the eastern island coastline as was observed for the 4 min. period results. Circular contours, with spacing wider than those over Chatham Sound, are seen at Milbanke Sound and Rennell Sound. As was the case for the 4 min. period results, a fairly large enhancement is observed over the narrow section of the channel between Aristazabal Island and the mainland.

3.6 Model Field Amplitude Results for Various Depths to the Conducting Layer within the Mantle

The magnetotelluric study at Victoria (British Columbia) carried out by Caner and Auld (1968) indicated a conducting layer of approximately 0.01 Sm^{-1} at a depth of 65 km. Oldenburg's (1981) results, based on magneto-telluric responses for several locations on the Pacific Plate, indicate the presence of a conductor at a depth depending on the lithospheric age. The conductivity achieves a maximum value of about 0.1 Sm^{-1} at a depth of approximately 70 km for lithospheric age of 1 Ma and the depth increases to 180 km for lithospheric age of 72 Ma.

The field components for simulated depths to the conducting layer of d = 100, 200, and 300 km for the E-Polarization and 4 min. period variations for traverses T2 and T3 are shown in Figs. 28 and 29 respectively. In general, the field components show an approximate 5% attenuation for changing the conducting layer positions from 300 km to 200 km. This indicates that for the simulated period studied, a conducting layer at a depth of 200 km or more has very little effect. When comparing the results for d = 200 km with those for d = 100 km, an attenuation of approximately 20% is observed for the electric and magnetic field (except H_y) anomalies. With the conducting layer nearer the surface a greater portion of the induced currents tend to flow in it. As a result, the current density at the sea-land interfaces near the surface of the earth is reduced and the coastal anomalies are attenuated. E_x is usually enhanced over a low conductivity region, that is, over the islands and the coastal region of the continent. With the conducting layer near the surface (d = 100 km), the apparent resistivity observed at the surface is decreased, especially over land, resulting in decreased E_x response. Comparing the H_y results for d = 200 km and d = 100 km, the anomalies are attenuated by about 12% over Hecate Strait, and by about 8% over the deep ocean. Thus it is seen that the attenuation of the H_y anomalies due to the conducting layer is affected

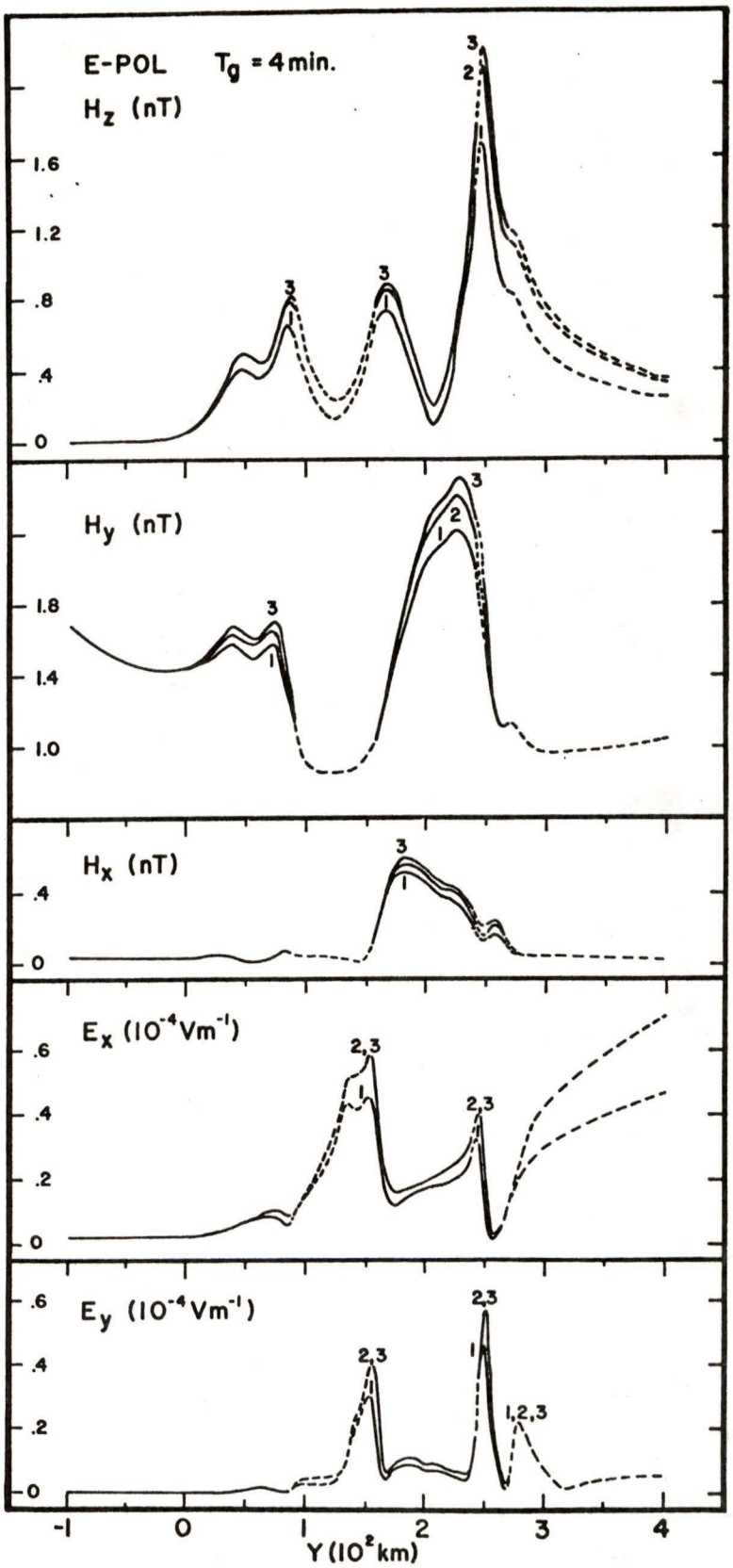

Fig. 28. Amplitudes of the field components along traverse T2 for simulated depths to the conducting layer of (1) 100 km, (2) 200 km, and (3) 300 km for a 4 min. period for E-Polarization.

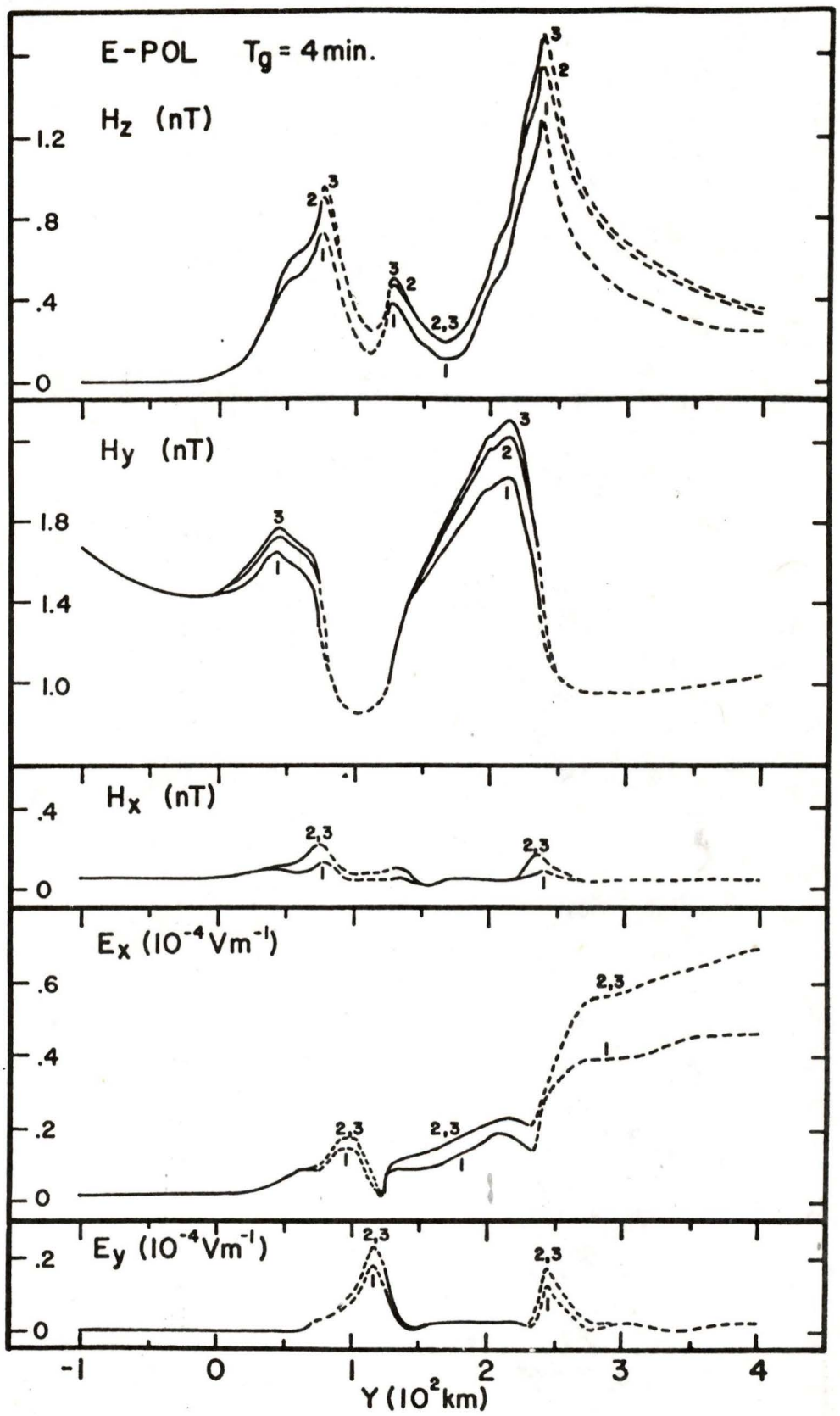

Fig. 29. Amplitudes of the field components along traverse T3 for simulated depths to the conducting layer of (1) 100 km, (2) 200 km, and (3) 300 km for a 4 min. period for E-Polarization.

by the conductivity of the upper region. The difference in the attenuation of H_y over Hecate Strait and over the deep ocean can be explained by the difference in thickness of the conducting ocean at the two locations. The effect of a subsurface conducting layer is diminished as the ocean depth increases. The attenuation of the H_z, E_x and E_y anomalies over (or near) the land masses is larger than the attenuation of the H_y anomalies over the conducting ocean where the conducting layer is shielded to a greater extent by the highly conducting ocean.

Measurements for traverses T1, T4, T5 and T6 as well as measurements for longer period variations (40 min. and 120 min.) for changing depth of the conducting layer were also carried out (see Appendix). The general behaviour of the field components for the longer periods was found to be very similar to that for the 4 min. period variation with the attenuation of the anomalies decreasing with increasing period. For 40 min. and 120 min. periods, the conducting layer thickness is much less than a skin depth, thus, the location of the conducting layer becomes insignificant.

Chapter 4

FIELD STATION RESULTS IN THE QUEEN CHARLOTTE ISLANDS REGION

4.1 Field Station Data Analysis

The three time-varying magnetic components Z (vertical), H (magnetic north-ward) and D (magnetic east-ward) were recorded at Prince Rupert, on the British Columbia mainland, and at Sandspit, on the Queen Charlotte Islands (October, 1979). The field station data was supplied by Mr. D.R. Auld of the Pacific Geoscience Centre. The D component measurements at Sandspit were not available due to equipment malfunction at the time of recording.

From the Prince Rupert station, 7 sections of 24 hour records containing considerable geomagnetic activity were selected for single station transfer function analysis, similar to that used by Everett and Hyndman (1967). The trend of the data for each component was removed by subtracting a least squares sloped straight line. The end effects were reduced by applying a cosine bell to the first and last 10% of the record (Kanasawich, 1975). Fourier transforms were computed for each 24 hour section. Stable average spectra were obtained by averaging symmetrically about selected centre frequencies (Parsen Window). For

each centre frequency, the Fourier amplitudes z, h and d of the respective magnetic components were calculated. These values were then used to obtain two components of the transfer function (A, B) satisfying the equation $z = Ah + Bd$. The in-phase and quadrature parts of the transfer function form the in-phase and quadrature induction arrows respectively. A and B are the north-south and east-west components of the induction arrow which points in the direction of the horizontal magnetic field that correlates best with the vertical magnetic field. In the present work, the direction of both the in-phase and quadrature induction arrows are reversed. Thus the in-phase arrow is consistent with the Parkinson Convention and points towards the current concentration (for two dimensional cases).

4.2 Comparison of Field Station Results with Model Results

Figures 30 and 31 present the in-phase and quadrature induction arrows at Tasu, Sandspit, Prince Rupert, Terrace, and Smithers. The upper diagrams show the analogue model results for 4, 40 and 120 min., while the lower diagrams show the field station results for 4, 10, 30, 40, 45, and 60 min. The field station induction arrows for Sandspit and Tasu were taken from the work of Miller (1973). The 4 and 40 min. field station results (1, 4) for Prince Rupert were supplied by Mr. D.R. Auld of the Pacific

Geoscience Centre, and the other results (2, 3, 5, 6) at Prince Rupert, as well as those at Terrace and Smithers, were adapted from the work of Dragert (1973).

In Fig. 30, the model in-phase arrows at Prince Rupert, Terrace, and Smithers all point in the general direction of Rose Point in response to the current concentration due to current channelling. With increasing period, the arrows decrease in length and rotate in the clockwise direction to point more towards the deeper Dixon Entrance. The field station arrows in the lower diagram at Prince Rupert point generally towards the Rose Point - Dixon Entrance region and agree with the model arrows. The magnitude of the 4 min. model induction arrow is much larger than that of the field station induction arrow. This may be explained in part by a possible over estimation in conductivity and thickness of the conducting sediments in Hecate Strait used for the analogue model. Due to the fragility of graphite, the material used for the model ocean, it was necessary to somewhat increase the depth of the model shallow seas at the coastal regions. With increasing period, the magnitude of the field station induction arrows first decreases then increases. The field station induction arrows at Terrace and Smithers point roughly in the north-west direction and rotate counter-clockwise with increasing period.

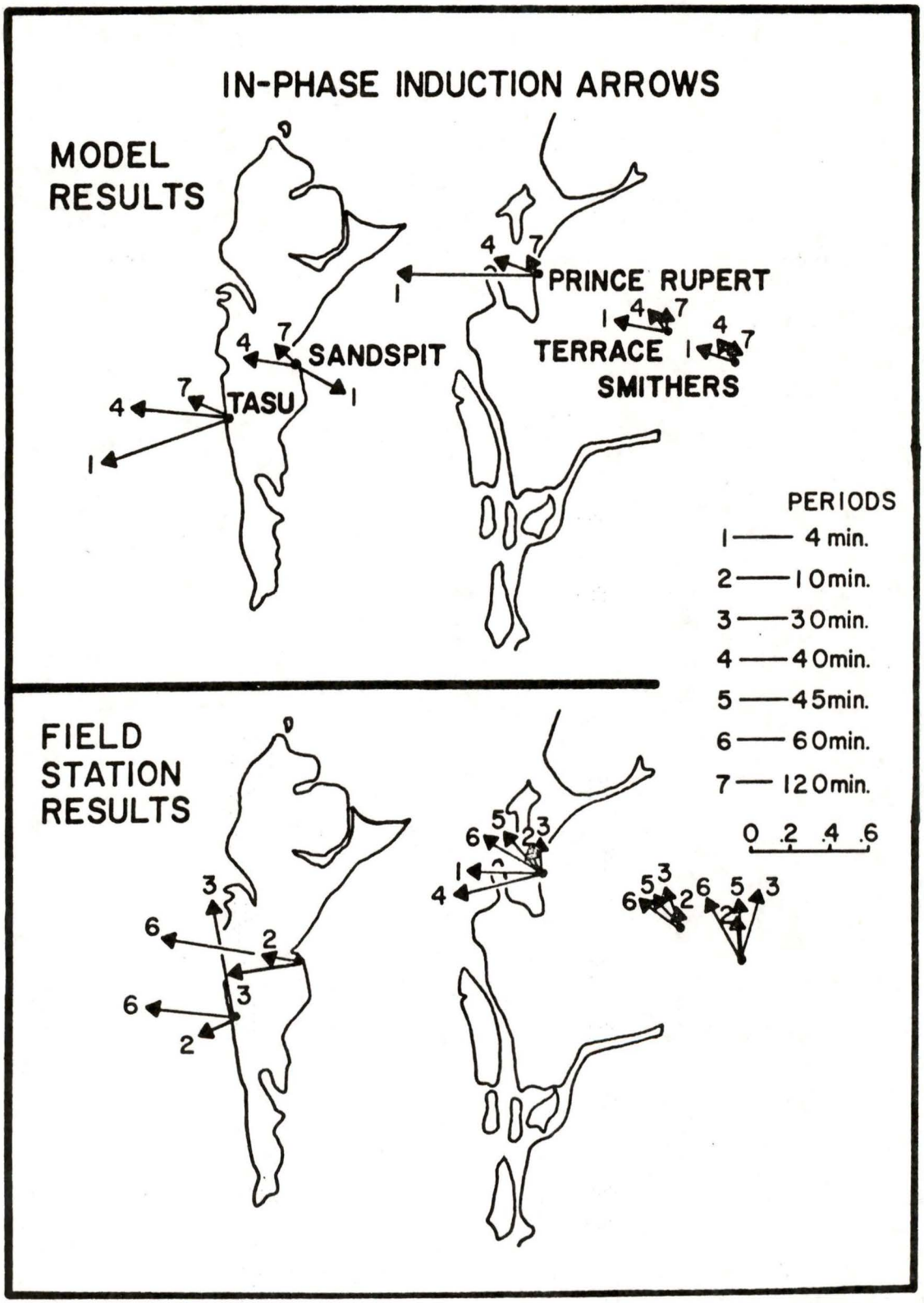

Fig. 30. In-phase induction arrows for field station and model results.

The 4 min. (1) model induction arrow at Sandspit points towards Hecate Strait while the 40 and 120 min. induction arrows (4, 7) point westward towards the deep ocean. The field station arrows all point westward towards the deep ocean. The difference between the model and field station short period induction arrows (1 for model results and 2 for field station results) may be due to the difference between the model and the geophysical system. Besides the possibility of over estimating the depth of sediments which would allow too much current in Hecate Strait in the model, the model has omitted well known geophysical features such as the Queen Charlotte Fault and the narrow shallow channel through the central region of the Queen Charlotte Islands near Sandspit. If these were included in the model, they would likely affect the magnitude and direction of the model induction arrows. The model induction arrows at Tasu all point towards the deep ocean, with the magnitude decreasing with increasing period. The field station induction arrows behave more irratically, both in changing direction and magnitude. The magnitude of the field station induction arrows are small at short periods and larger at long periods.

Figure 31 shows the quadrature induction arrows. Both model and field station arrows at Prince Rupert point roughly towards Rose Point. This direction can be accounted for by the large current concentration in the

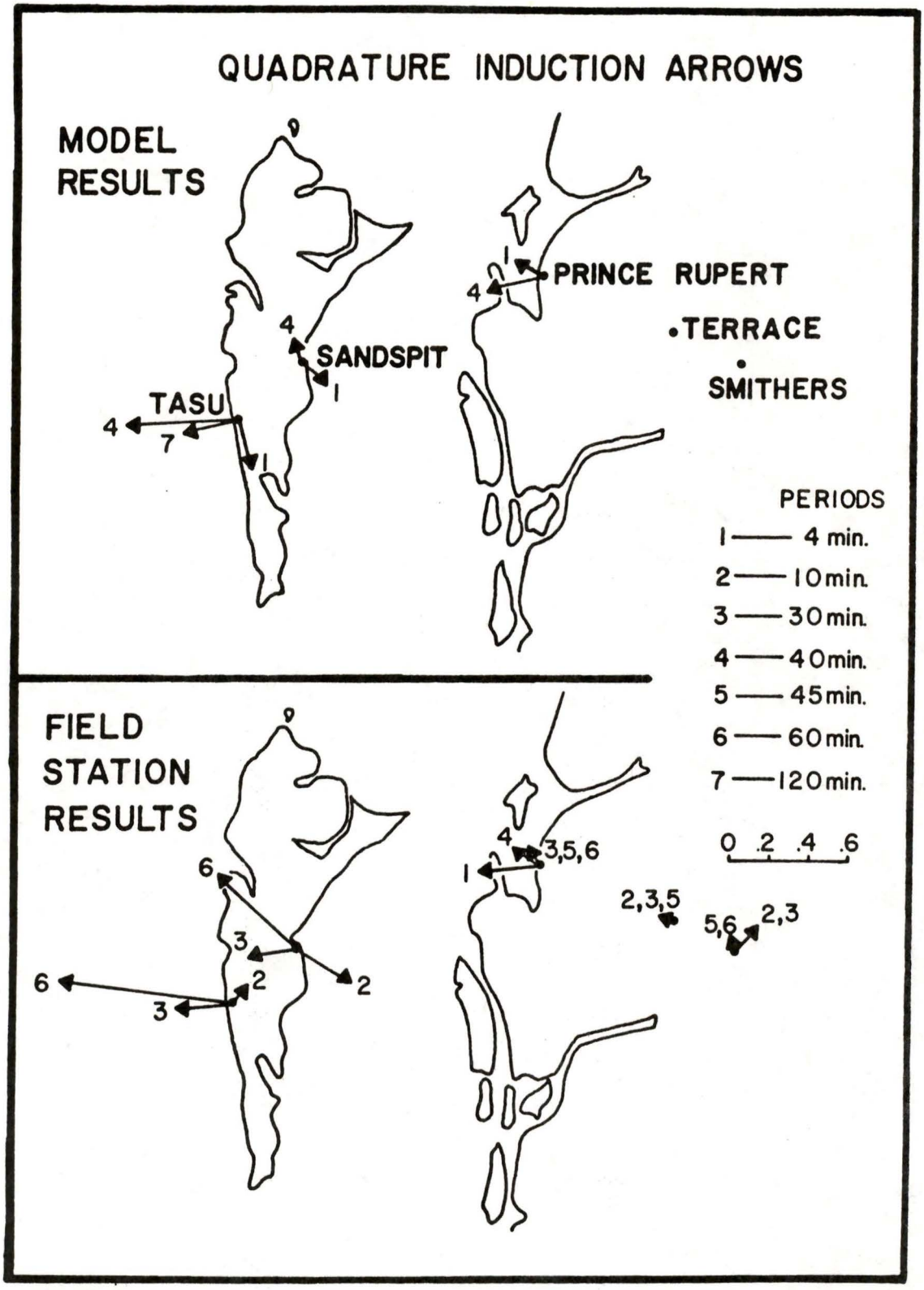

Fig. 31. Quadrature induction arrows for field station and model results.

Rose Point vicinity due to channelling and deflection of current. The model quadrature arrows at Terrace and Smithers are too small to be meaningful and are not shown. The magnitude of the field station quadrature arrows at Terrace and Smithers are of the order .1 or less. (It should be noted that arrows with magnitude .1 or less are not very reliable in direction.)

At Sandspit, both the model 4 min. quadrature arrow (1) and the field station 10 min. quadrature arrow (2) point towards Hecate Strait. At longer periods, both the model and field station quadrature arrows point in a more westerly direction towards the deep ocean. The field station arrows are longer than the model arrows. It is interesting that the 10 min. (2) field station in-phase and quadrature arrows point in opposite direction at both Sandspit and Tasu. This could indicate induced current at depth in these regions. This feature is not seen in the model results. At the longer period (3 to 7) the quadrature induction arrows at Tasu for both model and field station point towards the deep ocean as a result of currents induced at depth in the deep ocean.

The general agreement of the model and field station induction arrows indicates that the magnetic variations observed at the field stations are mainly a result of the coast effect. The difference between the two sets of data should reveal information on the subsurface structures of

the area that were not simulated in the model.

The ratio of the field station vertical magnetic field power density at Prince Rupert and Sandspit, for a range of periods, is shown in Fig. 32. The ratio is approximately 2 for 4 min. period, 3 for 40 min. period and 2 for 120 min. period. From model measurements, the ratio of the squares of the vertical field amplitudes calculated for the Prince Rupert and Sandspit locations are 2.4, for 4 min. period, 2.6 for 40 min. period and 1.8 for 120 min. period. Thus the field station values agree reasonably well with the analogue model values for the particular period variations studied.

It would be useful to carry out field observations at more locations for the purposes of confirming the model results and studying the tectonic structures. As stated earlier, magnetotelluric sounding measurements near Aristazabal Island and any of the ocean inlets would produce an enhanced value of magnetotelluric impedance. Other interesting locations are Rose Point, Banks Island region, areas near the northern and southern tips of the island, and points near large bays such as Chatham Sound and Milbanke Sound. Magnetic observations at these locations should provide support for the ideas of current channelling and current deflection in these areas. As for tectonic studies, field stations should not be located at or near a coastline since the large coastal effects would mask the smaller effects due to substructures.

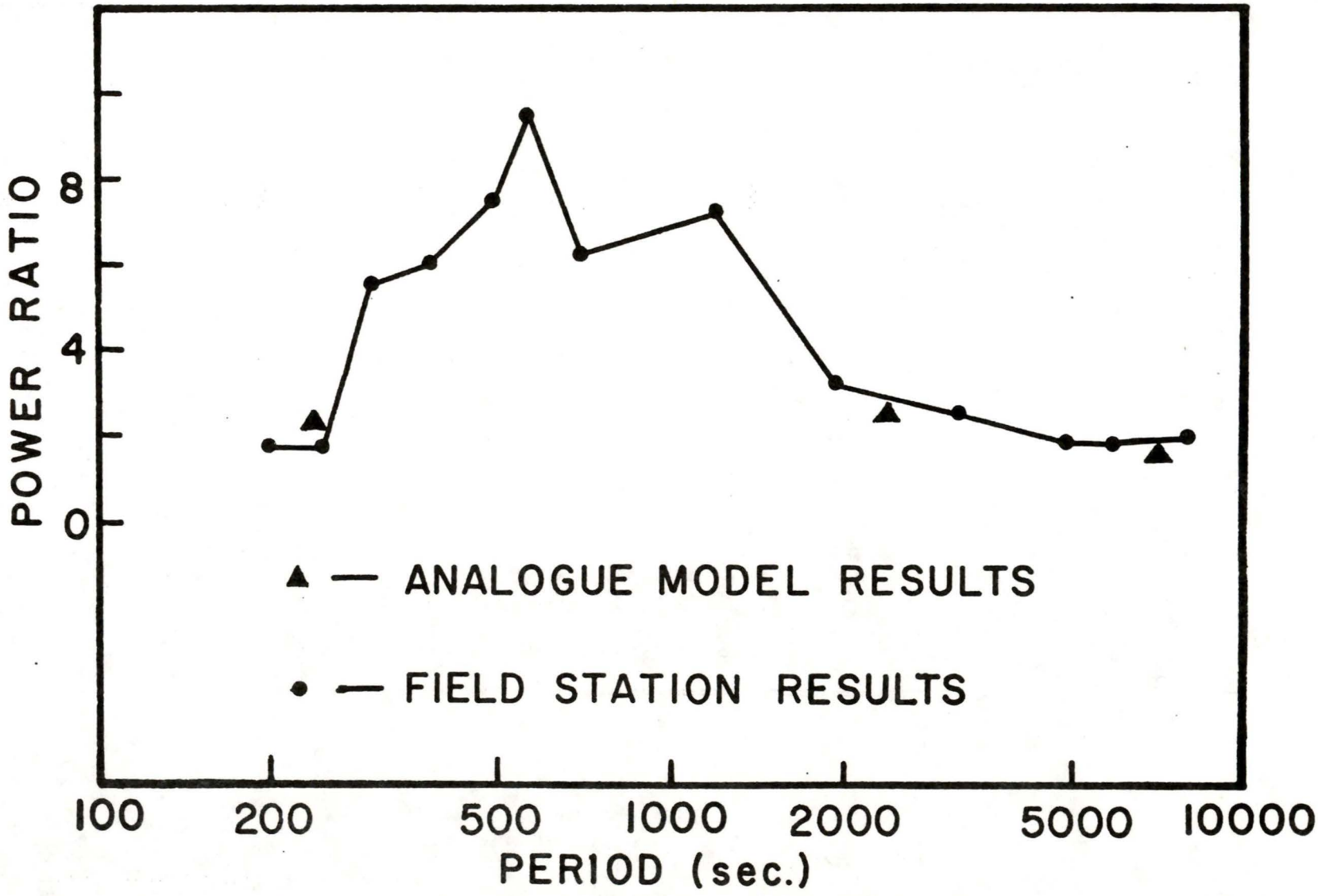

Fig. 32. The ratio of the vertical magnetic field power densities at Prince Rupert and Sandspit.

Chapter 5

SUMMARY AND CONCLUSIONS

5.1 The Effects of Current Channelling and Deflection

The analogue model results for the Queen Charlotte Islands region have brought out many interesting features. Conductive channelling is observed in Hecate Strait and in the Banks Island region for the E-Polarization of the source, especially at short periods as illustrated by the enhancements in H_z and H_x at the narrow channels near Banks Island and Aristazabal Island. Current deflection is emphasized in the neighbourhood of Rose Point for E-Polarization, and at the northern and southern tips of the Queen Charlotte Islands for H-Polarization. For E-Polarization, all the magnetic and electric field components studied show anomalies at or near Rose Point where a large current density exists due to current deflection at the wedge-shaped coastline. Field anomalies due to bays and capes are observed for both polarizations. H_z, H_x, and E_x respond to capes and bays and E_y shows large anomalies landward of bays. These four field components also respond to channelled currents in the ocean inlets with the electric fields showing the most striking

responses. Large enhancements in E_y at the end of ocean inlets suggest diffusion of currents into land.

5.2 The Effects of a Complex Coastline

For E-Polarization, current channelling and deflection by the complex and irregular island and continental coastlines lead to a wide range of field values over the Queen Charlotte Islands. At short periods, H_z generally shows larger coastal effects near the west coast than near the east coast, and is a factor of 4 (or more) greater at the coastline near the northern end than at the southern end due to the shape of the island coastline. H_z has a minimum value over the central region of the Queen Charlotte Islands (T2-T4), with a value about a factor of 4 smaller than at the coast.

H_y, at short periods, generally shows a broad minimum over the central regions, with increasing values as the east and west coastlines are approached. The coastal values are approximately 20% larger than the interior values. The electric fields E_x and E_y generally show large enhancements on the east coast and fall off rapidly over the island as the west coast is approached. Values near the east coast are factors of 3 to 5 greater than values near the west coast. With the relatively close proximity of the coast for all locations on the Queen Charlotte Islands, the complex island-continent coastlines and the

irregular shaped sea channels are expected to strongly influence the electric and magnetic field variations for all island locations. The effect of the sloping continental shelf region is important for all the magnetic components.

For the H-Polarization, all magnetic field components are essentially constant for points over the island, with H_y and H_z showing small gradients near the island coastlines. The E_y values are enhanced over the island, with the field generally increasing in traversing from the east coast to the west coast. This is opposite to that observed for the E-Polarization. E_x is sharply enhanced near both coastlines and has a broad minimum over the central regions of the island.

The coast effect, H_z/H_y, for the 4 min. period variations, has large values at the continental coastline and near Rose Point due to channelled current in Hecate Strait. An enhanced coast effect is observed over the entire Queen Charlotte Islands. The ratio is fairly constant near the central region of Hecate Strait. For the longer 40 min. period variations, the coast effect is decreased along the two coasts of Hecate Strait. This attenuation is due to the decrease of induced currents in Hecate Strait at longer periods. E_x/H_y, which is proportional to the magnetotelluric impedance, is a factor of 3 smaller at the continenatl coastlines than at inland

locations. However, the ratio is a factor of 2 greater at the ocean inlets than over the surrounding regions. Enhancements in E_x/H_y are observed on shore near bays.

5.3 The Effects of the Source Field Frequency

The analogue model results for the simulated 4, 40 and 120 min. period variations indicate that the behaviour of the fields over the Queen Charlotte Islands is highly frequency dependent. At certain coastal locations, H_z enhancements are a factor of 4 or 5 greater for the 4 min. period variation than for the 120 min. period variations. The effect of the deep ocean becomes more important as the period increases. For 40 min. period, the H_z anomalies at the east island coastline disappear. H_z increases sharply over the island reaching a large value over the west island coastline and continental margin. The H_z value at the west island coastline for 40 min. period is larger than that for 4 min. period. At longer periods, H_y becomes approximately constant over the island but shows enhanced values seaward of the west coast, while the enhancement over the shallow Hecate Strait decreases rapidly at longer period. The horizontal electric field components show a similar large range of values, responding strongly to deflected and channelled current.

From the contour diagrams, the behaviour of the in-phase and quadrature magnetic and electric fields for

the 40 min. period variations is generally similar to those for the 4 min. period. The enhancements decrease with increasing period, and at the longer period the quadrature part shows larger response than the in-phase part. The gradient of all field components over the island changes in a complicated way with changing period, as a result of frequency dependence of current channelling in Hecate Strait.

5.4 The Effects of the Conducting Layer in the Mantle

The 4 min. period model results indicate that as the depth to the conducting layer decreases from 200 km to 100 km the field enhancements (except H_y) at the coastlines are attenuated by approximately 20%. H_y attenuates by roughly 8% over the deep ocean and by 12% over Hecate Strait. There is relatively little change (5% or less) in any of the field anomalies in changing the position of the conducting layer from 300 km to 200 km.

5.5 Field Station Results

In general field station induction arrows are in agreement with the analogue model induction arrows. At short periods, the model in-phase induction arrows at locations along the two coasts of Hecate Strait point towards the strait in response to the channelled currents, while the short period field station in-phase induction

arrow at Sandspit points towards the deep ocean. This may be due to the effect of the Queen Charlotte Fault which is not simulated in the laboratory model and thus not observed in the analogue model results. At long periods, both the field station and model induction arrows at Sandspit and Tasu point towards the deep ocean as a result of currents induced at depth in the deep ocean. The ratio of the field station vertical magnetic field power densities is found to be in reasonably good agreement with the ratio of the squares of the model vertical magnetic field amplitudes at Prince Rupert and Sandspit for all period variations studied in the experiment.

The contour diagrams, describing the magnetic and electric field components of the Queen Charlotte Islands region in detail, suggest that certain locations would not be suitable for field station observations. Such locations are characterized by field contours with very large gradients (for example, areas near the coastlines and ocean inlets). In general, the difference between model and field station results should provide information on any sub-surface conductivity structures not simulated in the model. However, field station observations at locations such as Rose Point and near Aristazabal Island would be interesting for confirming the model results. The model results would also help to determine reference station locations for marine magnetic surveys.

REFERENCES

Ashour, A.A. 1950. The induction effect of electric current in a uniform circular disk. Quart. J. Mech. Applied Math., 3: 119-127.

Auld, D.R., Law, L.K. and Currie, R.G. 1979. Cross-over error and reference station location for a marine magnetic survey. Marine Geophys. Res., 4: 167-179.

Banks, R.J. 1972. The overall conductivity distribution of the earth. J. Geomag. Geoelectr., 24: 337-351.

Brewitt-Taylor, C.R. 1975. A model for the coast effect. Phys. Earth Planet. Inter., 10: 151-158.

Brewitt-Taylor, C.R. and Weaver, J.T. 1976. On the finite difference solution of two dimensional induction problem. Geophys. J. R. Astr. Soc., 47: 375-396.

Bullard, E.C. and Parker, R.L. 1970. Electromagnetic induction in the ocean. in The Sea, edited by A.E. Maxwell, Wiley-Interscience, New York.

Cagniard, L. 1953. Basic theory of the magnetotelluric method of geophysical prospecting. Geophysics, 8: 605.

Caner, B. and Auld, D.R. 1968. Magneto-telluric determination of upper mantle conductivity structure at Victoria, British Columbia. Can. J. Earth Sci., 5: 1209-1220.

Caner, B., Auld, D.R., Dragert, H. and Camfield, P.A. 1971. Geomagnetic depth sounding and crustal structure in western Canada. J. Geophys. Res., 76: 7181-7201.

Caner, B., Camfield, P.A., Andersen, F. and Niblett, E.R. 1969. A large-scale magnetotelluric survey in western Canada. Can. J. Earth Sci., 6: 1245-1261.

Caner, B. and Cannon, W.H. 1965. Geomagnetic depth-sounding and correlation with other geophysical data in western North America. Nature, 5000: 927-928.

Chan, G.H., Dosso, H.W. and Law, L.K. 1981a. An analogue model study of electromagnetic induction for cape and bay coastlines. Phys. Earth Planet. Inter., 25: 167-176.

Chan, G.H., Dosso, H.W. and Law, L.K. 1981b. Electromagnetic induction in the San Juan Bay region of Vancouver Island. Phys. Earth Planet. Inter. (in press)

Cochrane, N.A. and Hyndman, R.D. 1970. A new analysis of geomagnetic depth sounding data from western Canada. Can. J. Earth Sci., 7: 1208-1218.

Coggon, J.H. 1971. Electromagnetic and electrical modelling by the finite element method. Geophysics, 36: 132-155.

d'Erceville, I. and Kunetz, G. 1962. The effect of a fault on the earth's natural electromagnetic field. Geophysics, 27: 651-655.

Dosso, H.W. 1966a. A plane-wave analogue model for studying electromagnetic variations. Can. J. Phys., 44: 67-80.

Dosso, H.W. 1966b. Analogue model measurements for electromagnetic variations near vertical faults and dykes. Can. J. Earth Sci., 3: 287-303.

Dosso, H.W. 1966c. Analogue model measurements for electromagnetic variations near a coastline. Can. J. Earth Sci., 3: 917-936.

Dosso, H.W. 1969. Analogue model study of electromagnetic variations over an anisotropic conductor. J. Geomag. Geoelectr., 21: 647-653.

Dosso, H.W. 1973. A review of analogue model studies of the coast effect. Phys. Earth Planet. Inter., 7: 294-302.

Dosso, H.W. and Jacobs, J.A. 1968. Analogue model measurements of electromagnetic variations in the near field of an oscillating line current. Can. J. Earth Sci., 5: 23-29.

Dosso, H.W., Ramaswamy, V., Jones, F.W., Thomson, D.J. 1974. On the comparison of laboratory electromagnetic analogue model measurements and finite difference numerical calculations. Phys. Earth Planet. Inter., 9: 108-110.

Dosso, H.W., Nienaber, W. and Hutton, V.R.S. 1980a. An analogue model study of electromagnetic induction in the British Isles region. Phys. Earth Planet. Inter., 22: 68-85.

Dosso, H.W., Nienaber, W., Wright, J.A., Greenhouse, J.P. and Bailey, R.C. 1980b. An analogue model study of electromagnetic induction in the eastern coastal region of North America. Phys. Earth Planet. Inter., 23: 13-30.

Dragert, H. 1973. A transfer function analysis of a geomagnetic depth sounding-profile across central British Columbia. Can. J. Earth Sci., 10: 1089-1098.

Edwards, R.N., Law, L.K. and White, A. 1971. Geomagnetic variations in the British Isles and their relationship to electrical currents in the ocean and shallow seas. Phil. Trans. Roy. Soc. Lodon, Ser. A, 270: 289-323.

Everett, J.E. and Hyndman, R.D. 1967. Geomagnetic variations and electric conductivity structure in south-western Australia. Phys. Earth Planet. Inter., 1: 24-34.

Fischer, G. 1979. Electromagnetic induction effects at an ocean coast. Proc IEEE, 67: 1050-1060.

Frischknecht, F.C. 1971. Electromagnetic scale modelling. in Electromagnetic Probing in Geophysics, edited by J.W. Wait, The Golem Press, Boulder, Colorado.

Hermance, J.F. 1968. Model studies of the coast effect on geomagnetic variations. Can. J. Earth Sci., 5: 515-522.

Honkura, Y. 1971. Geomagnetic variation anomaly on Miyakejima Island. J. Geomag. Geoelectr., 23: 307-333.

Jones, F.W. 1974. The effect of an island and bay structure on alternating fields at three periods. Geophys. J. R. Astr. Soc., 36: 627-639.

Jones, F.W. and Lokken, J.E. 1975. Irregular coastline and channelling effects in three-dimensional geomagnetic perturbation models. Phys. Earth Planet. Inter., 10: 140-150.

Jones, F.W. and Pascoe, L.J. 1972. The perturbation of alternating geomagnetic fields by three-dimensional conductivity inhomogeneities. Geophys. J. R. Astr. Soc., 27: 479-485.

Jones, F.W. and Price, A.T. 1970. The perturbation of alternating geomagnetic fields by conductivity anomalies. Geophys. J. R. Astr. Soc., 20: 317-334.

Kanasewich, E.R. 1975. Time sequence analysis in geophysics. University of Alberta Press, Edmonton, Alberta.

Kertz, W. 1964. The conductivity anomaly in the upper mantle found in Europe. J. Geomag. Geoelectr., 15: 185-192.

Kulik, S.N., Rokityanskii, I.I., Fornarev, G.A. and Shneer, V.S. 1973. Simulation of coast effect in variation of geomagnetic vertical field component. Academy of Science of the Ukrainian SSR Publication, 54: 82-84.

Lahiri, B.N. and Price, A.T. 1939. Electromagnetic induction in non-uniform conductors, and the determination of the conductivity of the earth from terrestrial magnetic variations. Phil. Trans. Roy. Soc., London, A., 273: 509.

Lamb, H. 1883. On electrical motions in a spherical conductor. Phil. Trans. Roy. Soc., 174: 526.

Lambert, A. and Caner, B. 1965. Geomagnetic depth-sounding and the coast effect in western Canada. Can. J. Earth Sci., 2: 485-509.

Launay, L. 1970. Studies on edge effect through scale models. Ann. Geophys., 26: 805-810.

Lines, L.R. and Jones, F.W. 1973. The perturbation of alternating geomagnetic fields by an island near a coastline. Can. J. Earth Sci., 10: 510-518.

Lipskaya, N.V. 1953. On certain relationships between harmonics of the periodic variations of the terrestrial electric and magnetic fields. Izv. Akad. Nauk, USSR, Geophysics Series, 1: 41.

Miller, H.G. 1973. An analysis of geomagnetic variations in western British Columbia. Ph.D. thesis, University of British Columbia.

Nienaber, W., Dosso, H.W., Law, L.K., Jones, F.W. and Ramaswamy, V. 1976. An analogue model study of electromagnetic induction for island-continent ocean channels. Phys. Earth Planet. Inter., 13: 169-183.

Nienaber, W., Dosso, H.W., Law, L.K., Jones, F.W. and Ramaswamy, V. 1979a. An analogue model study of electromagnetic induction in the Vancouver Island region. J. Geomag. Geoelectr., 31: 115-132.

Nienaber, W., Dosso, H.W., Law, L.K., Jones, F.W. and Ramaswamy, V. 1979b. Electromagnetic induction in the Vancouver Island region-field station and analogue model results. J. Geomag. Geoelectr., 31: 599-613.

Nienaber, W., Dosso, H.W. and Hutton, V.R.S. 1981. Electromagnetic induction in the British Isles region-analogue model and field station results. Phys. Earth Planet. Inter. (in press)

Ogunade, S.O., Ramaswamy, V. and Dosso, H.W. 1974. Electromagnetic response of a conducting sphere buried in a conducting earth. J. Geomag. Geoelectr., 26: 417-427.

Ogunade, S.O. and Dosso, H.W. 1977. Subsurface electromagnetic response of a conducting sphere embedded in the lower layer of a two-layer earth. Acta. Geodaet., Geophys. et Montanist. Acad. Sci. Hung., 12: 311-314.

Oldenburg, D.W. 1981. Conductivity structure of oceanic upper mantle beneath the Pacific plate. Geophys. J. R. Astr. Soc., 65: 359-394.

Parker, R.L. 1968. Electromagnetic induction in a thin strip. Geophys. J. R. Astr. Soc., 14: 487-495.

Parkinson, W.D. 1959. Direction of rapid geomagnetic fluctuation. Geophys. J. R. Astr. Soc., 2: 1-14.

Parkinson, W.D. and Jones, F.W. 1979. The geomagnetic coast effect. Reviews of Geophysics and Space Physics, 17: 1999-2015.

Price, A.T. 1930. Electromagnetic induction in a conducting sphere. Proc. London Math. Soc., Ser. 2, 31: 217-224.

Price, A.T. 1931. Electromagnetic induction in a permeable conducting sphere. Proc. London Math. Soc., Ser. 2, 33:233-245.

Price, A.T. 1949. The induction of electric currents in non-uniform thin sheets and shells. Quart. J. Mech. Appl. Math., 2: 283-310.

Price, A.T. 1950. Electromagnetic induction in a semi-infinite conductor with a plane boundary. Quart. J. Mech. Appl. Math., 3: 385-410.

Price, A.T. 1962. The theory of magneto-telluric methods when the source field is considered. J. Geophys. Res., 67: 1907.

Ramaswamy, V. 1973. Electromagnetic Fields of a Horizontal Magnetic Dipole Situated Above and Within a Two-Layer Earth. Ph.D. Thesis, University of Victoria.

Ramaswamy, V. and Dosso, H.W. 1977. The response of a conducting cyclinder to the inducing fields of various sources. J. Geomag. Geoelectr., 29: 181-189.

Ramaswamy, V. and Dosso, H.W. 1978. Analogue model measurements for a horizontal magnetic dipole embedded within a conducting medium. Phys. Earth Planet. Inter., 17: 255-299.

Ramaswamy, V., Jones, F.W., Dosso, H.W. and Nienaber, W. 1980. A comparison of numerical, analogue model, and field-station vertical magnetic-fields for the Vancouver Island region. Phys. Earth Planet. Inter. 22: 60-67.

Ramaswamy, V., Nienaber, W., Dosso, H.W., Jones, F.W. and Law, L.K. 1975. Numerical and analogue model results for electromagnetic induction for an island near a coastline. Phys. Earth Planet. Inter., 11: 81-90.

Reddy, I.K. and Rankin, D. 1973. Magnetotelluric response of a two dimensional sloping contact by the finite element method. Pure and Appl. Geophys., 105: 847-857.

Rikitake, T. 1960. Electromagnetic induction in a hemispherical ocean by S_q. J. Geomag. Geoelectr., 11: 65-79.

Rikitake, T. 1961. S_q and ocean. J. Geophys. Res., 66: 3245-3254.

Rikitake, T. 1966. Electromagnetism and the Earth's Interior. Elsevier, New York.

Roden, R.B. 1964. The effect of an ocean on magnetic diurnal variations. Geophysics Journal, 8: 375-388.

Schmucker, U. 1959. Erdmagnetische Tiefensondierung in Deutschland 1957/59: Magnetogramme und Erste Auswertung. Abh. Akad. Wiss. Gott., Math. Phys. Kl., Beitr. z. I.G.J. Heft 5.

Schmucker, U. 1964. Anomalies of geomagnetic variations in the southwestern United States. J. Geomag. Geoelectr., 15: 193.

Schmucker, U. 1970. Anomalies of geomagnetic variations in the southwestern United States. Bull. Scripps Inst. Oceanography. 13.

Schuster, A. 1889. The diurnal variation of terrestrial magnetism. Phil. Trans. Roy. Soc., London, A, 180: 467.

Sinclair, G. 1948. Theory of models of electromagnetic systems. Proc. I.R.E., 36: 1364-1370.

Strangway, D.W. 1966. Electromagnetic scale modelling. in Methods and Techniques in Geophysics, ed. by S.K. Runcorn, Interscience, New York, 1-31.

Swift, C.M. 1967. A Magnetotelluric Investigation of an Electrical Conductivity Anomaly in the Southwestern United States, Ph.D. Dissertation, Massachusetts Institute of Technology, Cambridge, Massachusetts.

Thomsom, D.J., Ramaswamy, V. and Dosso, H.W. 1972. Model measurements of electromagnetic variations near a coastline for localized source fields. J. Geomag. Geoelectr., 24: 317-336.

Tikhonov, A.N. 1950. Determination of the electric characteristics of the deep strata of the earth's crust. Dok. Akad. Nauk USSR, 73: 295.

Vozoff, K. and Swift, C.M. 1968. Magnetotelluric measurements in the north German basin. Geophys. Prospect., 16: 454-473.

Wait, J.R. 1954. On the relation between telluric currents and the earth's magnetic field. Geophyscis, 19: 281.

Ward, S.H. 1967. The electromagnetic method. in Mining Geophysics, II, Soc. Expl. Geophysicists, Tulsa, Okla., 224-372.

Weaver, J.T. 1963. The electromagnetic field within a discontinuous conductor with reference to geomagnetic micropulsations near a coastline. Can. J. Phys., 41: 484-495.

Weaver, J.T. 1973. Induction in a layered plane-earth by uniform and non-uniform source fields. Phys. Earth Planet. Inter., 7: 226-281.

Weaver, J.T. and Thomson D.J. 1972. Induction in a non-uniform conducting half-space by an external line current. Geophys. J., 28: 163-185.

Weidelt, P. 1971. The electromagnetic induction in two thin half-sheets. Zeitschrift fur Geophysik, 37: 649-665.

Wiese, H. 1962. Geomagnetische Tiefentellurik Teil II: Die Streuchrichtung der Untergrundstrukturen des elektrischen Widerstandes, erschlossen aus geimagnetischen Variationen. Geofis. Pura. Appl., 52: 83-103.

Zienkiewicz, D.C. 1971. The Finite Element Method in Engineering Science. McGraw-Hill, New York.

APPENDIX

This section contains Figs. 33-41 that were prepared during the course of this study but are not included in the text.

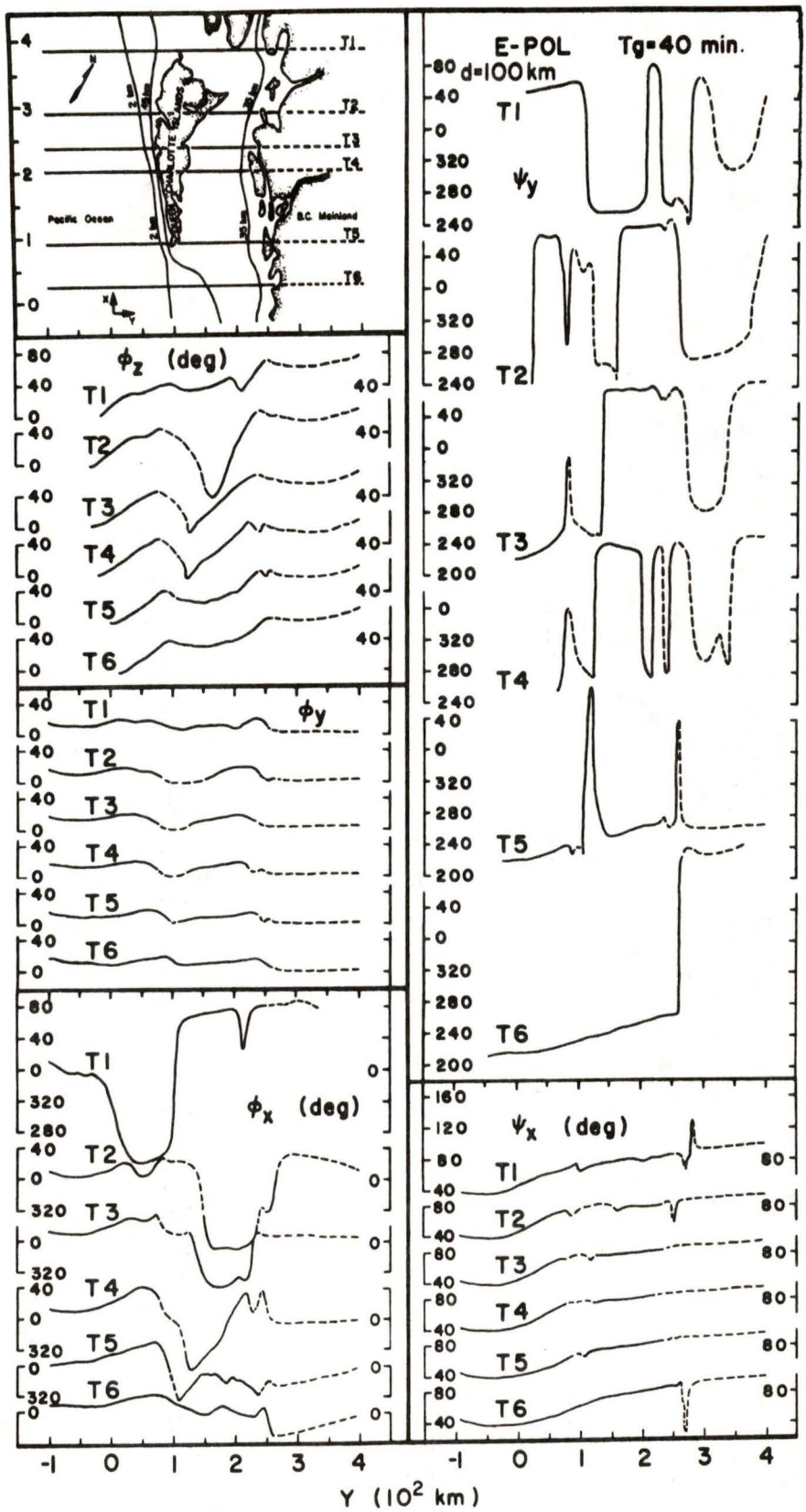

Fig. 33. Phases of the field components for traverses over the Queen Charlotte Islands model for a 40 min. period for E-Polarization.

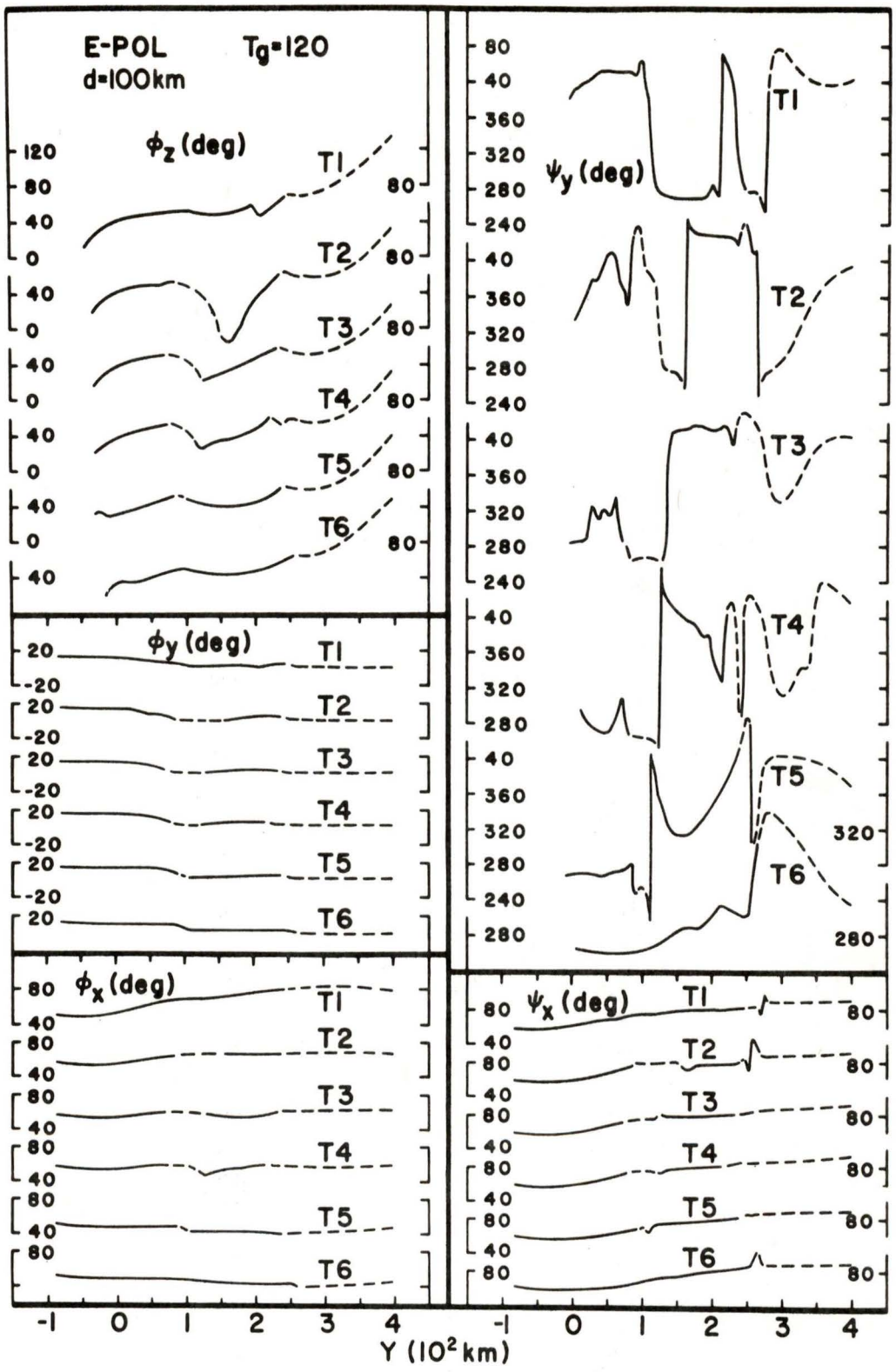

Fig. 34. Phases of the field components for traverses over the Queen Charlotte Islands model for a 120 min. period for E-Polarization.

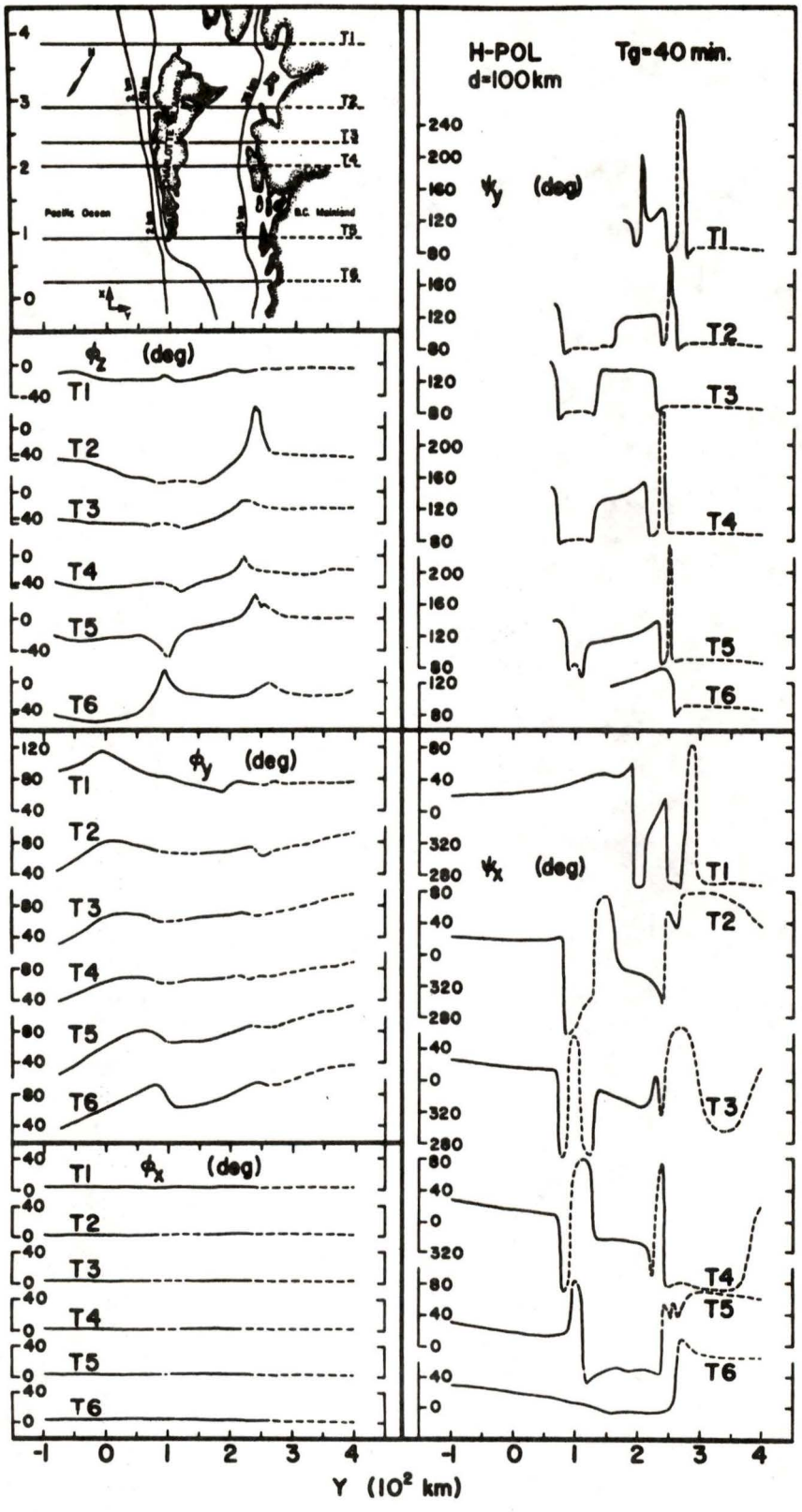

Fig. 35. Phases of the field components for traverses over the Queen Charlotte Islands model for a 40 min. period for H-Polarization.

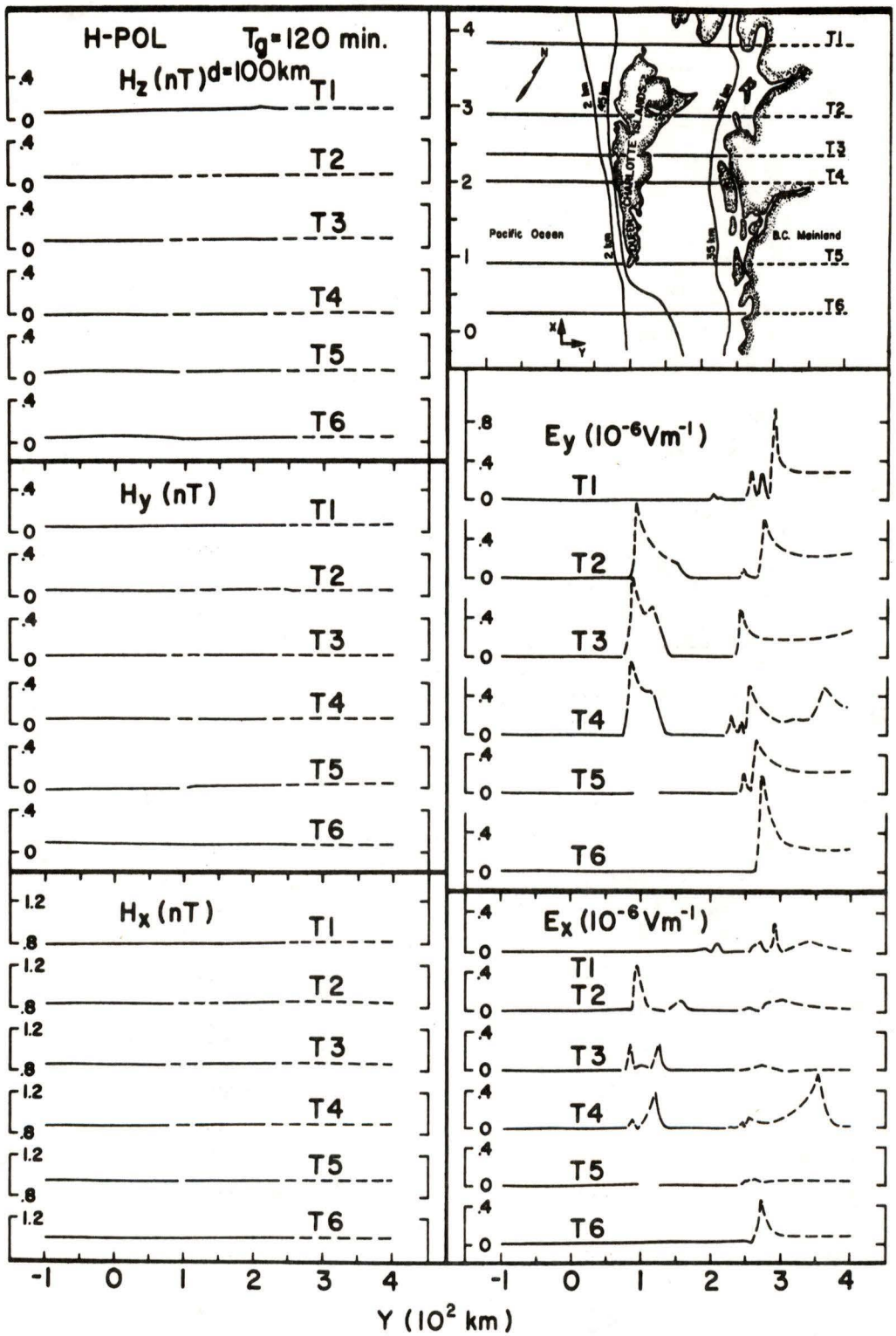

Fig. 36. Amplitudes of the field components for traverses over the Queen Charlotte Islands model for a 120 min. period for H-Polarization.

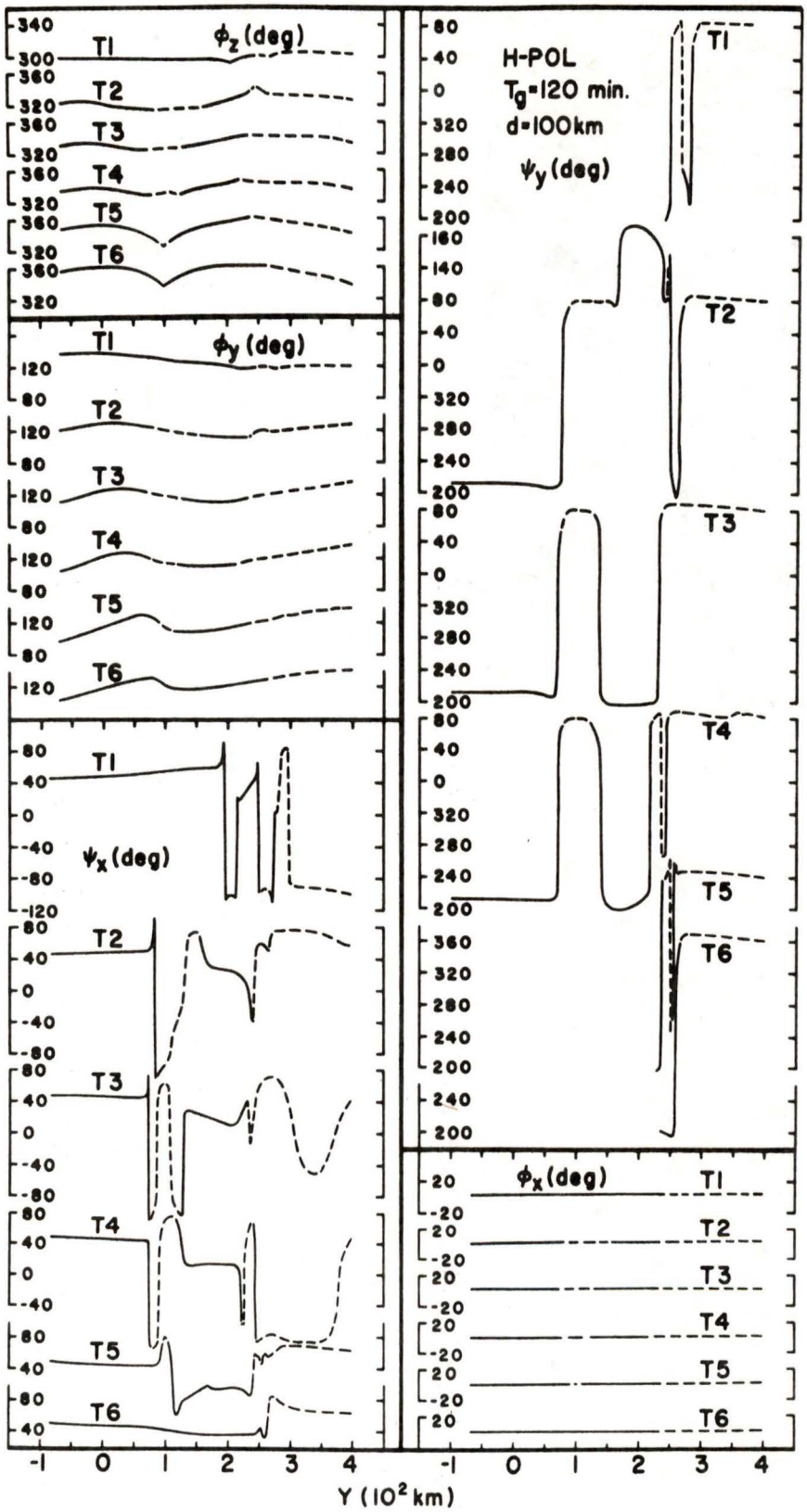

Fig. 37. Phases of the field components for traverses over the Queen Charlotte Islands model for a 120 min. period for H-Polarization.

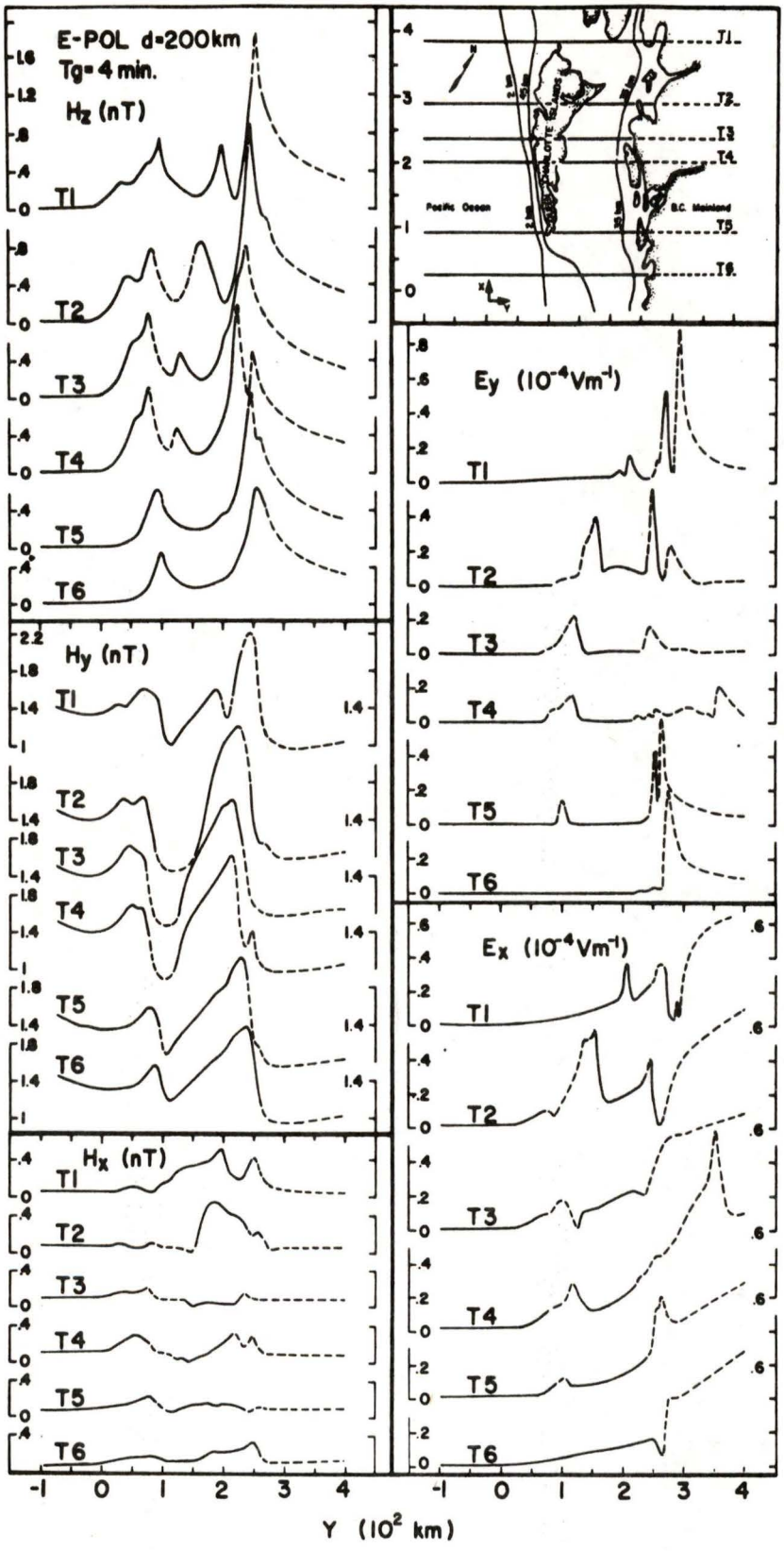

Fig. 38. Amplitudes of the field components for traverses over the Queen Charlotte Islands model for simulated depth to the conducting layer of 200 km for a 4 min. period for E-Polarization.

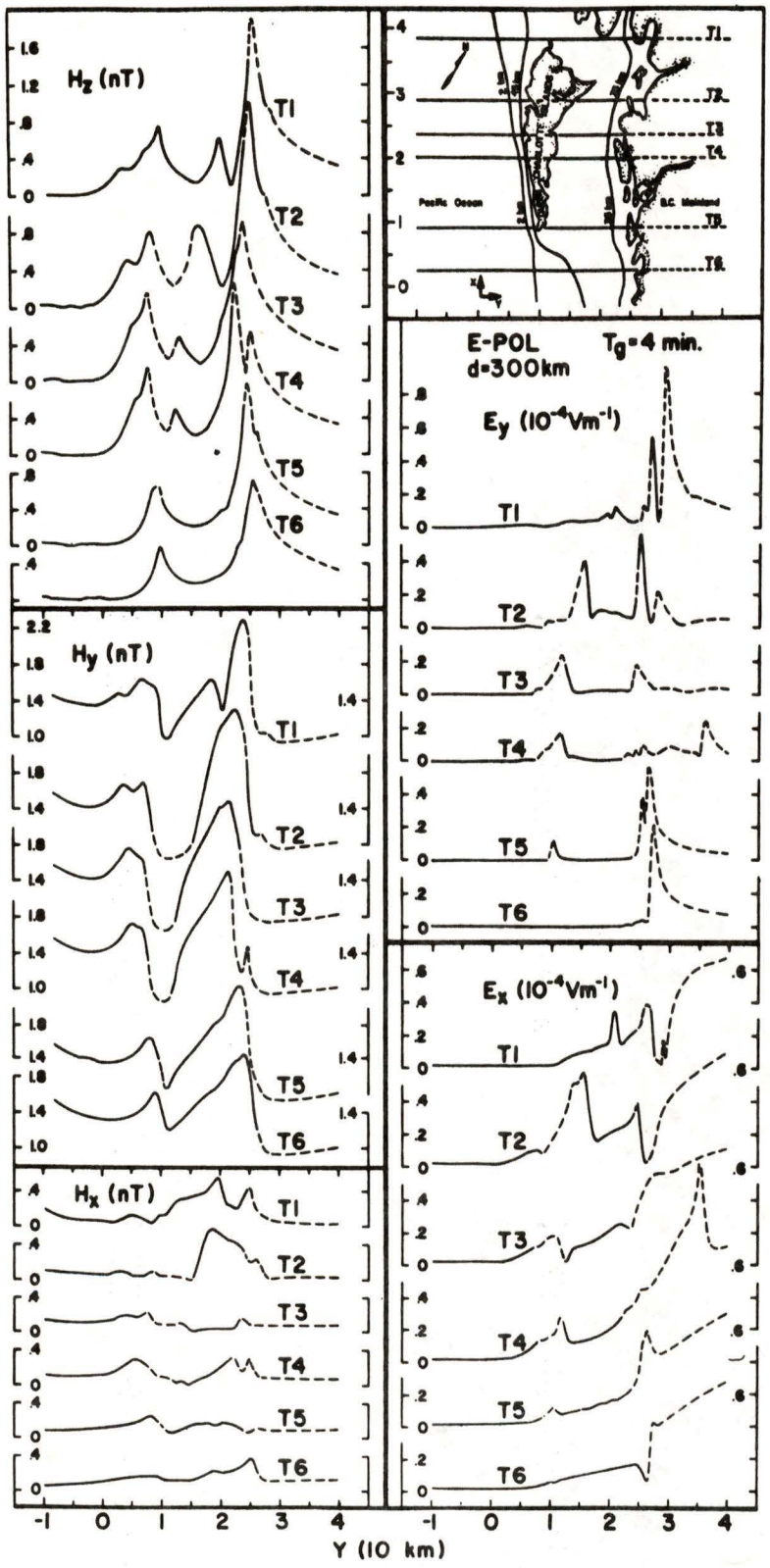

Fig. 39. Amplitudes of the field components for traverses over the Queen Charlotte Islands model for simulated depth to the conducting layer of 300 km for a 4 min. period for E-Polarization.

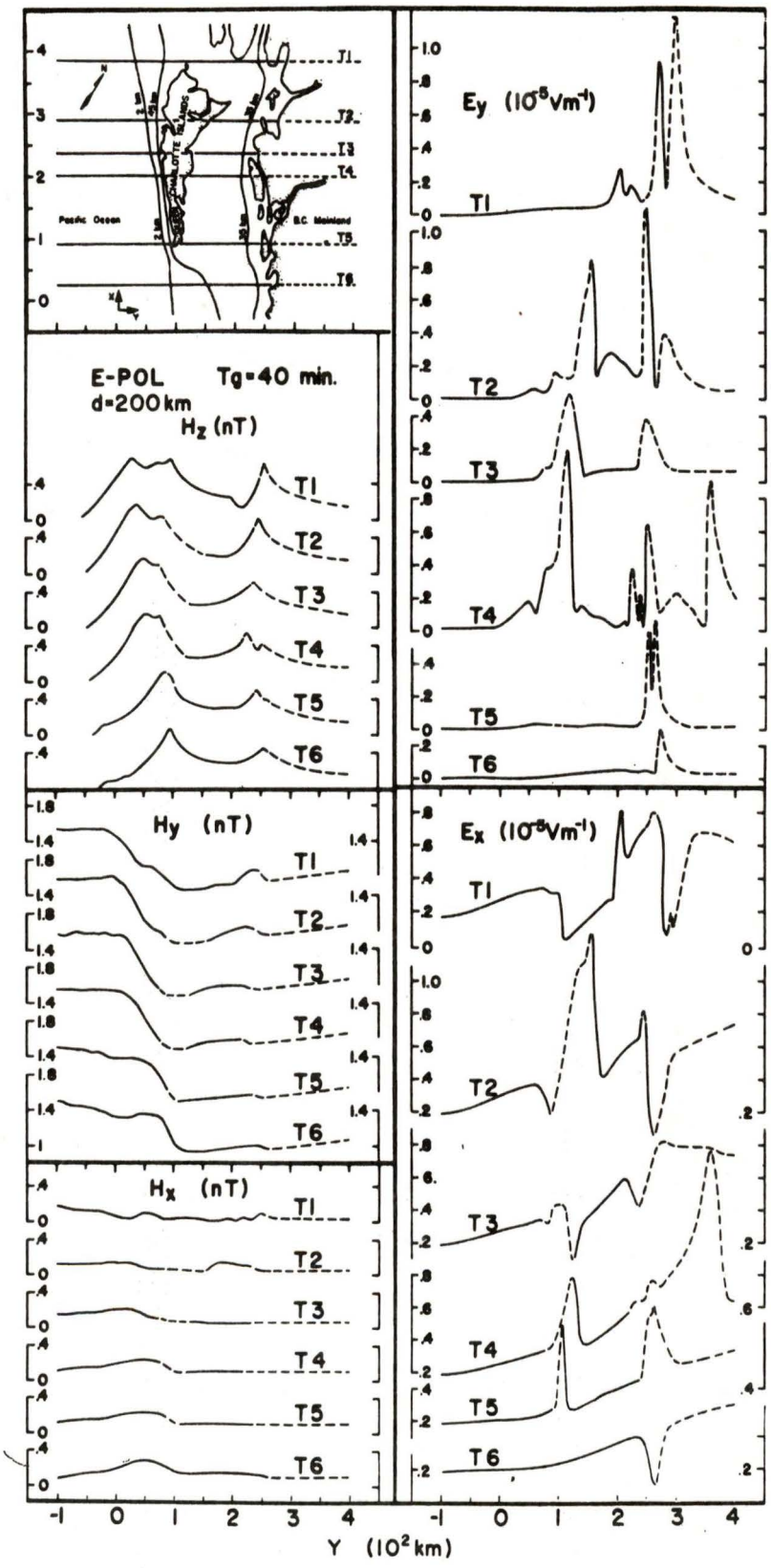

Fig. 40. Amplitudes of the field components for traverses over the Queen Charlotte Islands model for simulated depth to the conducting layer of 200 km for a 40 min. period for E-Polarization.

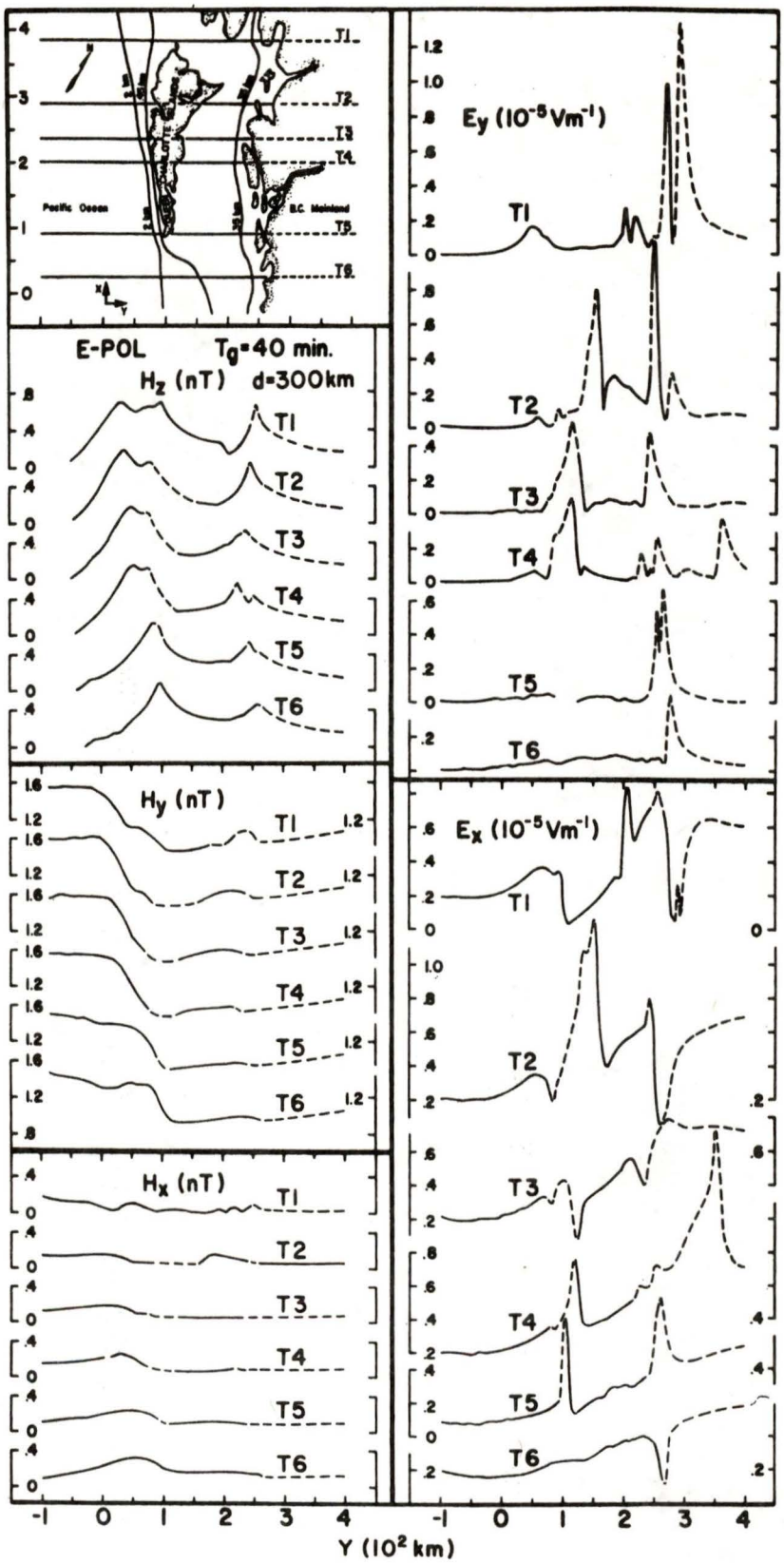

Fig. 41. Amplitudes of the field components for traverses over the Queen Charlotte Islands model for simulated depth to the conducting layer of 300 km for a 40 min. period for E-Polarization.

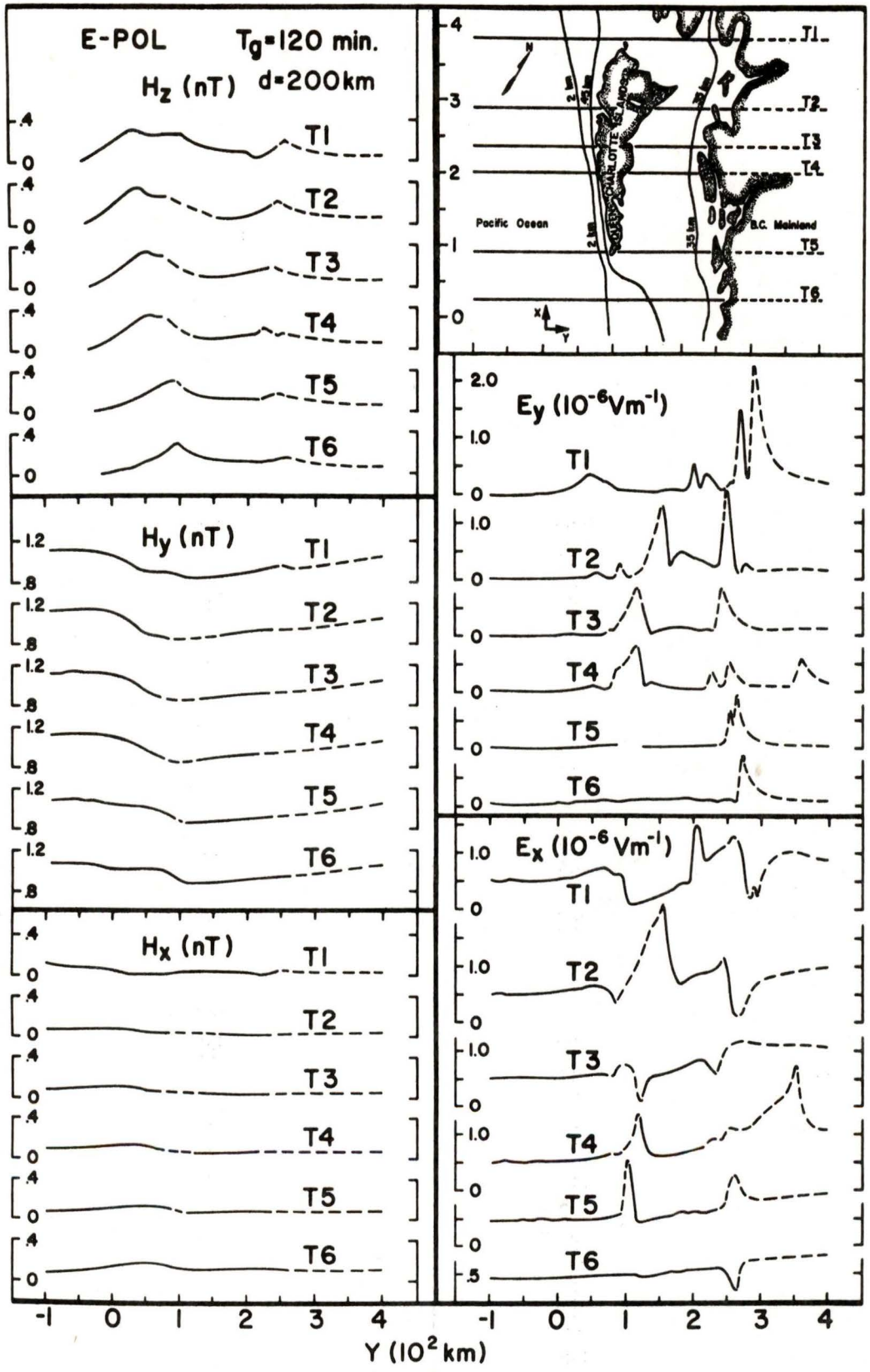

Fig. 42. Amplitudes of the field components for traverses over the Queen Charlotte Islands model for simulated depth to the conducting layer of 200 km for a 120 min. period for E-Polarization.

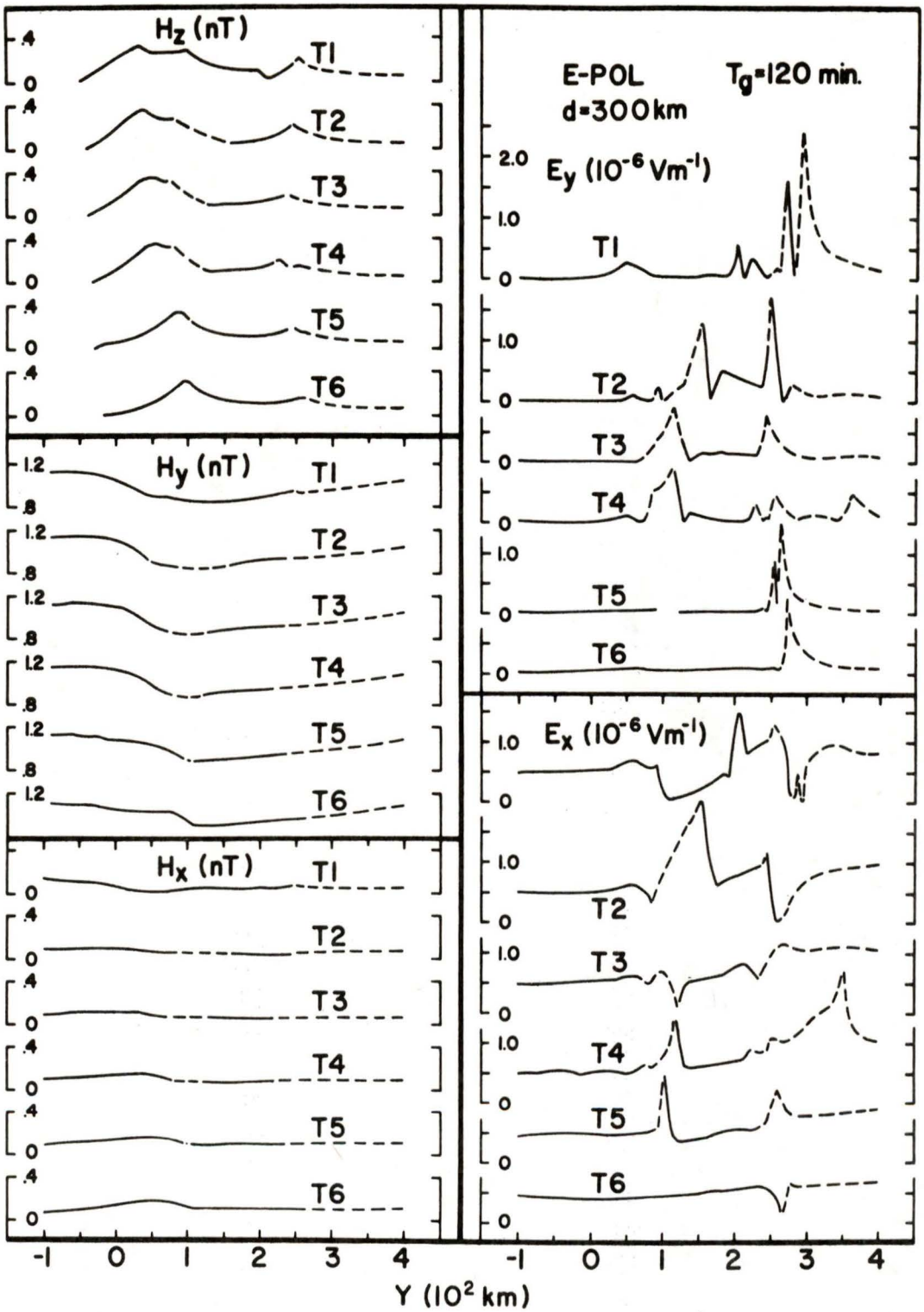

Fig. 43. Amplitudes of the field components for traverses over the Queen Charlotte Islands model for simulated depth to the conducting layer of 300 km for a 120 min. period for E-Polarization.

VITA

Surname: CHAN Given Names: EDWARD SU WAH

Place of birth: HONG KONG Date of Birth: AUGUST 26, 1955

Educational Institutions Attended, with Dates of Entering and Leaving:

UNIVERSITY OF VICTORIA 1973 to 1977

Degrees, Diplomas, Etc., Awarded, with Dates and Names of Institutions:

B.Sc. 1977 University of Victoria

Honours and Awards:

President's Scholarships, 1973/1974 and 1975/1976

N.S.E.R.C. Scholarships, 1979/1980 and 1980/1981

Papers Presented at Scientific Meetings:

Chan, E., Dosso, H.W., and Law L.K. 1979. An Electromagnetic Analogue Model Study of the Queen Charlotte Islands Region. Regional Meeting of the A.G.U. at Bend, Oregon.

Chan, E., Dosso, H.W., and Law L.K. 1980. Electromagnetic Induction for an Analogue Model of the Queen Charlotte Islands Region. Regional Meeting of the A.G.U. at Victoria, British Columbia.

Chan, E., Dosso, H.W., and Law L.K. 1980. A Model Study of the Electromagnetic Response of the Queen Charlotte Islands Region. Annual Fall Meeting of the A.G.U. at San Francisco, California.

PARTIAL COPYRIGHT LICENSE

I hereby grant the right to lend my thesis or dissertation (the title of which is shown below) to users of the University of Victoria Library, and to make single copies only for such users or in response to a request from the library of any other university, or similar institution, on its behalf or for one of its users. I further agree that permission for extensive copying of this thesis for scholarly purposes may be granted by me or a member of the University designated by me. It is understood that copying or publication of this thesis for financial gain shall not be allowed without my written permission.

Title of Thesis

An Analogue Model Study of Electromagnetic Induction in the Queen Charlotte Islands Region

Author [redacted]

signature

Edward S.W. Chan

name

July 1981

date